Electron Transfer Rates and Adsorption in the Electrochemistry of Cobalt-2, 2′-Bipyridine, Ruthenium Ammine Thiocyanate Complexes and cis-$[(C_5H_5)Fe(CO)P(C_6H_5)_2]_2$.

Thesis by

Brian Christopher Willett

In Partial Fulfillment of the Requirements

for the Degree of

Doctor of Philosophy

California Institute of Technology

Pasadena, California

1983

(Submitted September 17, 1982)

To Whom It May Concern

(You Know Who You Are)

ACKNOWLEDGMENTS

I wish to thank Dr. Fred C. Anson for his chemical insight, patience and many helpful suggestions, his July 4th parties, his stories about the "good old days" and Bozo the clown and the Happiness factor, and for not holding our tennis matches against me. In the same vein, I respectfully thank Dr. Harry Gray who showed me that even "older" chemists can play great tennis, if they are sneaky enough.

My tenure at Caltech has allowed me (or forced me, depending on how you look at it) to associate with many post-docs and graduate students, and I would like to thank them all one by one. Starting first with the graduate students I've known the longest: Mark Paffett for his computer expertise and for not beating me up when I mounted his desk six feet up on the wall; Roger Baar for his advice on Ruthenium chemistry, sports and women (solicited or not and not necessarily in that order); Dan Buttry who went from a long-haired hippie to a "serious, hard-working" student and a friend; Rich Durand who could stretch several mg of a compound a long, long, long way and could take a joke as well as give one; Jan Najdzionek for no other reason than he still owes me $20.00; Paul Neilson who gave new meaning to the words "background CV's"; Chi-Woo Lee (or Chuckles as we fondly call him) for providing a good laugh just by his presence; Steve Gipson for showing me the straight and narrow path (and who is the only student who can look Fred in the eye without looking up); Yu-min Tsou (the only person I know who dries his hair with a Waring blender) for showing me how much I learned while I was here.

And now for the post-docs: Dr. James Swartz for the companionship of another mechanistic organic chemist; Dr. Thomas Geiger for showing me how to live the singles life; Dr. Taka Shigehara for all the backgammon and chess games; Dr. Noboru Oyama, who once gave me a ride and I am luckily still alive to tell about it; Dr. Lorenz Walder, the best-dressed chemist I have ever met; Dr. Piotr Wrona who could talk for two hours without getting to the point and one hell of a soccer goalie; Dr. Patrick and Bernadette Martigny for the mixed doubles tennis matches; Dr. Takeo Ohsaka for showing me that some subjects transcend all language barriers and for being my personal bank machine; Dr. Hans-Rudolf Zumbrunnen for his friendship and the daily L.A. times; Dr. Carl Murray, who has a story for everything, for providing some competition in nerf-basketball; Dr. Mark Bowers, a kid after my own heart; and to all the other post-docs and professors I have known during my stay here - Thanks. Very special thanks go to Dr. Ann English for her friendship and all the tennis.

I especially want to acknowledge my friends from Indiana University, Dr. Dennis Peters (my former boss and racquetball partner), Dr. Bill Carroll and Dr. Dan La Perriere who are partly responsible for what I am today as a chemist and a person (both the good and the bad). And thanks to Henriette Wymar for typing this thesis.

Several inanimate objects also deserve mention, these include the beautiful National Parks (Zion, Bryce Canyon, Yosemite, Kings Canyon, Sequoia, Grand Canyon, Glacier, Yellowstone, Grand Tetons, Mount Ranier and Redwood), rock music, chili, Dr. Pepper, Colby cheese, candy bars and my '77 Camaro.

Finally, I thank my parents for their support these past twenty-five years (the last four in particular), both emotional (all the letters and calls) and financial (I would not have survived otherwise).

ABSTRACT

In Part I of this thesis, the electrochemical properties of cobalt(I)-2, 2′-bipyridine and cobalt(I)-6, 6′-dimethyl-2, 2′-bipyridine complexes were investigated, including their reactions with reducible substrates and their adsorption on mercury electrodes.

Electron transfer rate constants measured for cyclooctatetraene and cis-$[(C_5H_5)Fe(CO)P(C_6H_5)_2]_2$, molecules which undergo large intramolecular rearrangements upon electron transfer, in non-aqueous solvents with various tetraalkylammonium salts as supporting electrolytes are presented in Part II. The electrode kinetics were measured by cyclic voltammetry, chronocoulometry and AC impedance techniques. Values of the rate constants found were as large as 0.30 cm/sec.

Synthesis and adsorption behavior of several novel substituted ruthenium ammine complexes are discussed in Part III. The adsorption on mercury was used to distinguish between the two thiocyanate linkage isomers, $Ru(NH_3)_5NCS^{2+}$ and $Ru(NH_3)_5SCN^{2+}$. The coordination properties of ruthenium(II) were used to prepare trans-$Ru(NH_3)_4$(NCS)(4-vinylpyridine)Ru(EDTA), a binuclear ruthenium species.

TABLE OF CONTENTS

TABLE OF CONTENTS (continued)

Part I

Electrochemistry and Adsorption of Bis 2, 2′-Bipyridinecobalt(I) and Bis 6, 6′-Dimethyl-2, 2′-Bipyridinecobalt(I) in Acetonitrile

INTRODUCTION

Several recent reports by Anson and coworkers[1,2] have investigated the electrochemical and catalytic behavior of cobalt-2,2'-bipyridine complexes in acetonitrile. In the first of these,[1] the previously claimed catalytic reduction of acrylonitrile by a low-valent cobalt tris-bipyridine species[3] was shown not to involve reduction of the acrylonitrile by Co(I) but instead there was formation of an adduct between the Co(I)-bipyridine material and acrylonitrile. This adduct showed a new wave for reduction of Co(I) to Co(-I) which was at a potential positive of that for the Co(I) to Co(-I) wave in the absence of acrylonitrile, and had been mistakenly taken for a catalytic reduction wave. Formation of adducts with the Co(I)-bipyridine complex was also found to occur for other vinyl monomers. An important result from this work[1] was that the half-wave potential for reduction of the Co(II) tris-bipyridine species to the Co(I) complex was independent of added "free" 2,2'-bipyridine concentration, thus implying no loss of coordinated bipyridine ligand from the Co(I) compound during its electrolytic formation. Production of $Co(bipy)_3^+$ (bipy = 2,2'-bipyridine) by electroreduction of the tris-bipyridine cobalt(II) is in agreement with that reported earlier[4,5] but contrary to other investigations.[6-9] The $Co(bipy)_3^+$ is a characteristic dark blue with a λ_{max} at 601 nm ($\epsilon \sim 5,200$),[4,10] which has been assigned to a metal-to-ligand charge transfer. In the absence of any substrates, the cobalt tris-bipyridine complexes show well-behaved, reversible behavior for the Co(III) to Co(II) to Co(I) waves on both mercury and platinum electrodes.

A later study[2] investigated the electrocatalytic reduction of allyl chloride by the Co(I)-bipyridine complex in an inner-sphere electron transfer process to form 1,5-hexadiene and oligomers. Even greater catalytic rates were found for allyl chloride when cobalt(II) bis-bipyridine was electroreduced, however, even the $Co(bipy)_2^+$ was ineffective in catalyzing the reduction of allyl alcohol or acrylonitrile. One of the primary objectives of this study was to investigate further the electrochemistry and catalytic utility of the bis-bipyridine cobalt complex in acetonitrile solutions.

Chemical reductions of $Co(bipy)_3^{2+}$ with $NaBH_4$ or Na/Hg amalgam to form $Co(bipy)_3^+$ have shown that the Co(I) species may react with N_2O,[11] aromatic nitro compounds,[5] acetylene[12] and even ethyl bromide[12] but these reactions were always carried out with an excess of reducing agent present and the exact stoichiometry of the reactions was not determined. The catalytic reduction of nitrous oxide by the Co(I) was singled out for more detailed investigation in this study because the N_2O could possibly bind to the inner-sphere of the cobalt-bipyridine species and provide a simple model for oxygen reduction in cobalt-porphyrin complexes. However, as discussed in Part I, the reaction of N_2O and $Co(bipy)_n^+$ (where n = 2 or 3) was not as uncomplicated as was first thought.

In addition to discussing the bis-bipyridine cobalt electrochemistry and catalytic properties, Part I also reports the preparation and characterization of a highly hindered bis-6,6'-dimethyl-2,2'-bipyridine cobalt(II) whose electrochemistry more closely parallels the redox behavior of $Co(terp)_2^{2+}$[13] than that of $Co(bipy)_2^{2+}$. These results, along

with the adsorption behavior of the bis-bipyridine (substituted and unsubstituted) cobalt(I) on mercury electrodes in acetonitrile, have been published.[14]

EXPERIMENTAL

Materials. "Spectrograde" acetonitrile (Aldrich) was distilled first from CaH_2 and again from BaO just prior to use. (Burdick-Jackson) "UV quality" acetonitrile was used as received. "Polarographic grade" tetraethylammonium perchlorate and tetra-n-butylammonium perchlorate (Southwestern Analytical Company) were vacuum dried and used as supporting electrolytes without further purification. Tetra-n-butylammonium trifluoromethane sulfonate was prepared as described by Brandstrom.[15] Sodium perchlorate (G. F. Smith) was recrystallized twice from water and dried at 110°C. Nitrous oxide (Matheson) and n-butyl bromide (Matheson, Coleman, and Bell) were used as received. Allyl chloride (Eastman) was distilled prior to use. $Co(bipy)_3(ClO_4)_2$, $Co(bipy)_3(ClO_4)_3 \cdot 3H_2O$ and $Co(terp)_2(ClO_4)_2$ were synthesized according to standard procedures.[13,16] All these salts gave satisfactory elemental analyses as did 6,6′-dimethyl-2,2′-bipyridine, dmbp, synthesized according to a published procedure.[17] Elementary analysis of dmbp: C, 78.23%; H, 6.57%; N, 15.21%. Calculated: C, 78.45%; H, 6.82%; N, 15.41%. Solutions of $Co(bipy)_2^{2+}$ and $Co(dmbp)_2^{2+}$ were prepared by adding aliquots of a standard solution of $Co(ClO_4)_2 \cdot 2H_2O$ in acetonitrile to stoichiometric quantities of the ligands in the supporting electrolyte solution just prior to use. $[Co(terp)(bipy)(H_2O)][PF_6]_2$ was prepared according to Martel.[18]

Apparatus. Cyclic voltammograms were obtained with a Princeton Applied Research (PAR) Model 173 potentiostat driven by a PAR Model 175 universal programmer. Working electrodes were a commercial hanging mercury drop electrode (Metrohm), a static mercury drop electrode (PAR Model 303), a planar platinum button electrode or a pyrolytic graphite disk electrode mounted in glass with heat-shrinkable tubing.

Chronocoulometry experiments were accomplished by means of a computer-based apparatus similar to that described previously.[19] Controlled-potential electrolyses were conducted with the PAR Model 173 potentiostat equipped with a PAR Model 179 digital coulometer. The electrolysis cell employed was modeled after the design described by Moore and Peters.[20] Solutions were usually deoxygenated by bubbling with argon that had been passed through hot copper turnings. When more complete exclusion of oxygen was desired, the experiments were connected inside a controlled atmosphere box (Vacuum Atmospheres Company).

Rotating ring-disk measurements were performed according to conventional practice[21] inside the controlled atmosphere box. The Pt-ring, Pt-disk electrode, electrode rotator, and the bipotentiostat were from Pine Instrument Co. (Grove City, Pa.). An x-y-y' recorder (Hewlett Packard Model 7046) was used to record disk and ring current-potential curves simultaneously. A dual compartment cell was employed with a platinum wire auxiliary electrode and the reference electrode separated from the main cell compartment by a sintered glass frit.

The radius of the disk electrode was 0.301 cm (A = 0.285 cm^2). The inner and outer radii were 0.314 and 0.332 cm, respectively. The collection efficiency[21] (measured by reducing $Co(bipy)_3^{2+}$ at the disk and oxidizing the resulting $Co(bipy)_3^{+}$ at the ring in the absence of any substrates) was 0.19 in relatively good agreement with the value (0.18) calculated from the electrode geometry.[22] This electrode was cleaned by polishing with 0.3 μm alumina on a polishing cloth before use and on a kimwipe before each scan.

UV-VIS spectra were recorded with a Cary Model 219 Spectrometer or a Hewlett-Packard Model 8450A Spectrometer. Potentials were measured and are reported with respect to an aqueous Ag/AgCl reference electrode which has a potential ca. 45 mV more negative than a saturated calomel electrode. Experiments were conducted at the laboratory temperature, 22 ± 3°C.

RESULTS AND DISCUSSION

$Co(bipy)_3^{2+}$ and $Co(bipy)_2^{2+}$

The cyclic voltammetry of solutions containing cobalt(II) and bipyridine is particularly simple when the molar ratio of metal to ligand is one to three. As shown in Figure 1A, three waves appear at ca. +0.4, -0.9 and -1.5 volts corresponding to the Co(III)/Co(II), Co(II)/Co(I) and Co(I)/(-I) couples, respectively.[1,3] The first two couples appear completely reversible at scan rates from 0.02 to 10 volt s^{-1} (with a plot of peak current versus the square root of scan rate that is linear) while the last couple yields cathodic peak currents that are larger than their anodic counterparts at scan rates below

ca. 1 volt s^{-1}. The responses obtained are essentially identical at both mercury and platinum electrodes. The polarographic half-wave potential for the Co(II)/(I) couple is unaffected by the addition of as much as 0.1 M excess 2,2'-bipyridine[1] showing that no bipyridine molecules leave the inner coordination sphere of cobalt(II) during the reduction to cobalt(I).

Double potential step chronocoulometry[23] with solutions of $Co(bipy)_3^{2+}$ indicates little or no adsorption on mercury or platinum of the tris-bipyridine complexes of cobalt(III), (II) or (I). During controlled-potential reduction of $Co(bipy)_3^{2+}$, the current decreases exponentially with time and 1.0 faraday per mole of cobalt(II) is consumed. The resulting solution of $Co(bipy)_3^{+}$ are dark blue and appear stable for weeks when stored in an oxygen-free atmosphere.

There are significant changes in this simple pattern when the initial solution contains only two moles of 2,2'-bipyridine per mole of cobalt(II). Figures 1B and 1C show cyclic voltammograms for $Co(bipy)_2^{2+}$ at mercury and platinum electrodes. At mercury, a small wave appears ahead of the main Co(II) reduction peak and the corresponding anodic response includes a narrow, sharp wave typical of adsorbed species. In addition, a small, irreversible oxidation peak is observed at +0.14 V on mercury (its magnitude depends on the scan rate and the concentration of the complex) just prior to the small, reversible response corresponding to the Co(II)/(III) couple. The magnitude of this Co(II)/(III) response increases if the ligand-to-cobalt ratio is increased above 2 to 1 and decreases to zero when the ratio is reduced below ca. 1.8 to 1. At any fixed ratio, the response gives an

Figure 1. Cyclic voltammograms of $Co(bipy)_3^{2+}$ and $Co(bipy)_2^{2+}$ in acetonitrile.

A. 1.0 mM $Co(bipy)_3^{2+}$; mercury electrode (0.0255 cm^2); scan rate = 200 mV s^{-1}.

B. 1.8 mM $Co(bipy)_2^{2+}$; mercury electrode; scan rate = 100 mV s^{-1}.

C. 0.5 mM $Co(bipy)_2^{2+}$; platinum electrode (0.20 cm^2); scan rate = 200 mV s^{-1}.

Supporting electrolyte: A, B - 0.1 M tetraethylammonium perchlorate; C - 0.1 tetrabutylammonium trifluoromethane sulfonate.

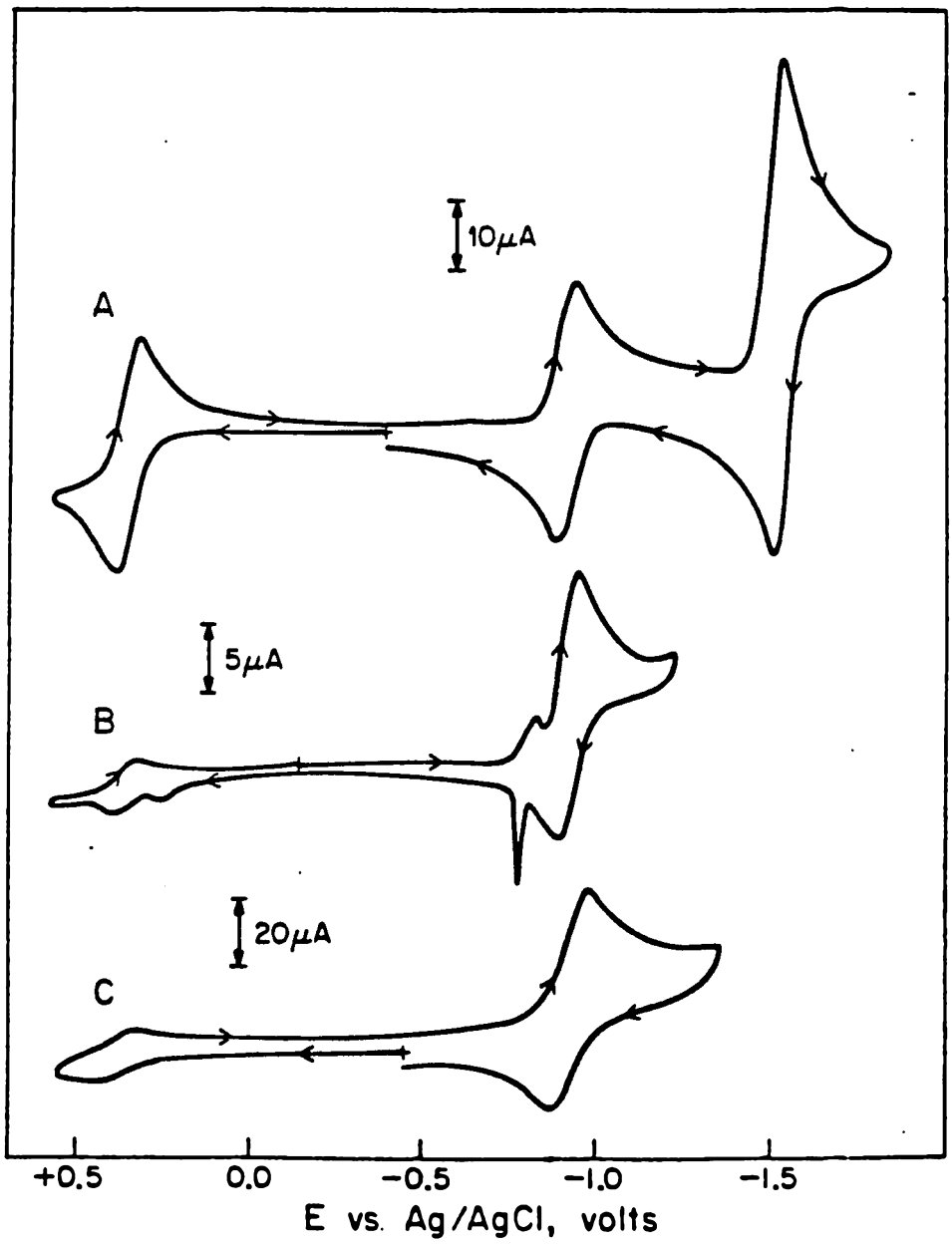
10μA
A
5μA
B
20μA
C
+0.5
0.0
−0.5
−1.0
−1.5
E vs. Ag/AgCl, volts

indication of the amount of $Co(bipy)_3^{2+}$ formed by ligand exchange reactions between species with fewer than three coordinated ligands. The irreversible wave at +0.14 V arises from the oxidation of cobalt metal as demonstrated by cyclic voltammetry on Hg with solutions of $Co(ClO_4)_2 \cdot 2H_2O$ in acetonitrile in the absence of bipyridine.

At platinum electrodes, no pre-wave or anodic spike appears at the potentials where the cobalt(II)/(I) couple is active (Figure 1C) suggesting that there is much weaker interaction between cobalt(I) and the platinum surface. At both electrodes, the peak current for reduction of $Co(bipy)_2^{2+}$ exceeds the value for the same concentration of $Co(bipy)_3^{2+}$ and the ratio of cathodic to anodic peak current is well above unity. The peak current ratio depends upon the concentration of the complex and the scan rate, approaching unity at sufficiently high scan rates. (A plot of peak current versus square root of scan rate is non-linear.)

The course of controlled-potential reductions of $Co(bipy)_2^{2+}$ also differs markedly from that of $Co(bipy)_3^{2+}$: With the latter complex, plots of the logarithm of the current vs. time are linear and 1.0 faraday is consumed per mole of cobalt(II). The former complex yields non-linear plots and consumes 1.3 to 1.4 faradays per mole. Changes in the color of the electrolysis solution also differ from those observed during the reduction of $Co(bipy)_3^{2+}$: The initially pale yellow solution develops a violet color during the first few minutes of the electrolysis before it acquires the deep blue color characteristic of $Co(bipy)_3^{+}$. No intermediate violet color precedes the appearance of the blue color when $Co(bipy)_3^{2+}$ is reduced.

Figure 2. UV-visible spectra of A, $Co(bipy)_2^+$ and B, $Co(bipy)_3^+$ in acetonitrile. Spectrum A, obtained from a partially reduced solution of $Co(bipy)_2^{2+}$, was scaled to correspond to 0.23 mM $Co(bipy)_2^+$. Spectrum B is for a 0.23 mM solution of $Co(bipy)_3^{2+}$ that was fully reduced to $Co(bipy)_3^+$.

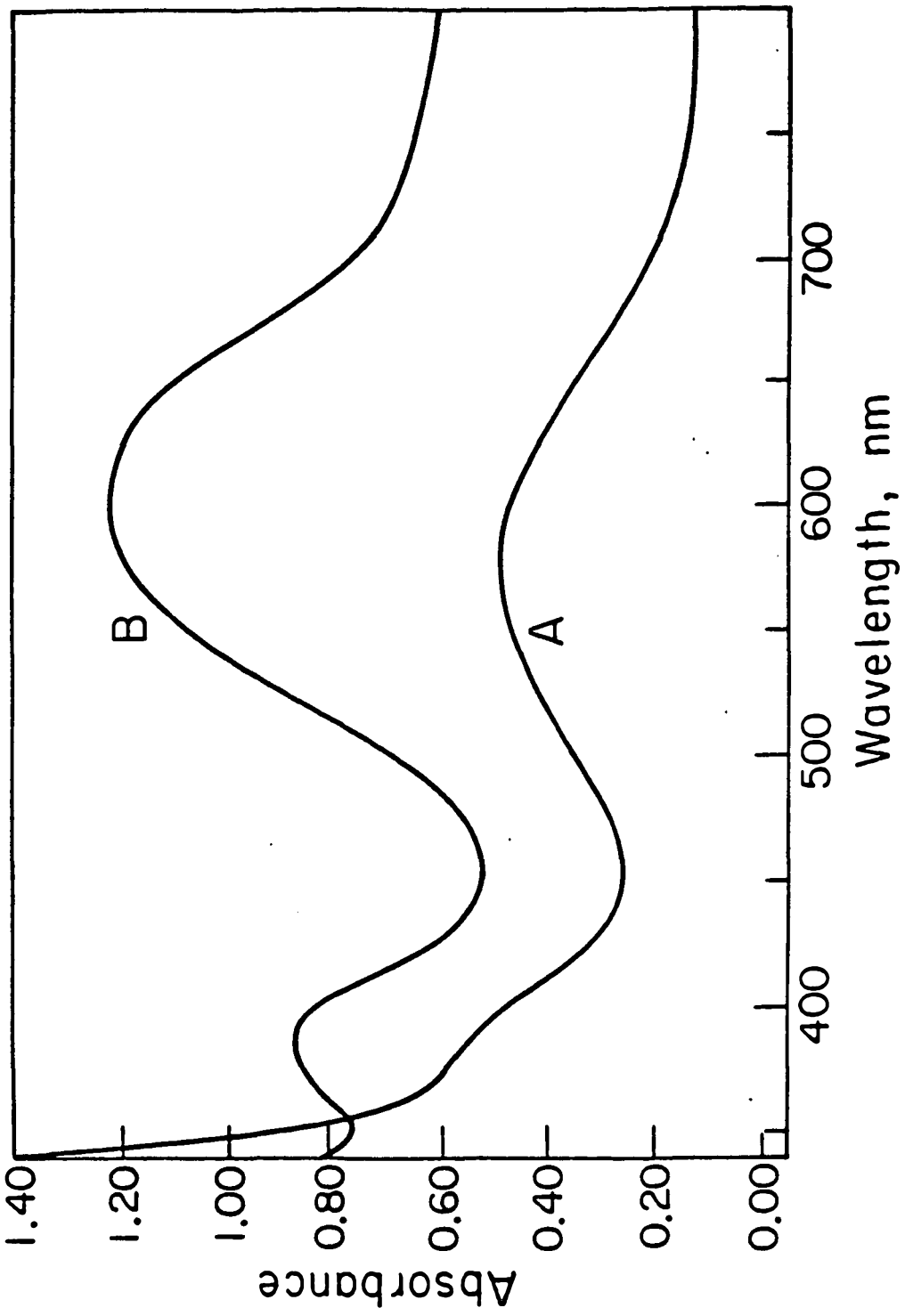
Absorbance
1.40
1.20
1.00
0.80
0.60
0.40
0.20
0.00
400
500
600
700
Wavelength, nm
A
B

Interruption of an electrolysis of $Co(bipy)_2^{2+}$ at an early stage when the solution is violet results in a fading of the violet color in a matter of minutes and restoration of the initial pale yellow color. (Both $Co(bipy)_2^{2+}$ and $Co(bipy)_3^{2+}$ are yellow). Curve A of Figure 2 is a spectrum of the violet solution. The spectrum was recorded as rapidly as possible after the electrolysis was interrupted. The spectrum of the stable, blue $Co(bipy)_3^{+}$ ion is shown for comparison in curve B. Although the precise composition of the violet solution is uncertain, the spectrum shown is believed to be dominated by $Co(bipy)_2^{+}$. ($Co(bipy)_2^{2+}$ and $Co(bipy)_3^{2+}$ absorb negligibly at wavelengths greater than 450 nm; the only likely interfering contaminant is $Co(bipy)_3^{+}$ and none was detected in the spectrum obtained after the violet color had disappeared).

Solutions of $Co(bipy)_2^{2+}$ that have been exhaustively electrolyzed at -1.2 volts have spectra that are identical to that of $Co(bipy)_3^{+}$, but only two-thirds of the initial cobalt is accounted for by the intensity of the absorption. Cyclic voltammograms show a reversible response at the potential corresponding to the $Co(bipy)_3^{2+}/Co(bipy)_3^{+}$ couple with peak currents corresponding to two-thirds of the cobalt initially present. The missing cobalt cannot be recovered by the addition of more bipyridine. It is believed to be in the form of cobalt metal that results from the decomposition of cobalt(I) complexes containing fewer than two bipyridine ligands as outlined in Scheme I.

SCHEME 1

$$Co(bipy)_2^{2+} + e \rightarrow Co(bipy)_2^{+} \quad (1)$$

$$2Co(bipy)_2^{+} \rightleftharpoons Co(bipy)_3^{+} + Co(bipy)^{+} \quad (2)$$

$$2Co(bipy)^{+} \rightarrow Co + Co(bipy)_2^{2+} \quad (3)$$

$$Co(bipy)_2^{2+} + e \rightarrow Co(bipy)_2^{+} \quad (1)$$

etc.

According to this scheme the net result of the electrolysis of a solution of $Co(bipy)_2^{2+}$ will be given by reaction 4:

$$Co(bipy)_2^{2+} + 4/3e^{-} \rightarrow 1/3\,Co + 2/3\,Co(bipy)_3^{+}. \quad (4)$$

This accounts for both the observed disappearance of one-third of the cobalt and the consumption of 1.3 to 1.4 faradays per mole of cobalt during the electrolysis.

Scheme 1 also accounts for the observation that the cathodic peak currents in cyclic voltammograms of 1 mM solutions of $Co(bipy)_2^{2+}$ exceed the anodic peak currents except at scan rates above ca. 2 V s^{-1}. Additional support for Scheme 1 comes from the observation that voltammograms obtained in solutions prepared by adding equimolar quantities of Co^{2+} and bipyridine to acetonitrile show new peaks that correspond to the deposition of cobalt metal as well as smaller peaks for the generation of $Co(bipy)_2^{+}$.

An alternative scheme can be written for the loss of $Co(bipy)_2^{+}$ involving its disproportionation to $Co(bipy)_2^{0}$ and $Co(bipy)_2^{2+}$. However,

Groshen et al.[24] have examined the electrochemistry of chemically synthesized $Co(bipy)_2^0$ and shown that it is thermodynamically unstable with respect to disproportionation to $Co(bipy)_2^+$ and $Co(bipy)_2^-$ (as is consistent with the absence of a wave for the reduction of $Co(bipy)_2^+$ to $Co(bipy)_2^0$ in the cyclic voltammetry of $Co(bipy)_2^{2+}$). Thus, if $Co(bipy)_2^+$ were to disproportionate it would have to proceed according to reaction 5:

$$3Co(bipy)_2^+ \rightarrow 2Co(bipy)_2^{2+} + Co(bipy)_2^- \qquad (5)$$

and the equilibrium constant for this reaction can be calculated from the relevant voltammetric peak potentials[24] to be ca. 10^{-40}. This is one reason that the observed decomposition of $Co(bipy)_2^+$ was ascribed to reactions such as those given in Scheme 1 instead of to direct disproportionation as depicted in reaction 5.

$Co(bipy)_2^+$ generated by the disproportionation of $Co(bipy)_2^0$ should also decompose via reactions 2 and 3 of Scheme 1. Groshens et al.[24] did not consider this possibility but the cyclic voltammograms they report for solutions prepared from $Co(bipy)_2^0$ contain prominent peaks at the potential of the Co(III)/Co(II) couple that were found in this study to appear only when tris bipyridine complexes are present (Figure 1). In addition, the peak current densities of the voltammograms shown in references 24 are about half as great as those of Figure 1 and of Groshens et al. (cf. Figure 2A of reference 24) under the same conditions when the solution is prepared from $Co(bipy)_2^{2+}$. The conductance of solutions prepared from $Co(bipy)_2^0$[24] is also much smaller than would be expected if all of the cobalt added were present as $Co(bipy)_2^+$

and $Co(bipy)_2^-$. Thus, we conclude that the disproportionation of $Co(bipy)_2^0$ in acetonitrile to yield $Co(bipy)_2^+$ and $Co(bipy)_2^-$ as described in reference 24 was accompanied by significant decomposition of the $Co(bipy)_2^+$ so that Co and $Co(bipy)_3^+$ were also produced by reactions 2 and 3 of Scheme 1.

Reactions of $Co(bipy)_2^+$ with Reducible Substrates

One objective in studying the electrochemical reduction of $Co(bipy)_2^{2+}$ was the possibility that $Co(bipy)_2^+$, with an open coordination site, would prove to be a better catalyst than $Co(bipy)_3^+$ for reductions of substrates that are difficult to reduce directly but might be activated by coordination to the Co(I) centers. Nitrous oxide was examined as a possible substrate because its reduction by borohydride in homogeneous solution is known to be catalyzed by cobalt-bipyridine complexes[11] and the direct electrochemical reduction of N_2O at mercury occurs at potentials much more negative than those where $Co(bipy)_2^{2+}$ is reduced.[25]

Cyclic voltammograms for the $Co(bipy)_3^{2+}$ and $Co(bipy)_2^{2+}$ in the absence and presence of N_2O are compared in Figure 3. The addition of N_2O produces very little change in the peak currents for the reduction of either complex. However, the anodic peak currents are decreased significantly and the bigger effect is shown by $Co(bipy)_2^{2+}$. The addition of N_2O also eliminates the adsorption pre- and post-waves exhibited by $Co(bipy)_2^{2+}$ at mercury electrodes. Chronocoulometric tests showed that the adsorption of the reduced complex is essentially eliminated by the addition of N_2O.

The lack of significant increases in the cathodic peak currents in Figure 3 in the presence of N_2O shows that the rate of its reduction by

$Co(bipy)_3^+$ or $Co(bipy)_2^+$ is not large under these conditions. However, the decrease in anodic current suggests that N_2O does react with $Co(bipy)_2^+$ (but not $Co(bipy)_3^+$) either to form a moderately stable adduct that is not oxidizable at potentials where $Co(bipy)_2^+$ is oxidized or to produce oxide (or hydroxide) ion that attacks the $Co(bipy)_2^+$ complex[26] thus decreasing the anodic peak current. The reaction also reduces the adsorption of $Co(bipy)_2^+$ suggesting that, if an adduct is formed, the coordination site at Co(I) that is occupied by the N_2O is essential for the formation of the adsorption bond to the mercury surface.

Repeated cycling of the mercury electrode in solutions of $Co(bipy)_2^{2+}$ and N_2O causes the voltammogram to collapse until amost no current flows. The response returns immediately at a fresh electrode. At a platinum electrode the voltammogram collapses almost immediately indicating a strong passivation of the electrode surface. Similar behavior results during controlled potential reductions of $Co(bipy)_2^{2+}$ at -1.2 volt in the presence of excess N_2O. The electrolysis current does not attain a steady level as would be expected if a catalytic reduction of the N_2O were proceeding. Instead the current decays (plots of log (current) vs. time are non-linear) reaching zero after ca. 1.7 faradays per mole of cobalt are passed through the solution. The resulting brownish-yellow solution contains a small quantity of a dark precipitate and exhibits no electrochemical responses at a fresh mercury drop electrode except for an anodic wave attributable to the presence of free bipyridine. It seems likely that the oxide ion[27] (or hydroxide ion) generated by the slow reduction of N_2O to N_2 attacks the cobalt-bipyridine complexes present, removing the cobalt from

Figure 3. Effect of N_2O on cyclic voltammograms of $Co(bipy)_2^{2+}$ and $Co(bipy)_3^{2}$.

A. 1.9 mM $Co(bipy)_3^{2+}$; platinum electrode;
initial potential -0.6 volt.

B. 2.0 mM $Co(bipy)_2^{2+}$; mercury electrode;
initial potential -0.4 volt.

Supporting electrolyte: 0.1 M tetraethylammonium perchlorate.

Scan rate = 200 mV s^{-1}.

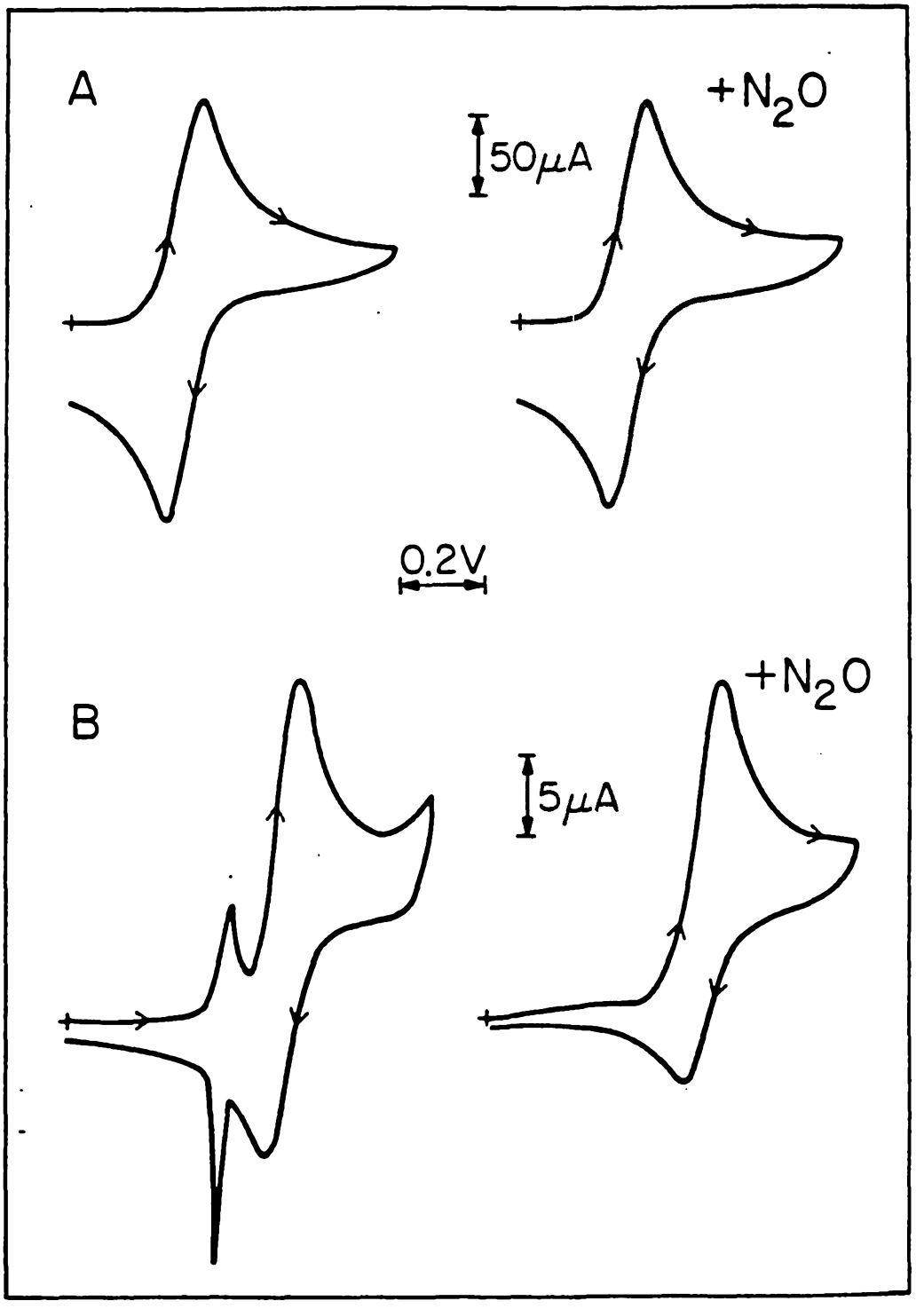
A
+N2O
50μA
0.2V
B
+N2O
5μA

solution and thereby halting the electrolysis. The substance produced by the reaction with the strong base is believed to form stable, passivating coatings on the surfaces of mercury and platinum electrodes that are responsible for the rapid decay in the current. The electrolysis could be prolonged a little by addition of proton donors, such as diethyl malonate, but no conditions were found where the $Co(bipy)_2^+$-facilitated reduction of N_2O could be sustained.

With substrates whose reduction does not liberate a strong base, e.g., alkyl halides, $Co(bipy)_2^+$ could conceivably serve as an effective reduction catalyst. However, the catalytic reaction would have to proceed relatively rapidly in order to avoid the loss of catalyst according to Scheme 1 with precipitation of cobalt metal. Rapid reduction is the case with allyl chloride[2] but with non-activated halides, e.g., n-butylbromide, the reaction with $Co(bipy)_2^+$ was too slow to be practical for electrosynthetic exploitation.

Catalysis of the reduction of allyl chloride by $Co(bipy)_2^+$ or $Co(bipy)_3^+$ was further studied by fast scan cyclic voltammetry and rotating ring-disk voltammetry. As anticipated from earlier work,[2] the rate of reduction of allyl chloride is faster when $Co(bipy)_2^+$ is the catalyst instead of $Co(bipy)_3^+$. Actually, with a 5-fold excess of allyl chloride present, scan rates greater than 2 V/sec show only a small amount of reaction between $Co(bipy)_3^+$ and the allyl chloride while scan rates greater than 500 V/sec are needed to obtain comparable responses with $Co(bipy)_2^+$. In addition, ring-disk experiments were performed with a 10-fold excess of the allyl chloride present (pseudo first-order conditions) to examine the kinetics of the catalytic reaction.

Qualitatively, the catalytic disk currents for $Co(bipy)_2^+$ are 3/2 to 3 times larger than those for $Co(bipy)_3^+$ and the corresponding anodic ring currents are smaller. In addition, it appears that the catalytic current for the reaction of the tris-bipyridine cobalt(I) species with allyl chloride is essentially independent of rotation rates above 400 rpm (see Figure 4).

Bis 6,6'-dimethyl-2,2'-bipyridine cobalt(II)

A cyclic voltammogram for $Co(dmbp)_2^{2+}$ recorded at a pyrolytic graphite electrode is shown in Figure 5A while 5B shows the response obtained at a mercury electrode. The reversible couples at -0.63 volt and -1.20 volt both correspond to one-electron processes, i.e., Co(II) $\rightleftharpoons$ Co(I) and Co(I) $\rightleftharpoons$ Co(0). The anodic wave at +0.32 volt is observed only at mercury and is therefore not attributable to the oxidation of Co(II) to Co(III). Instead, the wave is believed to arise from the oxidation of mercury to form $Hg(dmbp)_2^{2+}$ and Co^{2+}. The same wave appears in solutions containing only the uncoordinated ligand but its peak potential appears at a less positive value (+0.26 V), as expected. No corresponding anodic wave is present in solutions of $Co(bipy)_2^{2+}$ (or $Co(bipy)_3^{2+}$) probably because of the much greater stability (and/or smaller lability) of this complex.

No wave for the oxidation of Co(II) to Co(III) was found under any conditions at graphite or platinum electrodes, even in the presence of 10 mM uncoordinated ligand at potentials as positive as +1.5 volt. The two methyl substituents apparently produce sufficient steric crowding to prevent the formation of the tris complex[28] that would be required for the oxidation of Co(II) to Co(III) to proceed at accessible potentials.

Figure 4. Rotating disk currents in acetonitrile solutions at a platinum electrode for ● 1.8 mM $Co(bipy)_2^{2+/+}$, ○ catalytic reduction current from 1.8 mM $Co(bipy)_2^{2+/+}$ in the presence of 18 mM allyl chloride, ■ 1.8 mM $Co(bipy)_3^{2+/+}$, □ catalytic reduction current from 1.8 mM $Co(bipy)_3^{2+/+}$ in the presence of 18 mM allyl chloride, ▲ 1.8 mM $Co(bipy)_3^{+/-}$

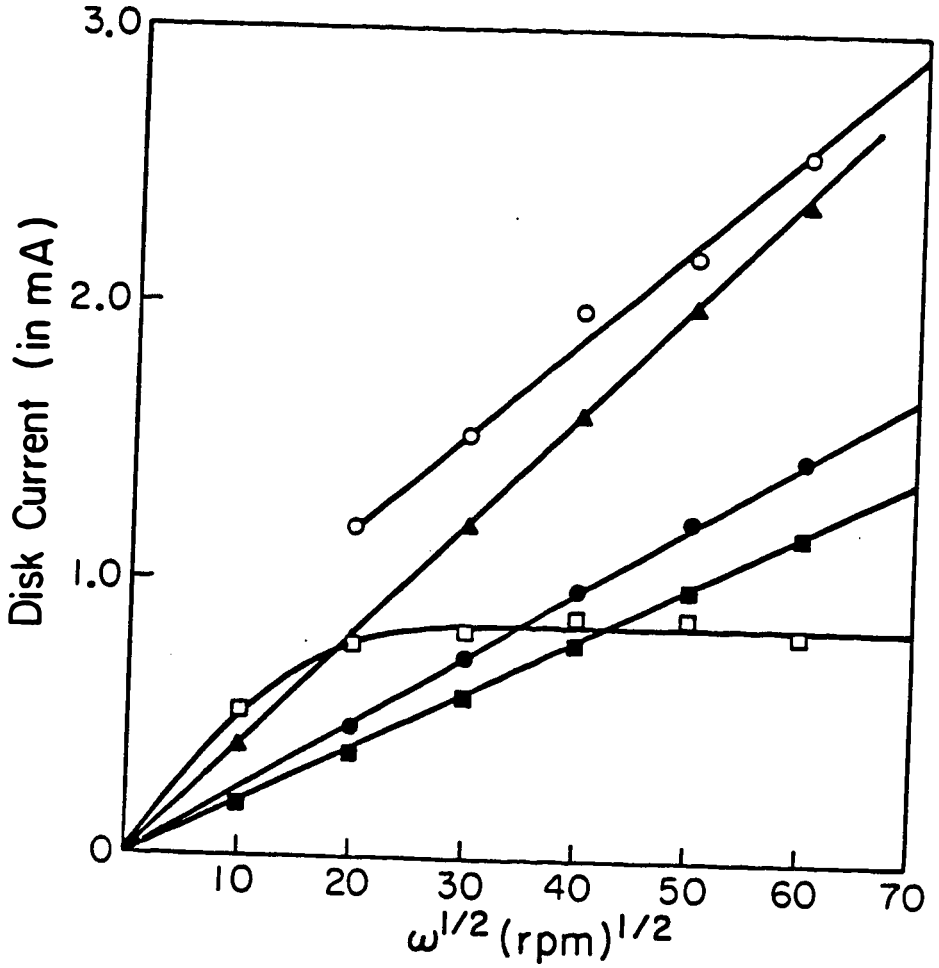
3.0
2.0
1.0
0
Disk Current (in mA)
10
20
30
40
50
60
70
ω^1/2 (rpm)^1/2

Figure 5. Cyclic voltammogram of 1.8 mM $Co(dmbp)_2^{2+}$ in acetonitrile. A. Pyrolytic graphite electrode. B. Mercury electrode. Scan rate: 100 mV s^{-1}. Supporting electrolyte: 0.1 M tetraethylammonium perchlorate.

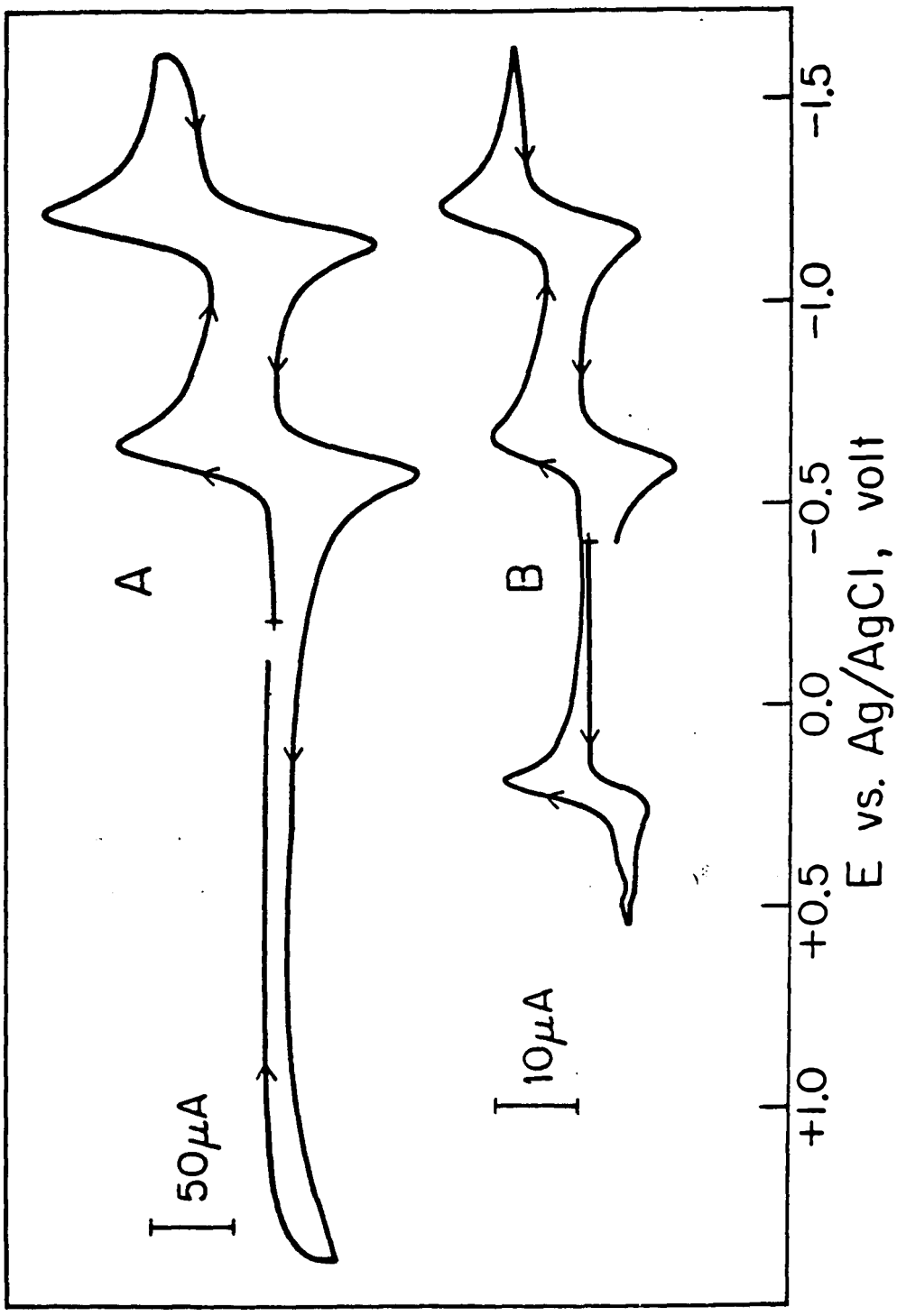
A
B
50μA
10μA
+1.0
+0.5
0.0
-0.5
-1.0
-1.5
E vs. Ag/AgCl, volt

The ratio of anodic to cathodic peak currents for the Co(II)/(I) and Co(I)/(0) waves in Figure 5A are close to 1.0 at all scan rates indicating that both of the reduced forms of the complex are much more stable than is $Co(bipy)_2^+$. This was confirmed by controlled-potential reduction of a solution of $Co(dmbp)_2^{2+}$ at -0.9 volt. Linear log (current) vs. time curves resulted and 1.05 faradays were consumed per mole of complex. The resulting purple solution (λ_{max} at 577 nm ($\epsilon \sim 5,600$)) showed no evidence of decomposition by pathways similar to those in Scheme 1. It was stable for days in the absence of oxygen. A spectrum of a solution of $Co(dmbp)_2^+$ is given in Figure 6, curve A.

Further reduction of $Co(dmbp)_2^+$ at -1.5 volt consumed an additional 1.07 faradays per mole of complex and produced a dark blue-black solution whose spectrum is shown in Figure 6, curve B. This reduced solution appeared stable for several hours in the absence of oxygen but cobalt metal precipitated from the solution if it was allowed to stand overnight.

Reduction of $Co(dmbp)_2^{2+}$ via two 1-electron steps and at more positive potentials than for $Co(bipy)_3^{2+}$ reduction is very similar to the electrochemical behavior of $Co(terp)_2^{2+}$ (see Figure 7), and, as discussed in the next section, their reactivities toward reducible substrates are also comparable.

Exposure of $Co(dmbp)_2^+$ to Reducible Substrates

The formal potential of the $Co(dmbp)_2^{2+/+}$ couple is about 400 mV more positive than that of the $Co(bipy)_2^{2+/+}$ couple. $Co(dmbp)_2^+$ is thus a much weaker reductant than $Co(bipy)_2^+$ and this is reflected in its inertness towards potentially reducible substrates. Addition of nitrous

Figure 6. UV-visible spectra of 0.23 mM solutions of (A) $Co(dmpb)_2^+$ and (B) $Co(dmbp)_2$ in acetonitrile.

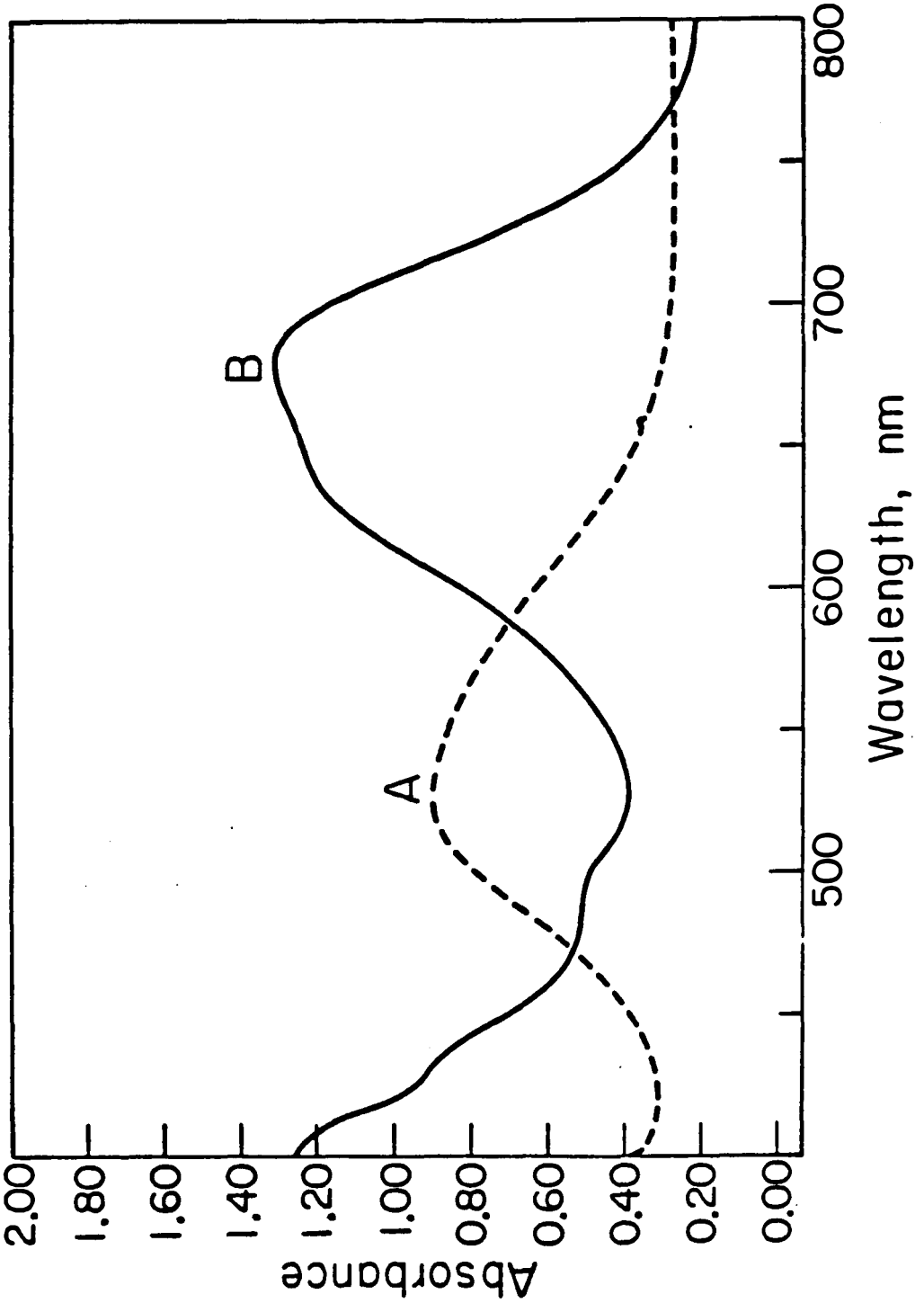
Absorbance
2.00
1.80
1.60
1.40
1.20
1.00
0.80
0.60
0.40
0.20
0.00
500
600
700
800
Wavelength, nm
A
B

Figure 7. 1.8 mM $Co(terp)_2(ClO_4)_2$ in CH_3CN containing 0.1 M tetraethylammonium perchlorate on (BPG) carbon at a scan rate of 50 mV/sec.

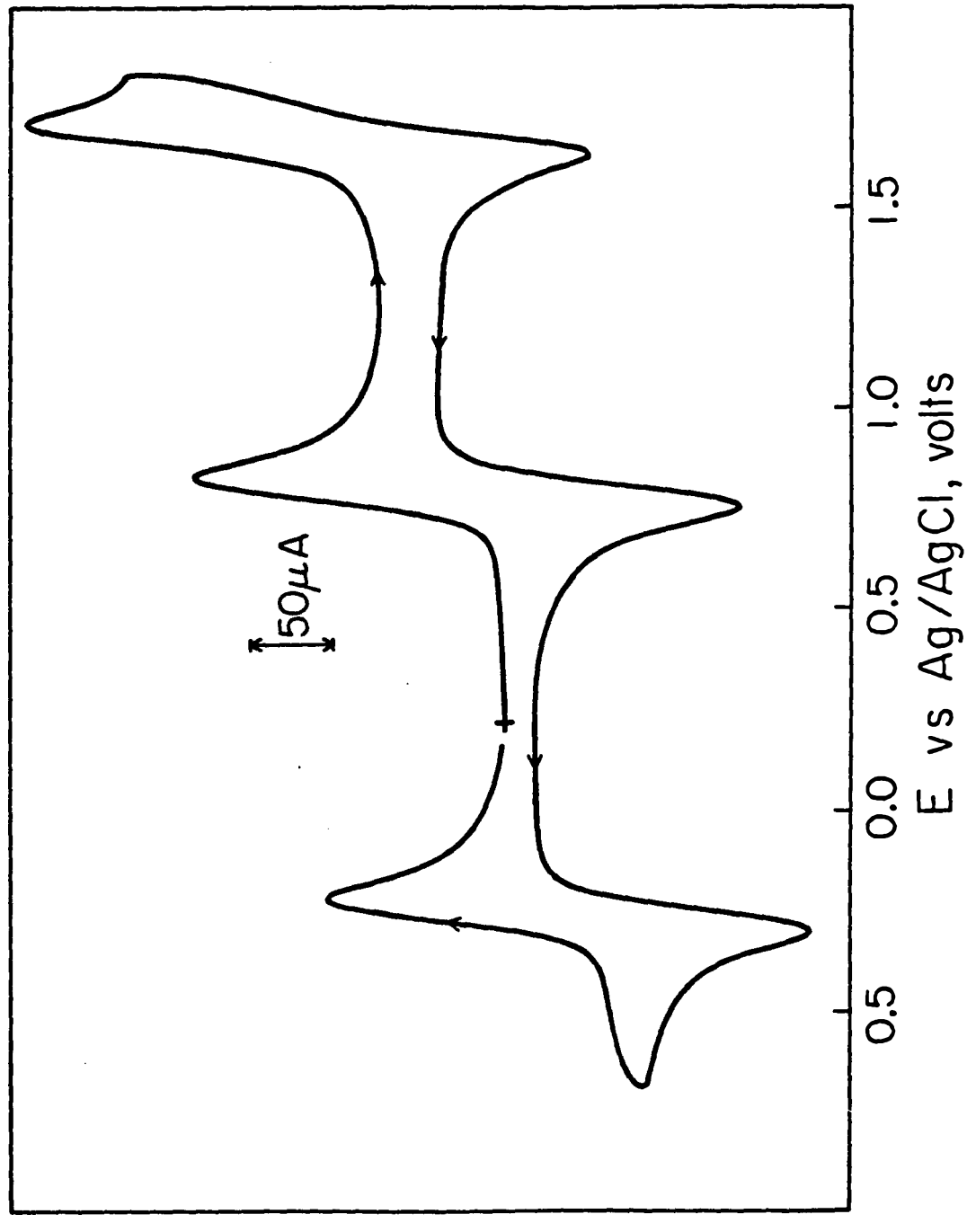
50μA
0.5
0.0
0.5
1.0
1.5
E vs Ag/AgCl, volts

oxide to solutions of $Co(dmbp)_2^{2+}$ produced no detectable changes in the cyclic voltammogram for the $Co(dmbp)_2^{2+/+}$ couple. In particular, and in contrast with the $Co(bipy)_2^{2+/+}$ couple, the anodic peak current was undiminished and the anodic peak potential did not shift in the presence of N_2O. This indicates that N_2O does not coordinate with $Co(dmbp)_2^{+}$ (and it is certainly not reduced at an appreciable rate). Supporting this interpretation was the failure of N_2O to affect the adsorption (vide infra) in the way that it did for $Co(bipy)_2^{+}$. Even the further reduction of the $Co(dmbp)_2^{+}$ to $Co(dmbp)_2^{0}$ was largely unaffected by the addition of nitrous oxide (less than a 10% decrease in the anodic peak current). Similar results were obtained with allyl chloride or acrylonitrile as the substrate, or when $Co(terp)_2^{+}$ and $Co(terp)_2^{0}$ were used as possible catalysts.

An alternate starting point for the preparation of a reactive Co(I) species which has an open coordination site was the $Co(terp)(bipy)(aq)^{2+}$ complex; however, in non-aqueous media, this compound undergoes rapid ligand reorganization to form $Co(terp)_2^{2+}$ and $Co(bipy)_2^{2+}$. Only when excess chloride ions are present could a single reduction wave for the $Co(terp)(bipy)(Cl)^{+}$ be observed with a half-wave potential exactly between the half-wave potentials for the bis-terpyridine and bis-bipyridine cobalt(II) species. Because of the necessity of chloride ion in the 6th coordination site, no further studies were carried out on this complex.

Adsorption of $Co(bipy)_2^{+}$ on Mercury

Chronocoulometry[23] showed no detectable adsorption ($<10^{-11}$ moles cm^{-2}) of $Co(bipy)_2^{2+}$ on mercury or platinum electrodes.

However, there was clear evidence for strong adsorption when mercury (but not platinum) electrodes were exposed to $Co(bipy)_2^+$. Because of the relatively rapid decomposition of $Co(bipy)_2^+$ (Scheme 1), it was not possible to prepare stable solutions in which the adsorption could be measured. Instead, solutions of $Co(bipy)_2^{2+}$ were employed and $Co(bipy)_2^+$ was generated at the electrode surface by adjusting its potential to -1.2 volt where the diffusion-limited reduction of $Co(bipy)_2^{2+}$ proceeded. At the end of the generation period (45 seconds was typical), the electrode potential was stepped to -0.4 volt where the diffusion-limited oxidation of $Co(bipy)_2^+$ proceeded. The resulting charge-time data were linearized by plotting charge vs. $(time)^{\frac{1}{2}}$ [23] and the quantity of $Co(bipy)_2^+$ adsorbed was estimated from the difference between the charge axis intercept and the corresponding value measured in a blank run in the pure supporting electrolyte. The slopes of the chronocoulometric plots of charge vs. $(time)^{\frac{1}{2}}$ were typically about half as large as those obtained in corresponding experiments in which the stable $Co(bipy)_3^{2+}$ complex was generated at the electrode and then reoxidized to $Co(bipy)_3^{2+}$. (A diffusion coefficient of $1.7 * 10^{-5}$ cm^2/sec was calculated from the chronocoulometric slopes for the $Co(bipy)_3^{2+}$.) The smaller slopes almost certainly result from the partial decomposition of $Co(bipy)_2^+$ during the period that it is generated. This means that the actual interfacial concentrations of $Co(bipy)_2^+$ that give rise to the adsorption cannot be measured precisely. The adsorption data are therefore presented by specifying the concentrations of the $Co(bipy)_2^{2+}$ solutions in which the $Co(bipy)_2^+$ was generated with the understanding that this provides only a qualitative measure of the effect of concen-

tration changes on the adsorption.

Table I summarizes the adsorption data at several concentrations of $Co(bipy)_2^{2+}$. The adsorption is clearly quite extensive, even from 0.1 mM solutions. The apparent maximum in the adsorption at a concentration of 0.45 mM may be the result of competition between the adsorbate and the increasing quantities of cobalt metal that are deposited on the mercury surface via reactions 2 and 3 as the concentration of $Co(bipy)_2^{+}$ increases.

Chronocoulometric charge-time transients for the reduction of $Co(bipy)_2^{2+}$ are strongly influenced by the fact that the $Co(bipy)_2^{+}$ formed at the electrode is adsorbed. Figure 8 shows that the slope of the charge-$(time)^{\frac{1}{2}}$ plot at times before the adsorption has attained its final value is larger for the reduction of $Co(bipy)_2^{2+}$ than of $Co(bipy)_3^{2+}$ where there is little or no adsorption of the reaction product. Chronocoulometric charge-$(time)^{\frac{1}{2}}$ transients for electrode processes in which an unadsorbed reactant is converted to an adsorbed product are usually no different from those obtained without product adsorption unless the adsorption results in large changes in the electric charge density on the electrode surface. The differential capacitance of the mercury electrodes at -1.2 volt showed no major increase in the presence of $Co(bipy)_2^{2+}$ so that the higher slope of curve B in Figure 8 cannot be attributed to changes in the surface charge density of the electrode. Instead, we believe the higher initial slope results from the further reduction of $Co(bipy)_2^{+}$ by one electron as it is adsorbed. Thus, the $Co(bipy)_2^{2+}$ that is reduced to adsorbed product consumes two electrons while only one electron is consumed in reducing unadsorbed $Co(bipy)_2^{2+}$

TABLE I

Adsorption on Mercury of the Product of the Reduction of $Co(bipy)_2^{2+}$ in Acetonitrile[a,b]

Concentration of $Co(bipy)_2^{2+}$, mM	$n\Gamma F$, μC[c]
0.11	12
0.14	16
0.23	42
0.45	100
0.9	78
1.8	78
3.6	88

a. Supporting Electrolyte: 0.1 M tetrabutylammonium trifluoromethane sulfonate.

b. The electrode potential was held for 45 seconds at -1.2 volts and then stepped to -0.4 volt for 100 msec.

c. To convert these values into mole cm^{-2}, n = 2 should be used (see text).

Figure 8. Chronocoulometric charge-$(\text{time})^{\frac{1}{2}}$ transients for the reduction of (A) $Co(bipy)_3^{2+}$ and (B) $Co(bipy)_2^{2+}$ at mercury electrodes. The potential was stepped from -0.4 to -1.2 volts. (C) Response obtained in the pure surporting electrolyte. Supporting electrolyte as in Figure 1B.

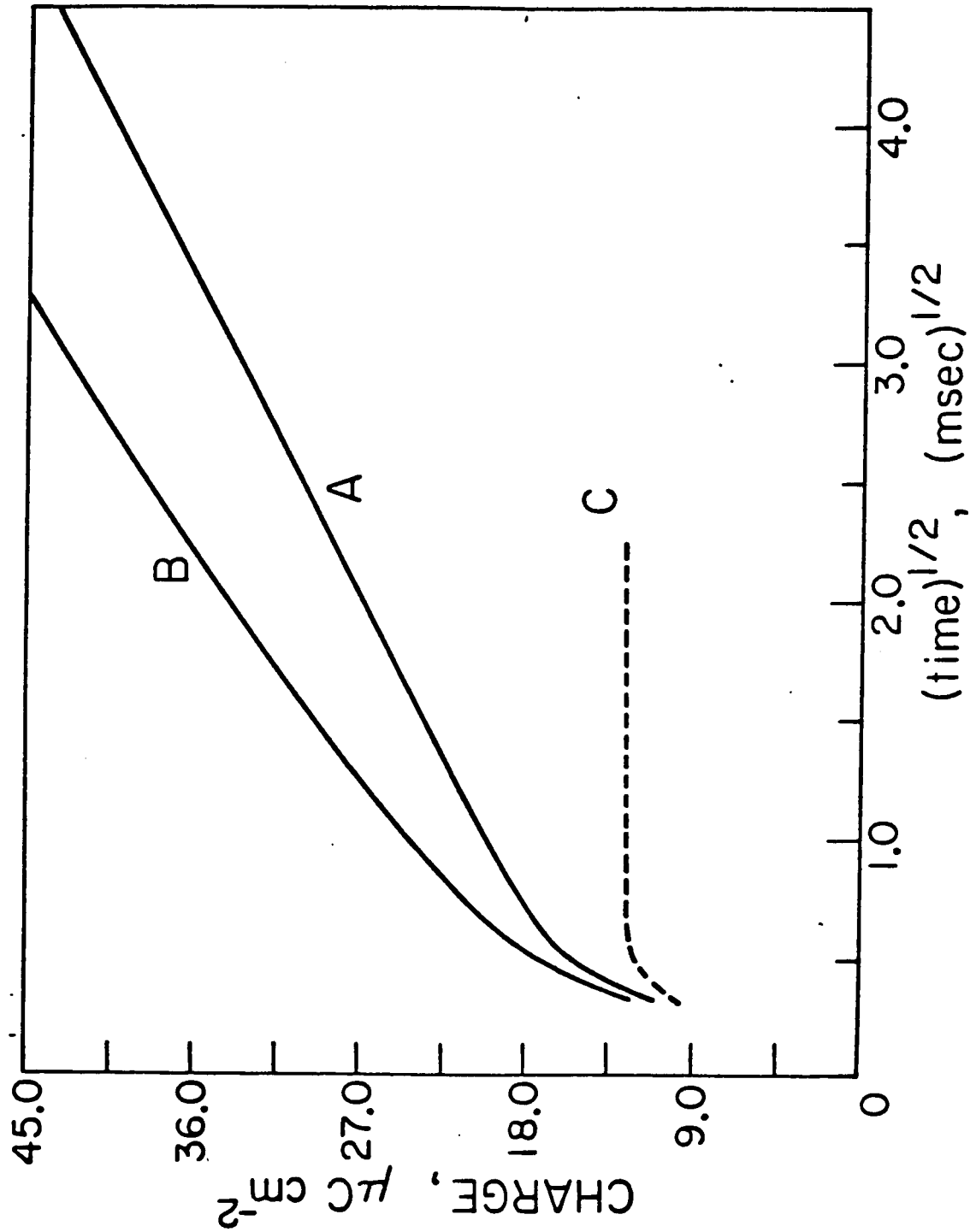
CHARGE, μC cm⁻²
45.0
36.0
27.0
18.0
9.0
0
1.0
2.0
3.0
4.0
(time)^1/2, (msec)^1/2
A
B
C

to unadsorbed $Co(bipy)_2^+$. The higher slope decreases toward the value expected for a one-electron reduction once the electrode surface is fully covered with the adsorbed product because continued reduction of $Co(bipy)_2^{2+}$ requires only one electron. Supporting this interpretation are the data in Table II which show that the ratio of the initial slopes of chronocoulometric plots for the reduction of $Co(bipy)_2^{2+}$ and $Co(bipy)_3^{2+}$ depends on the reactant concentration. The ratio approaches unity as the concentration increases because a smaller and smaller fraction of the $Co(bipy)_2^+$ generated at the electrode surface is adsorbed.

According to this interpretation, the species adsorbed is a complex of Co(0). The fact that the adsorption occurs on mercury but not on platinum or graphite electrodes indicates that the adsorption requires strong interaction with the mercury atoms on the electrode surface. A stabilizing interaction with the surface would also be required to overcome the intrinsic instability of $Co(bipy)_2^0$ demonstrated by Goshens et al..[24] Increasing the d electron density on the cobalt by reduction to cobalt(0) would be expected to favor the formation of a metal-metal bond with mercury. Similar surface coordination chemistry leading to adsorption on mercury was encountered in previous studies with low-valent complexes of cobalt[29] and rhodium.[30]

If two electrons are involved in the oxidation of the adsorbed cobalt complex, the molar quantities adsorbed are only half as great as might have been anticipated from the data of Table I. Nevertheless, the maximum quantities adsorbed represent more of the complex than could be accommodated in a close-packed monolayer with the bipyridine rings positioned parallel to the surface (ca. 1.5×10^{-10} moles cm^{-2} for

TABLE II

Ratio of Slopes of Charge-(Time)$^{\frac{1}{2}}$ Plots for the Reductions of $Co(bipy)_3^{2+}$ and $Co(bipy)_2^{2+}$ at Mercury Electrodes in Acetonitrile[a]

Concentration of complex, mM	Slope ratio[b]	$n\Gamma F/Q_{tot}$[c]
0.11	1.32	0.30
0.14	1.28	0.26
0.23	1.28	0.27
0.45	1.20	0.28
0.90	1.21	0.26
1.8	1.12	0.17
3.6	1.07	0.12

a. The potential was stepped from -0.4 to -1.2 volt for 100 msec. The slopes were obtained from a least-squares fit of the charge-time data. Supporting electrolyte as in Table I.

b. $\frac{\text{Slope for } Co(bipy)_2^{2+}}{\text{Slope for } Co(bipy)_3^{2+}}$

c. $n\Gamma F$ is the quantity of cobalt complex adsorbed at the end of 100 msec. It was estimated from the faradaic charge consumed in the first 0.2 msec after the potential was stepped from -1.2 volt back to -0.4 volt; Q_{tot} is the total faradaic charge passed during the recording of the charge-time transient.

a molecular diameter of 14 Å.[31] Adsorption with the bipyridine rings perpendicular to the electrode surface is conceivable, especially if the resulting "stack" of bipyridine ligands could interact cooperatively with one another because the very strong dependence of the adsorption on concentration (Table I) points to attractive rather than repulsive interactions between the adsorbing molecules.

The potential dependence of the adsorption was not clearly established because measurements were restricted to a narrow range of potentials by the proximity of the wave corresponding to the further reduction of $Co(bipy)_2^+$. A weak trend toward increased adsorption at more negative potentials appeared to be present. This might reflect the fact that the adsorption of $Co(bipy)_2^+$ is accompanied by its reduction; a step that proceeds only at more negative potentials in the absence of adsorption.

Addition of nitrous oxide or acrylonitrile to solutions of $Co(bipy)_2^{2+}$ greatly diminished the adsorption of subsequently generated $Co(bipy)_2^+$. Both of these molecules are likely to coordinate to the $Co(bipy)_2^+$ complex,[2] where they may block the position needed for the formation of the mercury-cobalt bond believed to be responsible for the adsorption.

The interpretation offered here for the pattern of adsorption exhibited by $Co(bipy)_2^+$ is supported by the adsorption behavior of the analogous cobalt complex of 6,6'-dimethyl-2,2'-bipyridine as discussed in the following section.

Adsorption of $Co(dmbp)_2^+$ on Mercury

Although the cyclic voltammograms for $Co(dmbp)_2^{2+}$ (Figure 5B) contain none of the hallmarks of adsorption evident in the voltammograms

of $Co(bipy)_2^{2+}$ (Figure 1B), chronocoulometric measurements revealed extensive adsorption of $Co(dmbp)_2^{+}$. The greater stability of $Co(dmbp)_2^{+}$ (compared with $Co(bipy)_2^{+}$) simplified the measurement of its adsorption on mercury. The complex was generated at the electrode surface in solutions of $Co(dmbp)_2^{2+}$ by adjusting the electrode potential to values between the $Co(dmbp)_2^{2+/+}$ and $Co(dmbp)_2^{+/0}$ waves for 45 seconds before stepping to -0.1 volt where the complex was reoxidized to $Co(dmbp)_2^{2+}$ at a diffusion controlled rate. The plots of anodic charge vs. $(time)^{\frac{1}{2}}$ had slopes that matched those for the corresponding steps for the reduction of $Co(dmbp)_2^{2+}$ showing that $Co(dmbp)_2^{+}$ was not disproportionating. (A diffusion coefficient of $1.4 * 10^{-5}$ cm^2/sec was calculated from the chronocoulometric slope.) In addition, the plots for the reduction of $Co(dmbp)_2^{2+}$ did not show the higher slopes exhibited in the analogous experiments with $Co(bipy)_2^{2+}$. This indicates that the reduction of $Co(dmbp)_2^{2+}$ to both adsorbed and unadsorbed $Co(dmbp)_2^{+}$ consumes only one electron and serves to support the previous interpretation of the higher slopes of the charge-$(time)^{\frac{1}{2}}$ plots for $Co(bipy)_2^{2+}$. The extent of adsorption of $Co(dmbp)_2^{+}$, determined from the intercepts of charge-$(time)^{\frac{1}{2}}$ plots for the step to -0.1 volt, is shown in Figure 9A as a function of the potential where the $Co(dmbp)_2^{+}$ was generated. The adsorption was measured over a sufficiently wide range of potentials to establish clearly that the adsorption increases at more negative potentials. Since no further reduction accompanies the adsorption of $Co(dmbp)_2^{+}$, the potential dependence must have a different origin than that suggested earlier for the case of $Co(bipy)_2^{+}$. The adsorbing species is cationic but the dependence seems too strong to be attributed

to simple electrostatic factors. Studies of metal-metal bonding in the adsorption of low-valent, transition-metal complexes are still too sparse to provide a basis for understanding the effect of electrode potential on the extent of adsorption. At the highest concentrations and most negative potentials, the adsorption reaches values almost as large as those obtained with $Co(bipy)_2^+$ and it clearly exceeds the value corresponding to a monolayer of complexes lying flatly on the electrode.

The adsorption of $Co(dmbp)_2$ was also measured chronocoulometrically by generating this complex at the electrode surface in solutions of $Co(dmbp)_2^{2+}$. The results, displayed in Figure 9B, show an even stronger potential dependence of the adsorption that passes through a rather sharp maximum. The decrease in adsorption at the most negative potentials could arise from preferential adsorption of the supporting electrolyte cations (although no adsorption of the tetraalkylammonium ions on mercury was indicated in the work by Fawcett[32]) but the factors underlying the large increase in adsorption at potentials positive of the maximum are not evident.

Figure 9. Potential dependence of the adsorption of (A) $Co(dmbp)_2^+$ and (B) $Co(dmbp)_2$ at mercury electrodes. The electrode was held for 45 sec. at the indicated potential in a solution of $Co(dmbp)_2^{2+}$ and then stepped to -0.1 volt for 100 msec. Concentration of $Co(dmbp)_2^{2+}$, mM: ● - 0.11; ○ - 0.23; ■ - 0.45; □ -0.90.
Supporting electrolyte: 0.1 M tetrabutylammonium trifluoromethanesulfonate.

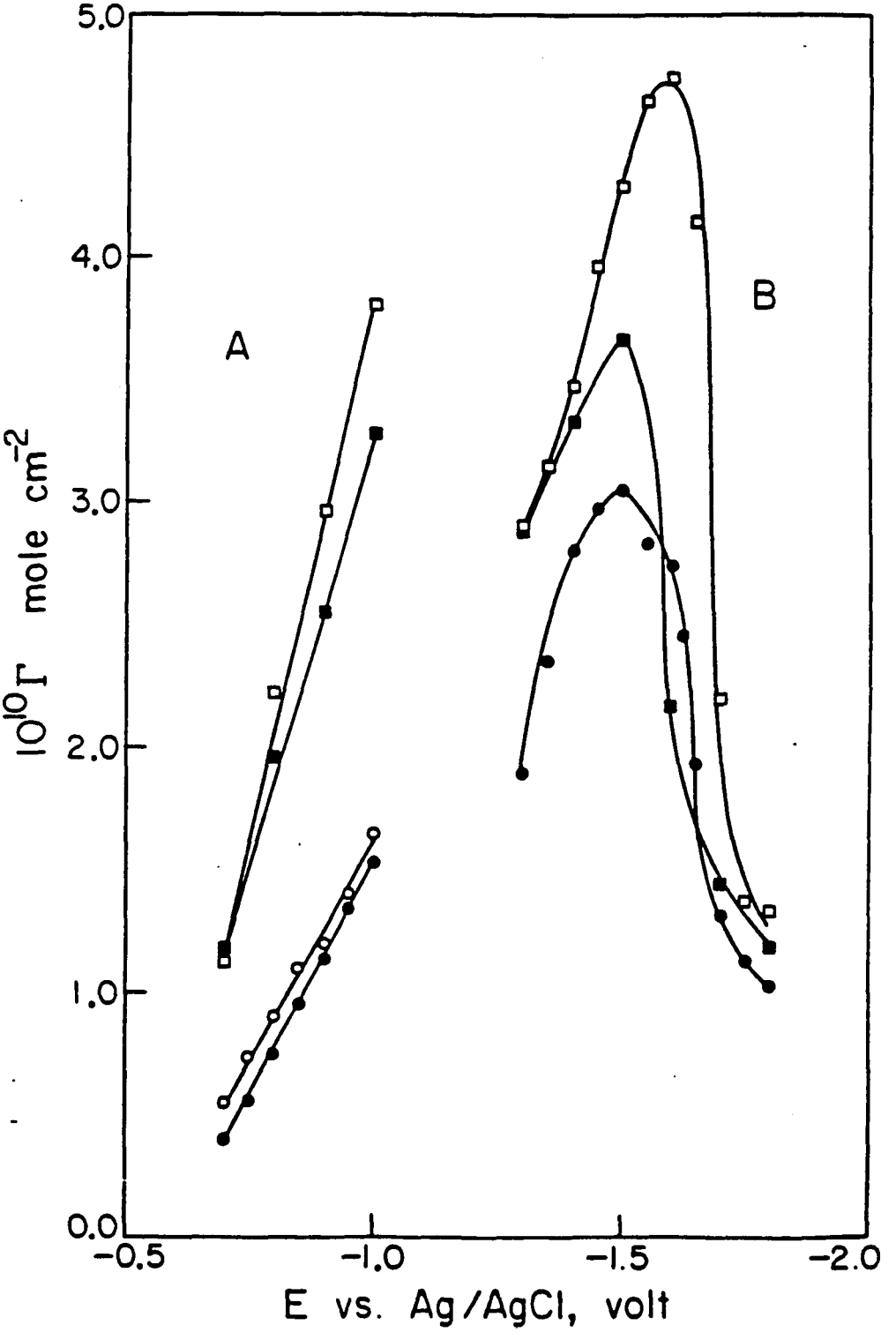
5.0
4.0
3.0
2.0
1.0
0.0
A
B
$10^{10}\Gamma$ mole cm^{-2}
−0.5
−1.0
−1.5
−2.0
E vs. Ag/AgCl, volt

CONCLUSIONS

This study has pointed to the intrinsic reactivity of $Co(bipy)_2^+$ that originates in its coordinative unsaturation and is expressed by its search for an additional ligand (Scheme 1) and by its strong interactions with the surface of mercury electrodes. Although highly reactive toward coordination reactions the bis-bipyridine cobalt(I) species was not sufficiently reactive as a reductant to be exploited as a catalyst for the reduction of N_2O or alkyl halide reduction. Only allyl chloride proved suitable as a substrate. The related complex, $Co(dmbp)_2^+$, is much more stable than $Co(bipy)_2^+$, is also strongly adsorbed on mercury and is even less reactive toward reducible substrates. Adsorption of both complexes is proposed to depend upon the formation of cobalt-mercury bonds and in the case of $Co(bipy)_2^+$, further reduction is believed to accompany adsorption so that the species adsorbed is a complex of Co(0).

REFERENCES AND NOTES

1. S. Margel, W. Smith and F. C. Anson, J. Electrochem. Soc., 125, 241 (1978).
2. S. Margel and F. C. Anson, J. Electrochem. Soc., 125, 1232 (1978).
3. N. Tanaka and Y. Sato, Bull. Chem. Soc. Japan, 41, 2059 (1968).
4. G. Waind and B. Martin, J. Chem. Soc., 551 (1958).
5. A. A. Vlek and A. Rusina, Proc. Chem. Soc., 161 (1961).
6. B. Martin and G. Waind, J. Chem. Soc., 169 (1958).
7. A. A. Vlek, Nature, 180, 753 (1957).
8. R. Prasad and D. B. Scaife, J. Electroanal. Chem., 84, 373 (1977).
9. B. Martin, W. R. McWinnie and G. M. Waind, J. Inorg. Nucl. Chem., 23, 207 (1961).
10. Y. Kaizu, Y. Torii and H. Kobayashi, Bull. Chem. Soc. Japan, 43, 3296 (1970).
11. R. Banks, R. Henderson and J. Pratt, Chem. Commun., 387 (1967).
12. G. Mestroni, A. Camus and E. Mestroni, J. Organometal. Chem., 24, 775 (1970).
13. S. Musumeci, E. Rizzarelli, S. Sammartano and R. P. Bonomo, J. Electroanal. Chem., 46, 109 (1973).
14. B. C. Willett and F. C. Anson, J. Electrochem. Soc., 129, 1260 (1982).
15. A. Brandstrom, Acta Chem. Scand., 3585 (1969).

REFERENCES AND NOTES

16. F. H. Burstall and N. S. Nyholm, J. Chem. Soc., 3570 (1952).

17. T. Kauffman, J. Konig and A. Woltermann, Chem. Ber., 109, 3864 (1976).

18. D. H. Huchital and A. E. Martell, Inorg. Chem., 13, 2966 (1974).

19. (a) G. Lauer, R. Abel and F. C. Anson, Anal. Chem., 39, 765 (1967); (b) J. A. Turner, Ph.D. Thesis, Colorado State University, 1977.

20. W. M. Moore and D. G. Peters, J. Am. Chem. Soc., 97, 139 (1975).

21. W. J. Albery and M. L. Hitchman, "Ring Disc Electrodes", Clarendon Press, Oxford, 1971.

22. W. J. Albery and S. Bruckenstein, Trans. Faraday Soc., 62, 1920 (1966).

23. J. H. Christie, R. A. Osteryoung and F. C. Anson, J. Electroanal. Chem., 13, 236 (1967).

24. T. G. Groshens, B. Henne, D. Bartak and K. J. Klabunde, Inorg. Chem., 20, 3629 (1981).

25. Z. Zagorski and J. Suwalski, J. Electroanal. Chem., 46, 353 (1973).

26. Addition of tetramethylammonium hydroxide to acetonitrile solutions of $Co(bipy)_3^{2+}$ or $Co(bipy)_2^{2+}$ causes the yellow color to fade. The only cyclic voltammetric response in the resulting solutions appears at potentials where mercury is oxidized in the presence of free bipyridine.

27. J. P. Collman, M. Marrocio, C. M. Elliot and M. L'Her, J. Electroanal. Chem., 124, 113 (1981).

REFERENCES AND NOTES

28. Addition of excess pyridine to a solution of the bis-6,6'-dimethyl-2,2'-bipyridine cobalt(II) showed some coordination of the pyridine to the inner-sphere of this complex (as evidenced by formation of a new wave) but upon reduction to the Co(I), the pyridine was expelled.

29. H. S. Lim and F. C. Anson, J. Electroanal. Chem., 31, 297 (1971).

30. J. Gulens, D. Konrad and F. C. Anson, J. Electrochem. Soc., 121, 1421 (1974).

31. (a) T. Saji and S. Aoyagui, Bull. Chem. Soc. Japan, 46, 2101 (1973); (b) R. C. Young, F. R. Keene and T. J. Meyer, J. Am. Chem. Soc., 99, 2468 (1977).

32. W. R. Fawcett and R. O. Loutfy, Can. J. Chem., 51, 230 (1973).

Part II

Electrode Kinetics for Electron Transfer to Cyclooctatetraene and cis-$[(C_5H_5)Fe(CO)P(C_6H_5)_2]_2$

INTRODUCTION

Determination of heterogeneous electron transfer rates to molecules which undergo large intramolecular rearrangements upon oxidation or reduction are of great current interest[1-7] because researchers are looking for experimental verification of electron transfer theories, such as the one proposed by Marcus,[8-10] which attempts to account for the physical factors which influence the rate.[1,2,11-14] Several of the major factors proposed to affect the rates of electron transfer include intramolecular rearrangements, solvent reorganization and the work terms associated with bringing the reactants and products together from the bulk.[8-10] A number of organic molecules have been studied in this context because of their large intramolecular rearrangements upon electron transfer. Examples include cyclooctatetraene,[6,15-17] its derivatives[16,17] and hindered stilbenes.[4] In addition, inorganic complexes such as $Co(NH_3)_6^{3+/2+}$, $Ru(NH_3)_6^{3+/2+}$ and several metal aquo species[2,3,18,19] have been investigated to determine the extent of the influence of intramolecular changes on the experimentally measured rates of electron transfer, both in solution and at electrodes.

The rate of electro-reduction of cyclooctatetraene has received much attention[6,15-17,20-22] because of the large intramolecular rearrangements that accompany reduction of the preferred, tub-shaped conformation of the neutral molecule[23-25] to the basically planar radical anion.[26-28] The reduction of cyclooctatetraene to its radical anion is governed by a small electron transfer rate, k_s, while

relatively fast electrode kinetics are observed for further reduction of the radical anion to the dianion. The latter process requires very little internal structural changes since the dianion is also flat.[26-30] These early studies were conducted in non-aqueous solvents containing tetra-n-butylammonium salts[6,16,17] (or tetrapropylammonium perchlorate[15]) as supporting electrolytes. Recent work has shown, both qualitatively[20,22] and quantitatively,[31] that the rate of electron transfer to such molecules is drastically affected by the size of the tetraalkylammonium cation used as supporting electrolytes: The smaller the cation size, the larger the rate constants.

In the present study, the first, one-electron reduction of cyclooctatetraene was reinvestigated in non-aqueous solvents containing tetraalkylammonium perchlorates of various sizes. The effect of the supporting electrolyte cation was found to dominate the factors that influence the heterogeneous rate constant, with the k_s for the first electron transfer becoming as large as that for the second electron transfer when tetramethylammonium perchlorate is the supporting electrolyte, despite the extent of the intramolecular rearrangements involved in the reduction.

In the past few years, several papers[32,33] have been published in which EXAFS (Extended X-Ray Absorption Fine Structure) Spectroscopy was used to obtain structural data for a series of dinuclear metal complexes and their ions in both the solid state and in solution. For many of these compounds, oxidation or reduction entails the making or breaking of a metal-metal bond which causes these molecules to enlarge or contract. Sometimes the distance

between the two metal centers changes by as much as 0.5 Å. One such system for which the EXAFS data exist for the neutral, mono- and dicationic species and for which fairly large internal rearrangements occur upon oxidation is $[(C_5H_5)Fe(CO)P(C_6H_5)_2]_2$. The reduction of this complex causes the distance between the two iron atoms to decrease from 3.498 Å in the neutral molecule to 3.14 Å in the monocation to 2.764 Å in the dication as an iron-iron bond is formed. At the same time other structural changes also occur.[34] This compound has been subjected to only a cursory examination electrochemically,[35] so it was decided to investigate its electrochemical behavior more extensively in acetonitrile with tetraalkylammonium salts as supporting electrolytes, the results of which are reported here.

EXPERIMENTAL

Materials. (Burdick-Jackson) "UV-quality" acetonitrile and dimethylformamide were used as received except in those situations where very dry solvent was needed, in which case the solvent/supporting electrolyte solution was first dried with Linde sieves (3 Å for acetonitrile, 4 Å for dimethylformamide) and then by several grams of activated alumina (Woelm neutral alumina heated at 300° C under vacuum overnight) per 25 ml. "Polarographic grade" tetraethylammonium perchlorate, tetra-n-butylammonium perchlorate (Southwestern Analytical Co.) and tetramethylammonium perchlorate (G. F. Smith) were vacuum dried and used as supporting electrolytes without further purification. Tetra-n-butylammonium trifluoromethane sulfonate was prepared as described by Brandstrom.[36] Cyclooctatetraene (Aldrich) was distilled under vacuum prior to use and kept under argon at 0°C. Ferrocene (ROC/RIC) and bis(pentamethylcyclopentadienyl) iron (Strem) were used as received, as was diphenylanthracene (Aldrich). cis-$[(C_5H_5)Fe(CO)P(C_6H_5)_2]_2$ was prepared according to the method of Hayter[37] and purified by column chromatography using neutral alumina and eluting with heptane containing increasing amounts of benzene. Fraction #5 (eluted with 60% benzene and 40% heptane) was collected and upon evaporation yielded fine, dark brown crystals of the desired product. Elemental analysis of cis-$[C_5H_5)Fe(CO)P(C_6H_5)_2]_2$: C, 63.4% and H, 4.5%. Calculated: C, 64.7% and H, 4.5%. Assignment of this fraction to the cis-isomer was based upon earlier work[37] that showed the trans-isomer eluting prior to the cis conformer (Fraction #3 in this study gave essentially

the identical electrochemistry as Fraction #5 but was not studied because it was only produced in small quantities) and because of its melting point above 285°C (the reported mp[37] for the cis-isomer is 302°C while for the trans it is 215°C).

Apparatus. Cyclic voltammograms at scan rates less than 1 V/sec were obtained with a Princeton Applied Research Model 173 potentiostat driven by a PAR Model 175 universal programmer and recorded on a Houston Model 2000 recorder. For scan rates greater than 1 V/sec, the PAR Model 175 was used to drive a home-built potentiostat[38] equipped with direct iR feedback capabilities (the iR feedback was set for each scan rate to a point just prior to oscillation of the system) and the resulting current-potential curve recorded on a Textronik Model 5000 Digital Scope and then transferred to a Houston recorder. Chronocoulometric measurements were accomplished by means of a computer-based apparatus.[39]

AC Impedance measurements were performed with a home-built potentiostat (used in the three-electrode configuration) in conjunction with the Ithaco Model 391A Lock-In Amplifier and a Fluke voltmeter. Working electrodes were a static mercury drop electrode (PAR Model 303) whose bevelled capillary had been modified[40] to reduce the internal resistance to ca. 1 Ω or a planar platinum wire sealed in glass (area = 0.009 cm^2), surrounded by a large platinum gauze electrode as the auxiliary electrode and with a silver wire as the pseudo-reference electrode. All electrodes were in the same solution to prevent phase shifts and no iR compensation was used. This system was tested with a mock cell consisting of precision resistors and

capacitors with values similar to those measured in real experiments at frequencies of 100 to 6000 Hz. First the in- and out-of-phase AC currents with a 5.00 mV AC signal applied to a circuit corresponding to a background solution (shown below) were measured. The best

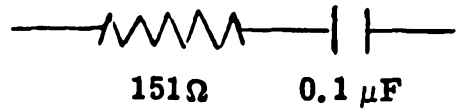

results (i.e., the measured resistance and capacitance matched the known values within 1%) were obtained at frequencies greater than 3000 Hz. Then a mock cell chosen to mimic the presence of slow electron transfer (drawn below) was examined. Analytical subtraction[41]

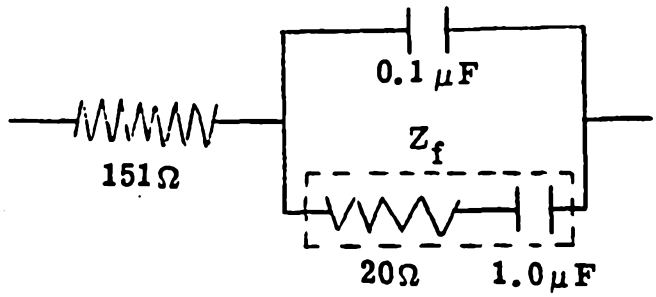

of the results obtained with the circuit corresponding to a background solution from those of the mock cell show that the precision of determining Z_f (the faradaic impedance due to electrode kinetics) by this method was better than 5%. For real chemical systems, best results were obtained with the potentiostat used in a 3-electrode configuration and with no iR compensation applied at frequencies between 150 to 800 Hz.

Controlled potential electrolyses were conducted with the PAR Model 173 potentiostat equipped with a PAR Model 179 Digital Coulometer. The electrolysis cell employed was modeled after the design of Moore and Peters.[42] Solutions were deoxygenated with argon but when more complete exclusion of oxygen was desired, the experiments were connected inside a controlled-atmosphere box (Vacuum Atmosphere Co.). UV-Visible spectra were recorded with a Hewlett Packard Model 8450A Spectrometer. Potentials were measured and are reported with respect to an aqueous Ag/AgCl reference electrode except in those cases where a silver wire pseudo reference electrode was used to reduce phase shifts. The Ag/AgCl electrode has a potential ca. 45 mV more negative than a saturated calomel electrode. Experiments were conducted at ambient temperature, 22° ± 2°C.

RESULTS AND DISCUSSION

Electron Transfer Rates to cis-$[(C_5H_5)Fe(CO)P(C_6H_5)_2]_2$

Cyclic voltammograms for 1 mM solutions of cis-$[(C_5H_5)Fe(CO)P(C_6H_5)_2]_2$ (I) in acetonitrile show two reversible, one-electron steps similar to those described by Dessy.[35] These waves, at -0.045 V and +0.29 V, (Figure 1) correspond to oxidation of the neutral parent molecule (Fe---Fe separation = 3.498 Å) to the radical cation (Fe---Fe separation = 3.14 Å) to the dication (Fe---Fe separation = 2.764 Å). The large changes in the Fe-Fe separation is due to formation of a metal-metal bond between the iron centers.[34] These oxidations were examined by cyclic voltammetry on both mercury and platinum electrodes. Chronocoulometry and voltammetry at high scan rates showed that there is some adsorption of the radical cation of I on mercury so that rate measurements were performed mainly on platinum electrodes. Some kinetic data were obtained on mercury by chronocoulometry only when starting with a solution of the neutral parent molecule.

Long term stability of the radical cation and dication in acetonitrile was determined by bulk electrolyses conducted in a controlled-atmosphere box. Oxidation of cis-$[(C_5H_5)Fe(CO)P(C_6H_5)_2]_2$ ($\epsilon_{442} \sim 3200\ M^{-1}\,cm^{-1}$) at +0.1 V until the current decayed to zero involved the loss of one electron per molecule and produced a blue ($\epsilon_{585} \sim 4500\ M^{-1}\,cm^{-1}$ and $\epsilon_{468} \sim 1600\ M^{-1}\,cm^{-1}$) solution of the radical cation which was stable for weeks. Further oxidation at +0.5 V yielded the dication (ca. 1.1 electrons per molecule were transferred)

Figure 1. Cyclic voltammogram of 1.0 mM cis-$[(C_5H_5)Fe(CO)P(C_6H_5)_2]_2$ in acetonitrile containing 0.1 M tetraethylammonium perchlorate at a scan rate of 100 mV/sec.

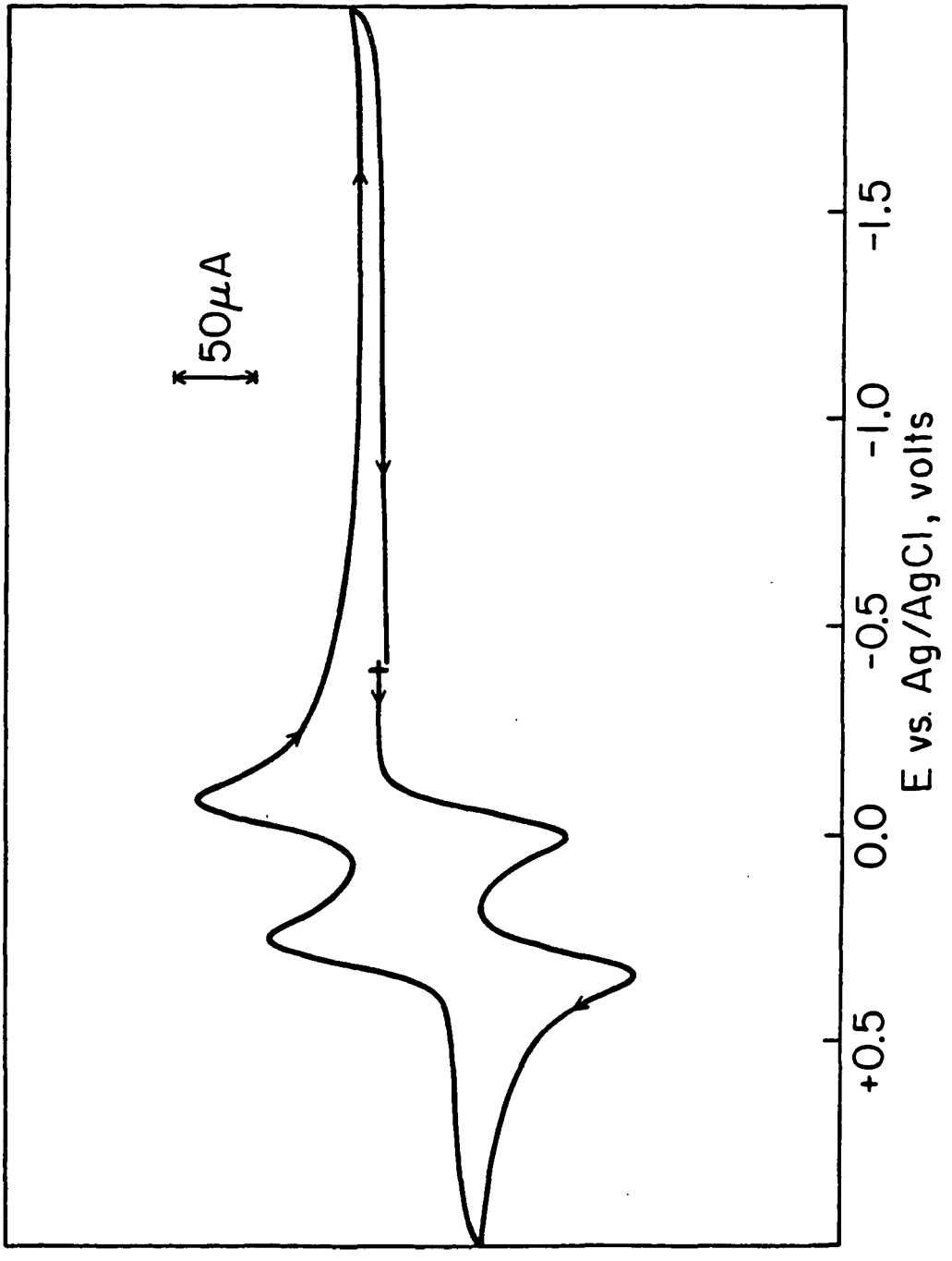
50μA
+0.5
0.0
-0.5
-1.0
-1.5
E vs. Ag/AgCl, volts

which was bright yellow ($\epsilon_{420} \sim 8000\ M^{-1}cm^{-1}$), not blue as reported by Dessy.[35] Decomposition of the dication discouraged attempts to measure the rate constant for the oxidation of the radical cation to the dication.

Heterogeneous electron transfer rate constants for the one-electron oxidation of $\hat{I}$, ferrocene and bis(pentamethylcyclopentadienyl) iron are reported in Table I. Ferrocene and the pentamethyl-ferrocene derivative were used as reference complexes because they undergo almost no inner-sphere reorganization upon oxidation.[43,44] Their half-wave potentials (+0.40 V for ferrocene and -0.11 V for bis(pentamethylcyclopentadienyl)iron) are also similar to that for $\hat{I}$ and their heterogeneous electron transfer rates have been measured previously.[45-47]

Rates of electron transfer were measured by cyclic voltammetry using the potential separation between the anodic and cathodic peak currents to calculate the rate constant according to the method of Nicholson and Shain[48] (see Appendix II). Measurements were made at scan rates from 100 mV/sec to 100 V/sec. Compensation of the ohmic potential drop was adjusted at each scan rate to reduce or eliminate this effect on the peak splitting. Calculations based on the peak current obtained at a scan rate of 100 V/sec and the solution resistance measured in separate AC impedance experiments showed that the contribution of the ohmic drop to the peak splitting without any added compensation would have amounted to about 20 mV at this scan rate (an error in the measured k_s of less than a factor of two for this case). Values of the measured rate constants for each complex in this study were essentially scan rate independent. The similarity of the k_s

TABLE I[a]

Rate Data for cis-$[(C_5H_5)Fe(CO)P(C_6H_5)_2]_2$, Ferrocene and Bis(pentamethylcyclopentadienyl) iron.

Compound	Solution[b]	Method[c]	k_g(cm/sec)	$D^{\frac{1}{2}}$[d] (cm/sec$^{\frac{1}{2}}$)
cis-$[(C_5H_5)Fe(CO)P(C_6H_5)_2]_2^{0/+}$	0.2 M TEAP in CH_3CN on Hg	Chrono	0.068	$3.2*10^{-3}$
"	0.3 M TEAP in CH_3CN on Pt	Cyclic	0.21	---
"	0.1 M TBAP in CH_3CN on Hg	Chrono[e]	0.054	$3.1*10^{-3}$
"	0.1 M TBAP in CH_3CN on Pt	Chrono[e]	0.14	$3.1*10^{-3}$
"	0.2 M TBAP in CH_3CN on Pt	Cyclic	0.29	$3.1*10^{-3}$
cis-$[(C_5H_5)Fe(CO)P(C_6H_5)_2]_2^{+/0}$[f]	0.2 M TBAP in CH_3CN on Pt	Cyclic	0.30	$3.1*10^{-3}$
$(C_5H_5)_2Fe^{0/+}$	0.2 M TEAP in CH_3CN on Hg	Chrono	0.31	$6.0*10^{-3}$
"	0.2 M TBA-TFMS in CH_3CN on Hg	Chrono	0.35	$5.7*10^{-3}$
"	0.2 M TEAP in CH_3CN on Pt	Cyclic	0.26	---
$(C_5(CH_3)_5)_2Fe^{0/+}$	0.2 M TEAP in CH_3CN on Pt	Cyclic	0.40	---

TABLE I (continued)

a. All solutions were 0.3 to 1.0 mM in substrate.

b. TEAP = tetraethylammonium perchlorate; TBAP = tetra-n-butylammonium perchlorate; TBA-TFMS = tetra-n-butylammonium trifluoromethane sulfonate.

c. Chrono = Chronocoulometry; Cyclic = Cyclic Voltammetry.

d. Diffusion coefficients were calculated from the chronocoulometric slopes[50] when stepping onto the diffusion-limited plateau or from the peak current in cyclics.

e. No iR compensation was used.

f. Formation of cis-$[(C_5H_5)Fe(CO)P(C_6H_5)_2]_2^+$ was accomplished by bulk electrolysis at +0.1 V of the neutral parent.

values for ferrocene found in the present work with that of previous workers[46,47] would tend to support the reliability of the cyclic voltammetric technique as applied here.

Application of chronocoulometry to the measurement of heterogeneous electron transfer rates in this study was accomplished according to a procedure outlined by Christie et al.[49] (see Appendix II). Substrate concentrations were limited to 1 mM or less because of solubility and adsorption problems. Electronic feedback was employed to reduce the uncompensated resistance. The electrode was stepped from potentials where no faradaic reaction occurs to potentials within ± 20 mV of the half-wave potential for the complex under study. Sufficiently long data acquisition times were used to insure that a plot of charge versus $(\text{time})^{\frac{1}{2}}$ became linear for at least 50% of the total time. Then extrapolation of the linear portion to time = 0 and subtraction of the double layer charge measured in a background solution[49] allowed calculation of the intercept on the $(\text{time})^{\frac{1}{2}}$ axis. The rate constant was determined from the maximum value of the intercept on the $(\text{time})^{\frac{1}{2}}$ axis, which occurs at the half-wave potential for the substrate when the transfer coefficient is 0.5, and a diffusion coefficient measured from a potential step to the diffusion-limited plateau of the wave.[49]

The rate constants listed in Table I for cis-$[(C_5H_5)Fe(CO)P(C_6H_5)_2]_2$, ferrocene and pentamethyl-ferrocene are quite similar despite the fact that large intramolecular changes accompany the oxidation of $\hat{I}$ but not for the other two reactants. The rate constants are not corrected for double layer effects[51] but the corrections would be similar for all three

molecules because their half-wave potentials are not very different. The possibility that the oxidation of $\underset{\sim}{I}$ proceeds through a high energy intermediate which has only minimal intramolecular rearrangements before it relaxes into the conformation observed in the solid state was checked by starting an experiment with an electrogenerated solution of the radical cation and measuring the k_s for reduction back to the neutral parent. The rate constant was found to be independent of which half of the redox couple was studied. However, it should be pointed out that this experiment does not exclude the possibility that there may be molecular-distance differences between the molecules in the solid state and in solution, although this is considered unlikely.

Thus, it appears that the heterogeneous rate constant for $\underset{\sim}{I}$ is quite large in spite of the large changes in the Fe-Fe distance and the other rearrangements[34] which accompany electron transfer. This is contrary to what might have been expected (a priori) on the basis of Marcus' theory.[8-10] However, due to the complexity of the overall rearrangements and the lack of physical data, it was not possible to calculate how large the inner-sphere energy should be; thus only qualitative arguments are possible. The similarity in rate constants for $\underset{\sim}{I}$, ferrocene and pentamethyl-ferrocene (the latter two undergo only very little intramolecular changes upon oxidation[43,44]) seems to indicate that the electron transfer rate for all three reactants is basically controlled by the outer-sphere solvent reorganization energy. The lack of an effect from the large Fe-Fe distance changes on the rate of oxidation of $\underset{\sim}{I}$ may be due to compensatory changes in other parts of the molecule or these intramolecular changes represent only a small fraction of the total

energy for activation for electron transfer to $\underset{\wedge}{I}$ because of the bond energies involved.

Several other trends in Table I deserve comment: The oxidation of $\underset{\wedge}{I}$ is slower on mercury than on platinum electrodes; changes in the nature of the supporting electrolyte (i.e., the sizes of the anion or cation) produced only small changes in the rates; the rate constant for the pentamethyl-ferrocene derivative is larger than that for ferrocene which is consistent with the relative homogeneous self-exchange rate constants for these compounds.[52] The effect of the electrode material on the rate of electron transfer to $\underset{\wedge}{I}$ could reflect a real difference between the energy of activation for electron transfer on the two electrodes (although none is predicted by Marcus theory[8-10] for simple outer-sphere reactions). However, it could also be the result of adsorption of the radical cation of $\underset{\wedge}{I}$ on mercury since there is no difference in the rate constant for ferrocene on the same two electrodes. The insensitivity of the rate constants to the size of the cation or anion of the supporting electrolyte is notable because several examples of systems showing contrary behavior have been reported.[20,22,31] One of these is discussed in the next section.

Electron Transfer Rates to Cyclooctatetraene

An organic compound whose rate of reduction has been widely studied and found to be rather low is cyclooctatetraene (COT). The low value of k_s for the first electron transfer to this molecule has been attributed to large intramolecular rearrangements.[6,15-17] Upon reduction by one electron, COT rearranges from tub-shaped[23-25] to a

planar (or nearly planar) radical anion.[26-28] The radical anion can be further reduced to a planar dianion.[26-30] In most of the previous studies,[6,16] tetra-n-butylammonium perchlorate was used as the supporting electrolyte and the rate constant for the first reduction step is reported as 0.002 cm/sec while that for the second is 0.15 cm/sec. A somewhat higher rate constant for the first step (k_s = 0.008 cm/sec) was reported when tetra-n-propylammonium perchlorate was the supporting electrolyte.[15] Recently Evans et al.[31] have shown that the nature of the supporting electrolyte cation can produce very large effects on heterogeneous electron transfer rate constants. For example, the rate of reduction of t-nitrobutane in acetonitrile increased by over a factor of 10^2 when the supporting electrolyte cation was changed from tetra-n-pentylammonium to hexadecyltrimethylammonium.[31] Qualitatively similar results for the reduction of COT in dimethylformamide have been reported by Fry et al.[20] and by Parker et al.[22]

To extend these studies on the rate of reduction of COT as a function of the size of the supporting electrolyte cation, AC impedance measurements[53] were performed on solutions of COT in acetonitrile or dimethylformamide. Supporting electrolytes tested were tetra-n-butylammonium, tetraethylammonium and tetramethylammonium perchlorates. The resulting rate constants along with those for diphenylanthracene and perylene, which were employed as model compounds, are listed in Table II. The values of k_s were calculated from the intercepts (R_{CT}) of plots of the in-phase impendance (R_s) versus (2π frequency)$^{-\frac{1}{2}}$ [41,53] (see Appendix II). Data were obtained from measurements of the in-phase and out-of-phase AC currents at the DC potential of maximum

in-phase current for each substrate at each frequency with a 5.00 mV AC potential applied. Corrections for the solution resistance and double layer capacitance were applied by analytical subtraction[41] of values of these parameters obtained in a background solution at the same potential as that used when the substrate was present. Examples of such plots for COT and the model complexes are presented in Figures 2-6. In evaluating the values of k_s it was assumed that the transfer coefficient, α, was 0.5 and that the diffusion coefficients for the oxidized and reduced species were equal. No attempt was made to correct for double layer effects[51] because the necessary data do not yet exist.

The values for the rate constants measured in this study for the first reduction of COT, of diphenylanthracene and of perylene in acetonitrile solutions are very similar to those found earlier (Table II). As anticipated from the investigations of Fry et al.[20] and Evans et al.,[31] the rate constant for COT in tetramethylammonium/dimethylformamide solutions is approximately 50 times larger than the rate measured with tetra-n-butylammonium perchlorate as the supporting electrolyte. In fact, the rate constant in the former electrolyte is within a factor of two of that for the reduction of $COT^{\cdot-}$.[6,55] The larger rates in supporting electrolytes containing the smaller cations has been ascribed in part to a difference in the location of the Outer Helmholtz Plane[31] or possibly to discreteness-of-charge effects.[56] However, the observed variation in rates is too large to be totally accounted for by these factors.[31] Another possible source of the effect is ion pairing between the tetraalkylammonium cation and the radical anion of COT, although

TABLE II

Rate Data for Cyclooctatetraene, Diphenylanthracene and Perylene

Compound[a]	Solution[b]	k_s(cm/sec)	$D^{\frac{1}{2}}$[c] (cm/sec$^{\frac{1}{2}}$)
Diphenylanthracene$^{0/-}$	0.3 M TBAP in CH_3CN	1.7	$3.5*10^{-3}$
"	0.1 M TEAP in CH_3CN	1.0[e]	---
Perylene$^{0/-}$	0.3 M TEAP in CH_3CN	7.1	$4.4*10^{-3}$
"	0.5 M TBAP in DMF	5[f]	---
COT$^{0/-}$	0.3 M TBAP in CH_3CN	0.004	$3.2*10^{-3}$
"	0.1 M TBAP in DMF	0.002[g]	---
"	0.3 M TEAP in CH_3CN	0.019	$3.2*10^{-3}$
"	0.15 M TMAP in DMF[d]	0.24	$3.2*10^{-3}$

a. All solutions were 0.5 to 1.0 mM in substrate.

b. All measurements were on mercury electrodes. TBAP = tetra-n-butylammonium perchlorate; TEAP = tetraethylammonium perchlorate; TMAP = tetramethylammonium perchlorate.

c. Diffusion coefficients were evaluated from the slopes of chronocoulometric plots[50] except for COT for which a previous measured value was employed.[6,16,21]

d. Dimethylformamide was used because of the insolubility of TMAP in acetonitrile.

e. From reference 54.

f. From reference 14.

g. From reference 6.

Figure 2. Impedance vs. $(2\pi \text{ frequency})^{-\frac{1}{2}}$ plots for 0.47 mM perylene in acetonitrile containing 0.35 M tetramethylammonium perchlorate on mercury. ● In-phase impedance (R_S); ■ Out-of-phase impedance ($\frac{1}{2\pi \text{ frequency } C_S}$).

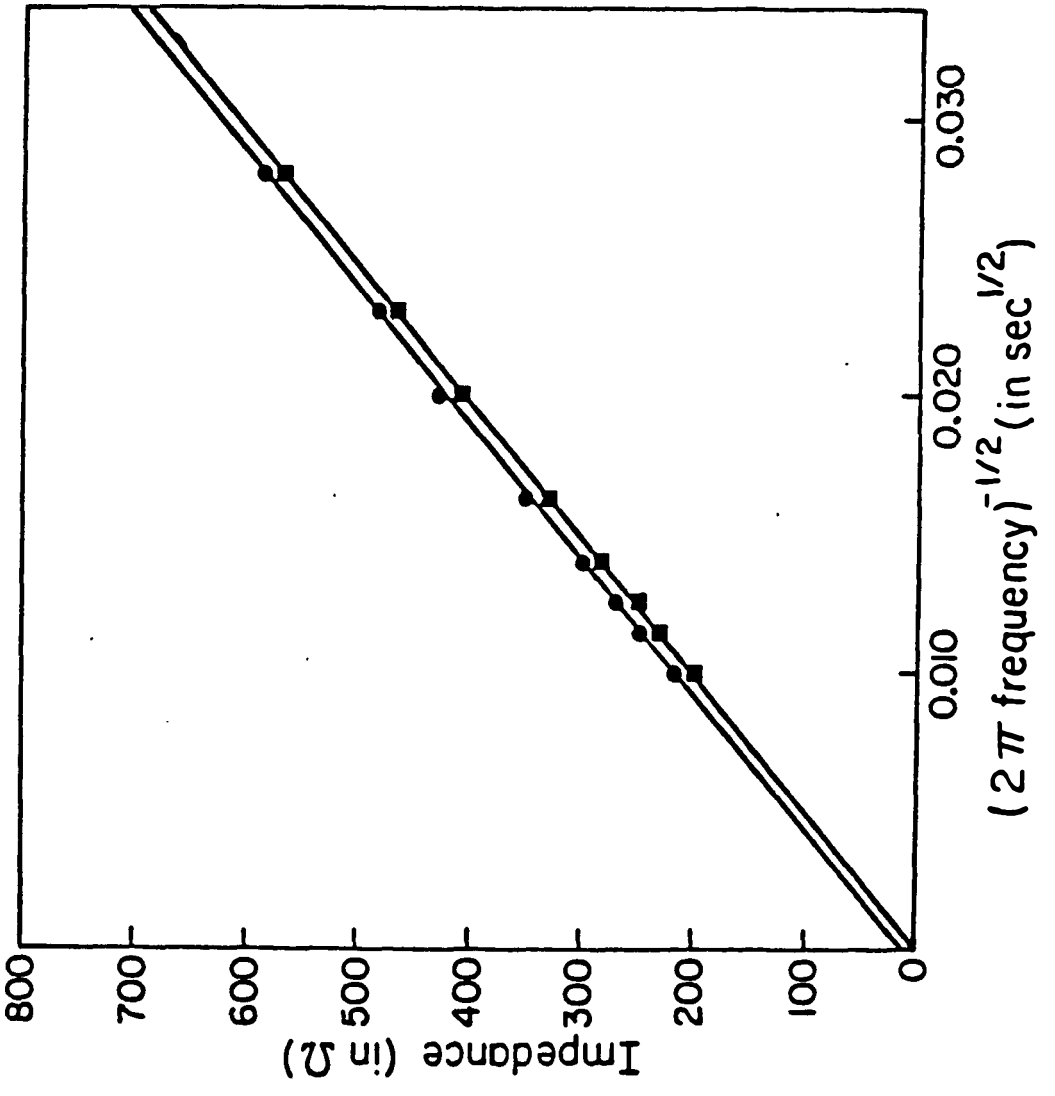
Impedance (in Ω)
800
700
600
500
400
300
200
100
0
0.010
0.020
0.030
(2π frequency)$^{-1/2}$ (in sec$^{1/2}$)

Figure 3. Impedance vs. $(2\pi \text{ frequency})^{-\frac{1}{2}}$ plots for 0.6 mM diphenylanthracene in acetonitrile containing 0.3 M tetra-n-butylammonium perchlorate on mercury. ● In-phase impedance (R_s); ■ Out-of-phase impedance ($\frac{1}{2\pi \text{ frequency } C_s}$).

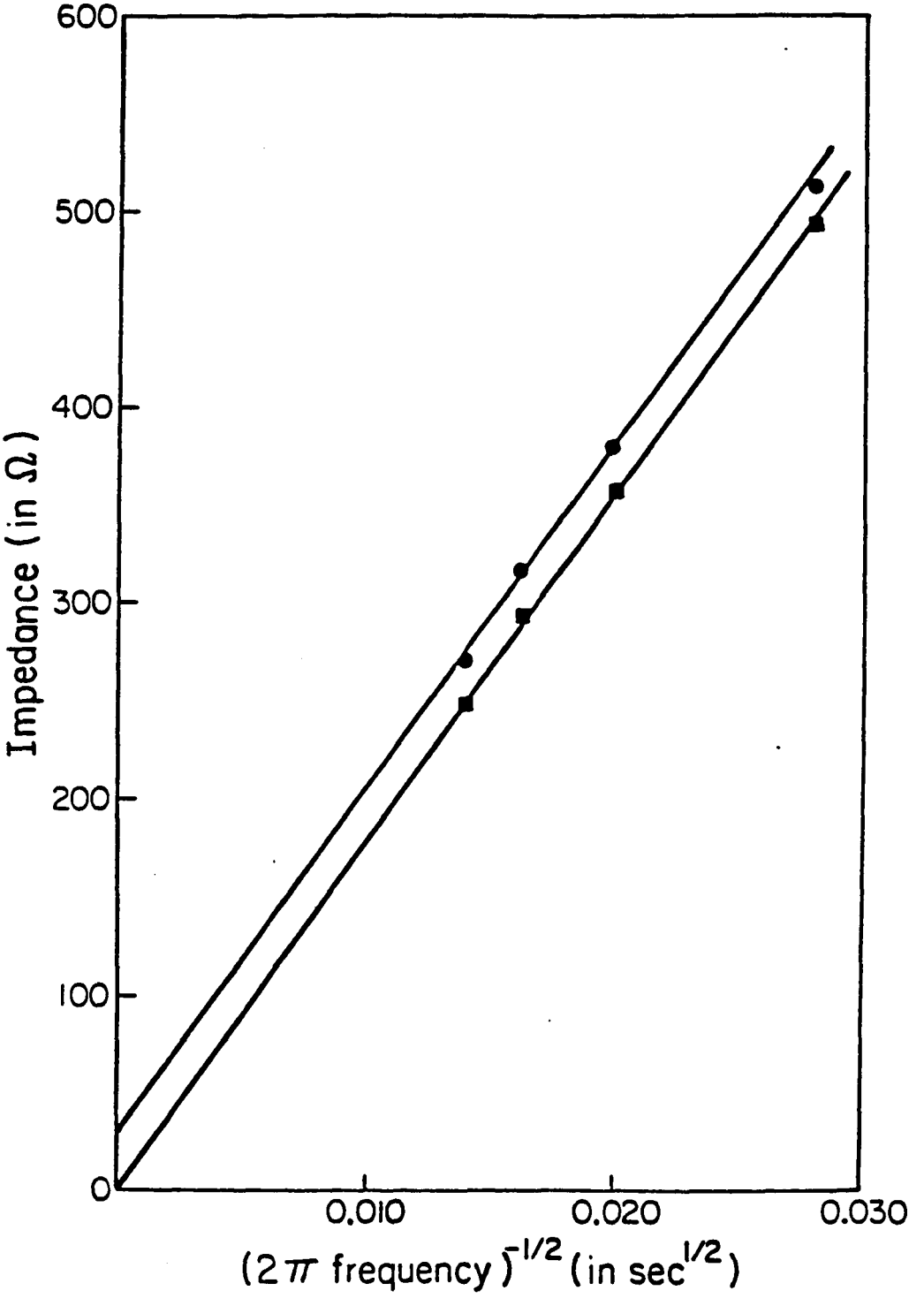
600
500
400
300
200
100
0
Impedance (in Ω)
0.010
0.020
0.030
(2π frequency)^-1/2 (in sec^1/2)

Figure 4. Impedance vs. $(2\pi \text{ frequency})^{-\frac{1}{2}}$ plots for 1.0 mM cyclooctatetraene in acetonitrile containing 0.2 M tetra-n-butylammonium perchlorate on mercury. ● In-phase impedance (R_s); ■ Out-of-phase impedance ($\frac{1}{2\pi \text{ frequency } C_s}$).

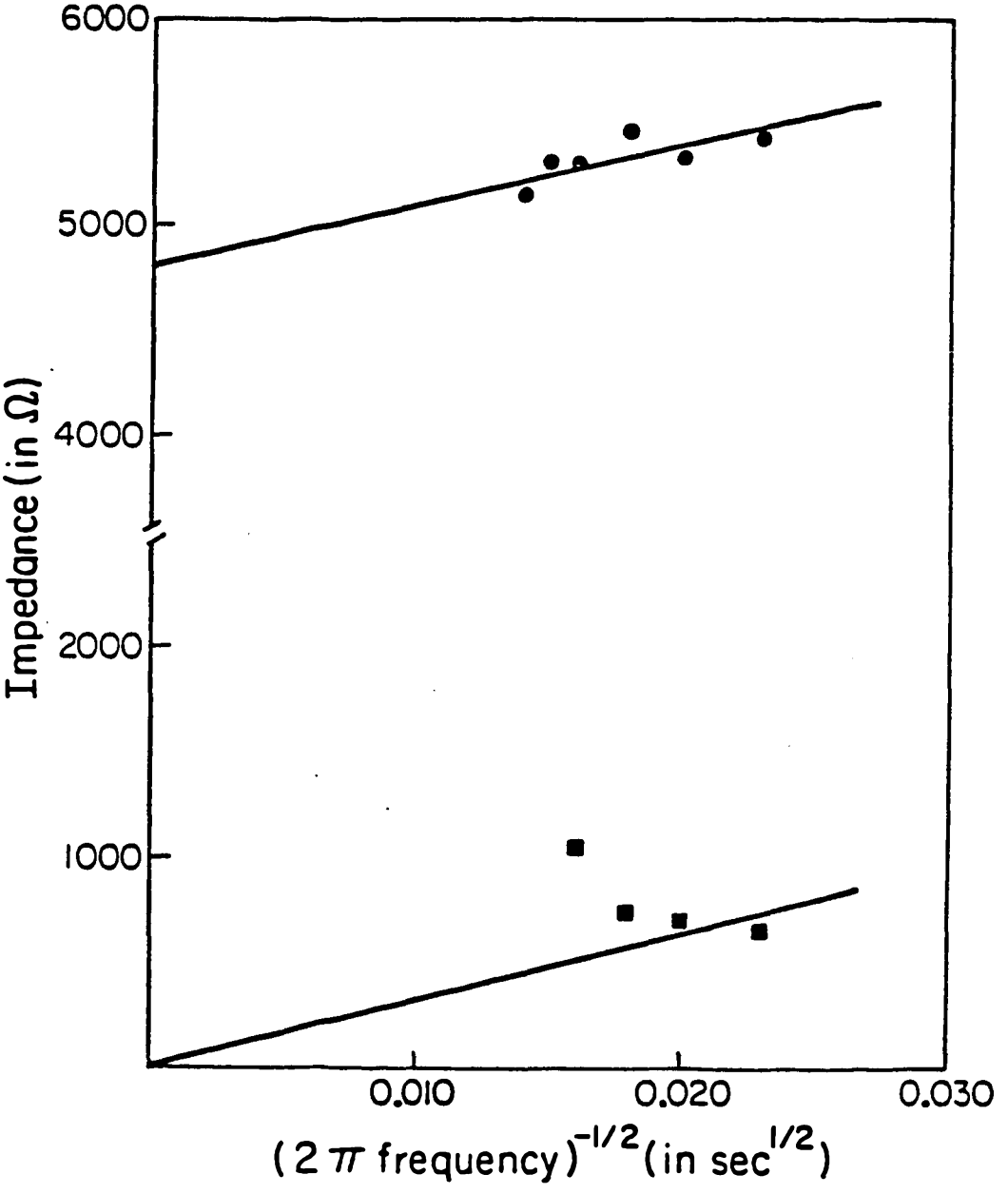
6000
5000
4000
2000
1000
Impedance (in Ω)
0.010
0.020
0.030
(2π frequency)^-1/2 (in sec^1/2)

Figure 5. Impedance vs. $(2\pi \text{ frequency})^{-\frac{1}{2}}$ plots for 1.0 mM cycloocta-tetraene in acetonitrile containing 0.3 M tetraethylammonium perchlorate on mercury. ● In-phase impedance (R_s); ■ Out-of-phase impedance ($\frac{1}{2\pi \text{ frequency } C_s}$).

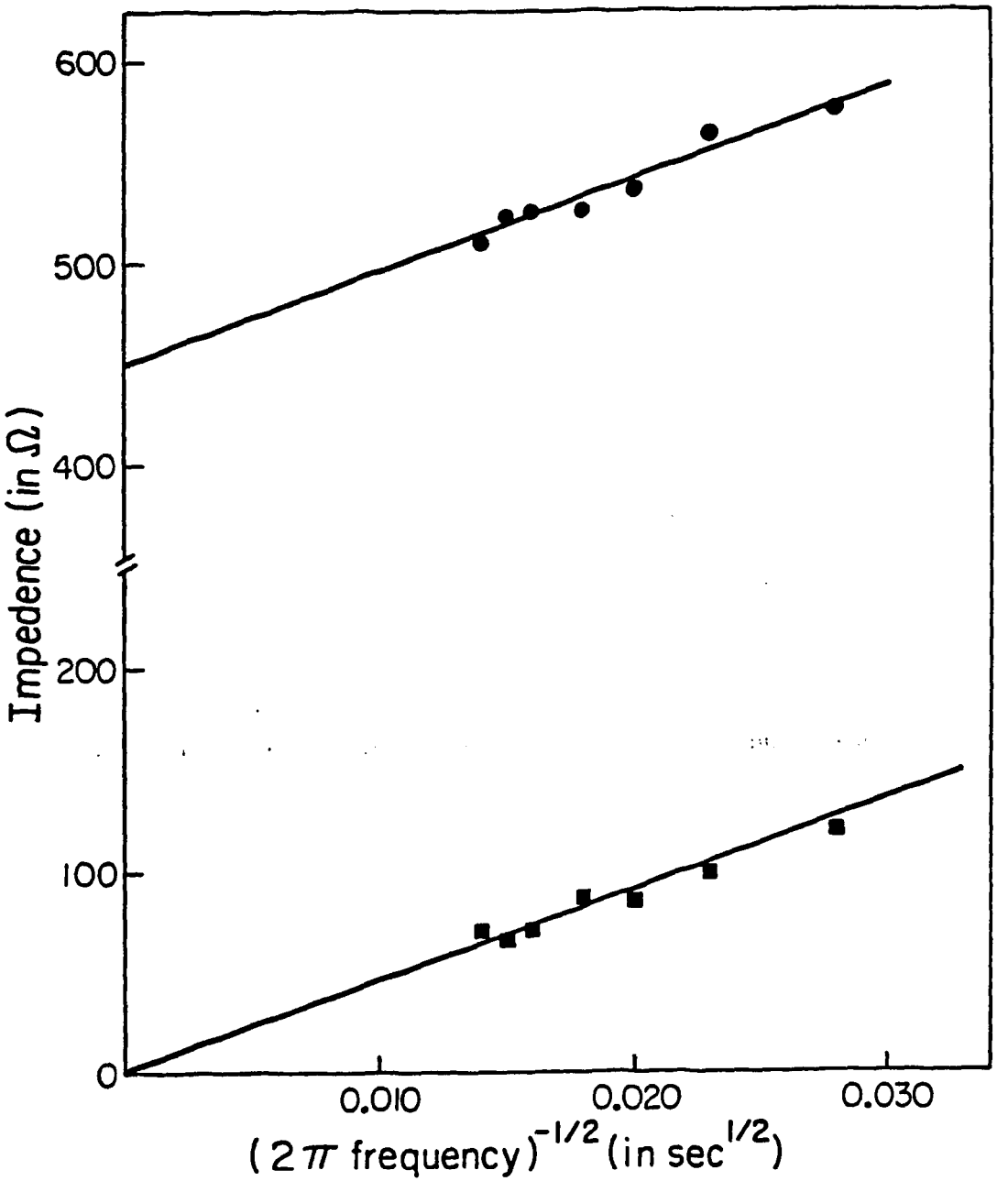
600
500
400
200
100
0
Impedence (in Ω)
0.010
0.020
0.030
(2π frequency)^-1/2 (in sec^1/2)

Figure 6. Impedance vs. $(2\pi \text{ frequency})^{-\frac{1}{2}}$ plots for 1.0 mM cycloocta-tetraene in dimethylformamide containing 0.15 M tetramethyl-ammonium perchlorate on mercury. ● In-phase impedance (R_S); ■ Out-of-phase impedance ($\frac{1}{2\pi \text{ frequency } C_S}$).

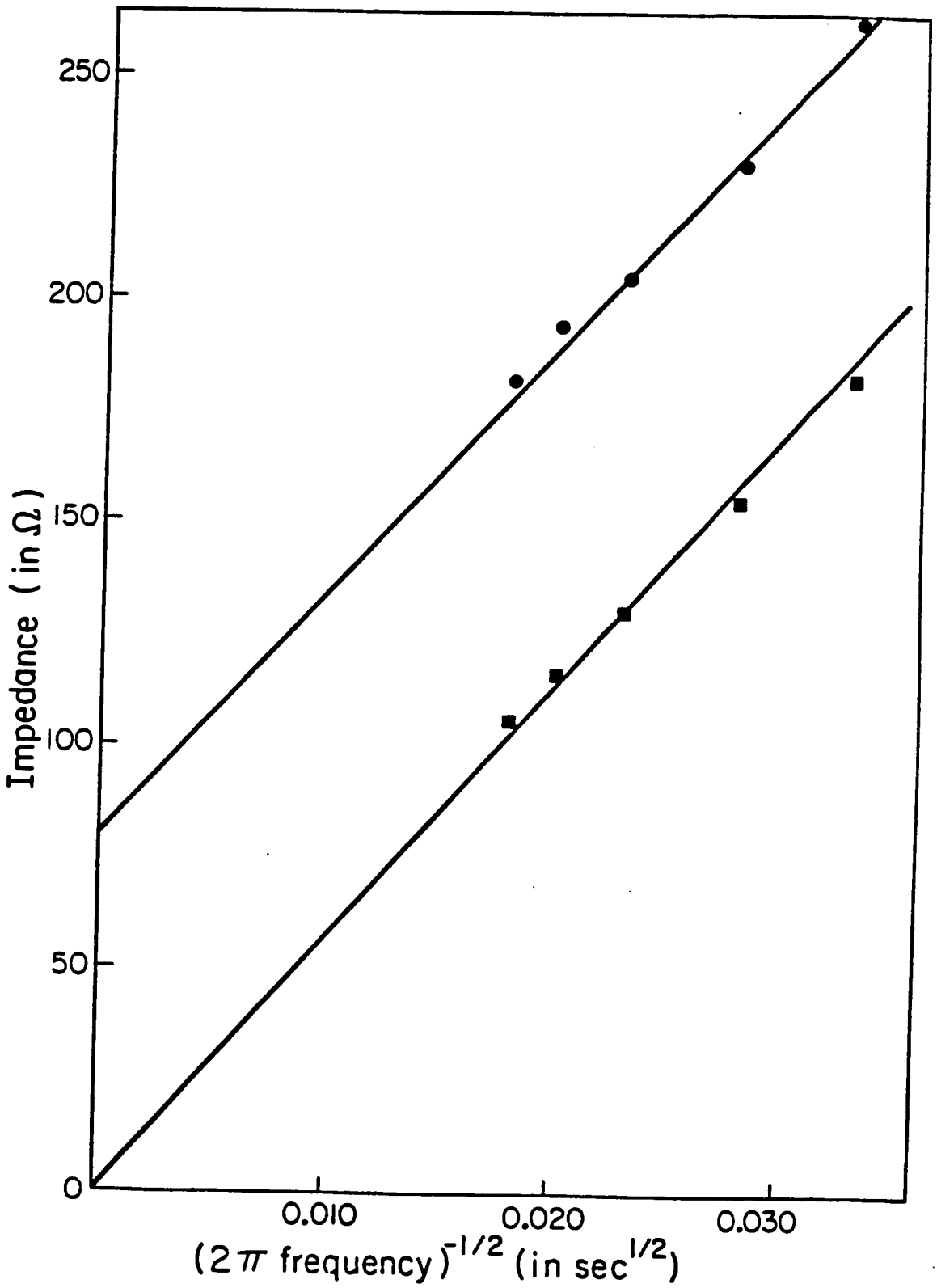
250
200
150
100
50
0
Impedance (in Ω)
0.010
0.020
0.030
(2π frequency)$^{-1/2}$ (in sec$^{1/2}$)

ESR of homogeneous solutions of $COT^{\cdot -}$ in the presence of various cations showed no evidence of such ion pairing.[57,58]

All of the factors responsible for the effect of the nature of the supporting electrolyte on the rate constant have not yet been elucidated but the fact remains that k_s for the first reduction of COT can be as large as 0.24 cm/sec, despite the major structural changes that result from the reduction. The large magnitude of the k_s values for both COT and $\underset{\frown}{I}$ are in the range where the outer-sphere, rather than the inner-sphere, reorganization energy dominates the factors that control the electrode reaction rate.[7,10] Thus it appears that much care must be taken in predicting how large an effect the inner-sphere structural changes will have on the rate constant for electron transfer, especially when it is not possible to calculate the latter from bond length changes and bond strengths using Marcus theory.[8-10] It would be very interesting to know if the homogeneous self-exchange rates for these species followed the behavior of their heterogeneous rates and if similar increases in the rates of electron transfer could be observed for other complexes with large intramolecular structural changes when changing the supporting electrolyte cation from tetra-n-butylammonium to tetramethylammonium. Unfortunately, such data are not yet available.

CONCLUSIONS

Two complexes, cis-$[(C_5H_5)Fe(CO)P(C_6H_5)_2]_2$ and cyclooctatetraene, which are known to have large intramolecular structural rearrangements upon oxidation and reduction, respectively, have been studied via cyclic voltammetry, chronocoulometry and AC impedance techniques. Heterogeneous electron transfer rate constants were measured for these species in non-aqueous solvents and were as high as 0.25 cm/sec, a rate usually associated with electron transfer limited only by the outer-sphere reorganizational energy. Although the reasons behind such large rates for these species have not been fully elucidated, it seems possible that compensatory structural changes in other parts of the molecule may lower the barrier to electron transfer. In any case, this study has clearly shown that it is not justified to associate large structural changes with slow electron transfers in general.

REFERENCES AND NOTES

1. M. Chou, C. Creutz and N. Sutin, J. Am. Chem. Soc., 99, 5615 (1977).
2. B. S. Brunschwig, C. Creutz, D. H. Macartney, T. K. Sham and N. Sutin, submitted for publication, Disc. Faraday Soc., 1982.
3. J. M. Hale in "Reaction of Molecules at Electrodes", N. S. Hush, Ed., Wiley, New York, 1971.
4. R. Dietz and M. E. Peover, Disc. Faraday Soc., 45, 154 (1968).
5. M. E. Peover and J. S. Powell, J. Electronanal. Chem., 20, 427 (1969).
6. B. J. Huebert and D. E. Smith, J. Electroanal. Chem., 31, 333 (1971).
7. B. Tulyathan and W. E. Geiger, Jr., J. Electroanal. Chem., 109, 325 (1980).
8. R. A. Marcus, Electrochim. Acta, 13, 995 (1968).
9. R. A. Marcus, J. Phys. Chem., 67, 853, 2889 (1963).
10. R. A. Marcus, J. Chem. Phys., 43, 679 (1965).
11. M. J. Weaver and E. L. Yee, Inorg. Chem., 19, 1936 (1980).
12. G. M. Brown and N. Sutin, J. Am. Chem. Soc., 101, 883 (1979).
13. T. Saji, Y. Maruyama and S. Aoyagui, J. Electroanal. Chem., 86, 219 (1978).
14. H. Kojima and A. J. Bard, J. Am. Chem. Soc., 97, 6317 (1975).
15. R. D. Allendoerfer and P. H. Rieger, J. Am. Chem. Soc., 87, 2336 (1965).
16. a) H. Kojima, A. J. Bard, H. N. C. Wong and F. Sondheimer, J. Am. Chem. Soc., 98, 5560 (1976).

REFERENCES AND NOTES (continued)

b) L. B. Anderson and L. A. Paquette, J. Am. Chem. Soc., 94, 4915 (1972).

17. L. B. Anderson, J. F. Hansen, T. Kakihana and L. A. Paquette, J. Am. Chem. Soc., 93, 161 (1971).

18. P. Siders and R. A. Marcus, J. Am. Chem. Soc., 103, 741 (1981).

19. N. Sutin in "Tunneling in Biological Systems", Academic Press, New York, 1979.

20. A. J. Fry, C. S. Hutchins and L. L. Chung, J. Am. Chem. Soc., 97, 591 (1975).

21. W. H. Smith and A. J. Bard, J. Electroanal. Chem., 76, 19 (1977).

22. B. S. Jensen, A. Ronlan and V. D. Parker, Acta Chem. Scand., B29, 394 (1975).

23. F. A. Anet, J. Am. Chem. Soc., 84, 671 (1962).

24. O. Bastiansen, L. Hedberg and K. Hedberg, J. Chem. Phys., 27, 1311 (1957).

25. D. H. Lo and M. A. Whitehead, J. Am. Chem. Soc., 91, 238 (1969).

26. P. J. Kimmel and H. L. Strauss, J. Phys. Chem., 72, 2813 (1968).

27. H. L. Straus, T. J. Katz and G. K. Fraenkel, J. Am. Chem. Soc., 85, 2360 (1963).

28. M. J. S. Dewar, A. Harget and E. Haselbach, J. Am. Chem. Soc., 91, 7521 (1969).

29. R. H. Cox, L. H. Harrison and W. K. Austin, Jr., J. Phys. Chem., 77, 200 (1973).

REFERENCES AND NOTES (continued)

30. T. J. Katz, J. Am. Chem. Soc., 82, 3784 (1960).

31. D. A. Corrigan and D. E. Evans, J. Electroanal. Chem., 106, 287 (1980).

32. R. E. Ginsburg, R. K. Rothrock, R. G. Finke, J. P. Collman and L. F. Dahl, J. Am. Chem. Soc., 101, 6550 (1979).

33. B. Teo, P. Eisenberger and B. M. Kincaid, J. Am. Chem. Soc., 100, 1735 (1978).

34. J. D. Sinclair, Ph.D. Thesis, University of Wisconsin, Madison, Wisconsin, 1972.

35. R. E. Dessy, R. Kornmann, C. Smith and R. Haytor, J. Am. Chem. Soc., 90, 2001 (1968).

36. A. Brandstrom, Acta Chem. Scand., 3585 (1969).

37. a) R. G. Hayter, Inorg. Chem., 2, 2031 (1963).
b) R. G. Hayter and L. F. Williams, J. Inorg. Nucl. Chem., 26, 1977 (1964).

38. D. J. Barclay, E. Passeron and F. C. Anson, Inorg. Chem., 9, 1024 (1970).

39. a) G. Lauer, R. Abel and F. C. Anson, Anal. Chem., 39, 765 (1967).
b) J. A. Turner, Ph.D. Thesis, Colorado State University, 1977.

40. The capillary was modified by carefully breaking-in-two, inserting a thin platinum wire (2 inches long) between the two halves and then resealing the capillary back together with heat shrinkable tubing until an airtight fit was obtained. This should allow an unimpeded mercury flow when growing a new drop, but once the

REFERENCES AND NOTES (continued)

mercury drop is extruded, the surface area should not change with time. Connections to the working electrode (i.e., the capillary) were now made to this platinum wire.

41. A. J. Bard and L. R. Faulkner, "Electrochemical Methods", Ch. 9, Wiley, New York, 1980.

42. W. M. Moore and D. G. Peters, J. Am. Chem. Soc., 97, 139 (1975).

43. T. Bernstein and P. H. Herbstein, Acta Cryst., B24, 1640 (1968).

44. J. W. Bats, J. J. de Boer and D. Bright, Inorg. Chim. Acta, 5, 605 (1971).

45. J. W. Diggle and A. J. Parker, Electrochim. Acta, 18, 975 (1973).

46. M. Sharp, M. Petersson and K. Edstrom, J. Electroanal. Chem., 109, 271 (1980).

47. Roger Parsons, Private Communication, 1980.

48. a) R. S. Nicholson and I. Shain, Anal. Chem., 36, 1251 (1964).
b) R. S. Nicholson, Anal. Chem., 38, 1406 (1966).

49. a) J. H. Christie, G. Lauer and R. A. Osteryoung, J. Electroanal. Chem., 7, 60 (1964).
b) P. J. Lingaine and J. H. Christie, J. Electroanal. Chem., 10, 284 (1965).

50. F. C. Anson, Anal. Chem., 38, 54 (1966).

51. a) P. Delahay, "Double Layer and Electrode Kinetics", Ch. 9, Interscience, New York, 1965.
b) A. N. Frumkin, Z. Phys. Chem., 164, 121 (1933).

REFERENCES AND NOTES (continued)

52. a) E. S. Young, M. S. Chan and A. C. Wahl, J. Phys. Chem., 84, 3094 (1980).

b) E. S. Young, M. S. Chan and A. C. Wahl, J. Phys. Chem., 79, 2049 (1975).

53. a) M. Sluyters-Rehbach and J. H. Sluyters, J. Electroanal. Chem., 4, 1 (1970).

b) J. E. B. Randles, Disc. Faraday Soc., 1, 11 (1947).

c) D. E. Smith in "Electroanalytic Chemistry", A. J. Bard, Ed., Volume 1, Ch. 1, 1966.

54. M. E. Peover and B. S. White, J. Electroanal. Chem., 13, 93 (1967).

55. The rate constant for reduction of $COT^{\cdot-}$ in dimethylformamide containing 0.15 M tetramethylammonium perchlorate measured in this study was within a factor of two of that measured for reduction of COT in the same media; based upon a comparison of the in-phase AC currents for each process.

56. W. R. Fawcett, J. Chem. Phys., 61, 3842 (1974).

57. G. R. Stevenson and J. G. Concepcion, J. Phys. Chem., 76, 2176 (1972).

58. G. R. Stevenson and I. Ocasio, J. Phys. Chem., 79, 1387 (1975).

PART III

Synthesis and Properties of Several Novel Ruthenium Ammine Complexes. Some Applications of Electrochemistry to the Study of Reaction Rates, Formal Potentials and Adsorption.

INTRODUCTION

In the past ten years the chemical, spectral and electrochemical behavior of ruthenium ammine species has received considerable attention,[1] both for a variety of ruthenium(II) pentaammine[2-4] and tetraamine[5] complexes and also for some ruthenium(III) ammine compounds.[4,6] The effects of various ligands on the formal potential for the Ru(III/II) couple and on the position of the metal-to-ligand charge transfer (MLCT) band have been investigated.[3-7] Basically, the results from these studies show that the greater the π-accepting ability of the ligand, the more positive is the formal potential for the ruthenium(II/III) couple. This trend is due to stabilization of the ruthenium(II) oxidation state relative to the ruthenium(III). Low spin Ru(II) is d^6 and a good π-back-donor while d^5 Ru(III) is a π-acceptor. For ligands which are not π-bonding, greater stability of the Ru(III) oxidation state relative to the Ru(II) is found for those ligands with the larger ligand field strength, with a subsequent negative shift in the formal potential.[6] In some cases, there exists a correlation between the formal Ru(II/III) potential for the substituted ruthenium pentaammine complex and the position of the visible absorption (MLCT) band of the ruthenium(II) species.

The large differences in the chemical and coordinative properties of Ru(III) versus Ru(II) pentaammine species have been used to prepare complexes which are coordinately stable in one oxidation state but, upon electron transfer, rapidly rearrange to accommodate an entirely new ligand environment. Although it has been possible to measure the rates

of coordination and aquation of various ligands in the substituted ruthenium ammines spectrally,[2,5,8] cyclic voltammetry has proven to be particularly useful in examining the kinetics of ligand substitutions when the reaction rates fall within the time domain of the cyclic scan.[3,4,6] The results of investigations into the aquation and coordination rates for a wide variety of ligands and substituted ruthenium(II) ammine complexes appear to show that both these processes occur via a dissociative mechanism.[2,9] In addition, studies with cis- and trans-ruthenium(II) tetraammines have indicated that there is a trans-labilizing effect[3,5] in these species, although those factors which govern this effect are not fully understood. In the present investigation, cyclic voltammetry has been employed to monitor both aquation and coordination rates for several novel ruthenium(II) ammine complexes.

An interesting compound that has been prepared is the ruthenium-(III) pentaammine isothiocyanate,[4] in which the NCS^- ligand is believed to be N-bound to the ruthenium atom. However, recent work of Taube[10] and Isied[11] have provided a synthetic route to the corresponding S-bonded isomer, $Ru(NH_3)_5SCN^{2+}$. To distinguish between other similar NCS linkage isomers, infrared spectroscopy has been applied.[12-14] The feature best used to differentiate the two isomers was found to be the intensities (and to a lesser extent the position) of the C-N stretching mode at approximately 2050 cm^{-1}. The N-bound species has a greater intensity than free thiocyanate[4] while the S-bonded complex has lower intensity, although great care must be taken to compare only measurements in identical media. In the present investigation it was found that cyclic voltammetry, visible absorption spectroscopy and the extent of

adsorption on mercury could also be used to distinguish the two linkage isomers of thiocyanate-substituted ruthenium pentaammine complexes.

Preliminary investigations into the adsorption behavior of $Ru(NH_3)_5NCS^+$ on mercury electrodes have shown that this complex displays moderate adsorption, probably via the isothiocyanate ligand.[15] This fact, coupled with a convenient synthesis of a compound that can be used as the starting point for formation of trans-substituted ruthenium tetraammines,[5,8] has been exploited to prepare complexes which can both coordinate other redox molecules and adsorb on mercury electrodes. Formation of such molecular anchors is exciting because they could be used to hold various redox couples at a known distance from mercury electrodes and allow measurement of electron transfer rates to the attached redox center. The effects of attaching redox catalysts at a known distance from the electrode on the electrode kinetics for these species are important parameters to understand in the field of attached redox catalysts,[16] and for which very little data are currently available.[17] In the present report, the preparation, characterization and electrochemistry of several molecular anchor-redox couple assemblies will be further explored.

EXPERIMENTAL

Materials. $[Ru(NH_3)_5Cl]Cl_2$ was prepared from $Ru(NH_3)_6Cl_3$ (Matthey Bishop, Inc.) as described in the literature[18] by dissolving 7.0 g of $Ru(NH_3)_6Cl_3$ in 150 ml of 6 N HCl and refluxing for four hours. Upon cooling the solution, a yellow precipitate is formed and collected by filtration. After washing this solid with cold 20 ml-portions of 6 N HCl, CH_3OH and acetone, it was redissolved in 0.1 N HCl by heating, then filtered hot and allowed to slowly cool to room temperature. After several days the bright yellow crystals (5 g) were collected and washed with CH_3OH.

trans-$Ru(NH_3)_4(HSO_3)_2$ was synthesized according to a method outlined by Vogt et al.[18] 2.0 g of $[Ru(NH_3)_5Cl]Cl_2$ was dissolved in 80 ml of distilled water containing 2.83 g of $NaHSO_3$. While slowly bubbling SO_2 through this solution it was heated to a temperature between 75-80°C for one hour. Then the solution was cooled down to 0°C, with continued bubbling of SO_2 through solution, to precipitate out the white solid. The product (1.8 g) was then washed with cold water and ethanol.

trans-$[Ru(NH_3)_4(SO_2)Cl]Cl$ was used as the starting point for synthesis of other trans-substituted ruthenium tetraammine complexes. It was prepared from trans-$Ru(NH_3)_4(HSO_3)_2$[18] by dissolving 1.35 g of this compound in 150 ml of boiling 6 N HCl; it dissolves only slowly turning the color of the solution red. This solution was filtered hot to remove a black side-product and reheated to dissolve any crystals that may have precipitated. Finally the solution was cooled down in a refrigerator overnight to precipitate orange-brown, needle-shaped crystals (0.5 g) of the desired product which were washed with cold

10-ml portions of 6 N HCl and CH_3OH.

$[Ru(NH_3)_5NCS](ClO_4)_2$ was prepared from $[Ru(NH_3)_5Cl]Cl_2$ by electrochemical reduction of a 10 mM solution at -0.6 V[4] to form $Ru(NH_3)_5(H_2O)^{2+}$ followed by addition of excess NaSCN, air oxidation until a dark-red colored solution is formed and precipitation of the purple perchlorate salt with excess $NaClO_4$.

$[Ru(NH_3)_5SCN](PF_6)_2$, the S-bound thiocyanate isomer, was synthesized by dissolving 25 mg of $(NH_3)_5Ru\text{-}S\text{-}S\text{-}Ru(NH_3)_5^{4+}$[10,11] (kindly donated by Stephen Isied) in 2 ml of deoxygenated water which contained 10 mg of $NaHCO_3$. Then 100 mg of NaCN were added and the solution was stirred in air for 30 minutes in a well-ventilated hood. After addition of several drops of trifluoroacetic acid to acidify the solution and further stirring in air, this solution was chromatographed on an ion-exchange resin (Sephadex SP-C50-120) eluting first with water, then 0.02 M trifluoroacetic acid (TFA) and finally with 0.2 M TFA to remove a purple band which contained the desired complex. After concentration of the purple solution, the PF_6^- salt was precipitated by the addition of excess NH_4PF_6.

trans-$Ru(NH_3)_4(NCS)(SO_4)$ was obtained from trans-$[Ru(NH_3)_4(SO_2)Cl]Cl$ via the following reaction sequence. To 5 ml of deoxygenated water containing 0.25 g of $NaHCO_3$ were added 0.2 g of trans-$[Ru(NH_3)_4(SO_2)Cl]Cl$ and excess NaSCN (0.2 g). The solution was stirred until all the solid material had dissolved. Then 0.5 ml of 12 N HCl was added as quickly as possible (gas and heat were evolved), followed by 0.5 ml of 30% H_2O_2 within <u>five</u> seconds. If hydrogen peroxide is added much after five seconds, even just a few seconds,

the yield of the desired product decreases considerably. The addition of H_2O_2 produces a dark-red solution from which an orange-red solid can be precipitated by the addition of 50 ml of a 30% ethanol/70% ether mixture. This solid was redissolved in a minimal amount of water and chromatographed on a Sephadex G-10 column with distilled water as the elutant. Only the dark-orange band was collected and concentrated by rotary evaporation. Finally, the solid was dried at room temperature under vacuum.

trans-$Ru(NH_3)_4(NCS)_2^+$ was generated by electrochemically reducing 0.1 g of trans-$Ru(NH_3)_4(NCS)(SO_4)$ in 0.2 M CF_3COOH at -0.6 V to produce trans-$Ru(NH_3)_4(NCS)(H_2O)^+$, followed by addition of excess NaSCN (0.2 g) and air-oxidation. The resulting solution was concentrated by rotary evaporation and chromatographed on the Sephadex SP-C50-120 column. Unfortunately it was not possible to precipitate the PF_6^- salt, even after the addition of a large excess of NH_4PF_6, so only qualitative spectral and electrochemical measurements were feasible.

Ethylenediaminetetraacetatoruthenium(III), $Ru(EDTA)(H_2O)^-$, was prepared and donated by Roger Baar.[19]

Ruthenium analyses[20] were performed on all solid samples studied by cyclic voltammetry and visible absorption spectroscopy in this study. This procedure was accomplished by dissolving several mg of the desired ruthenium complex in 5 ml of 2 M KOH, which also contained 100 mg of $K_2S_2O_8$. Then the solution was heated for 30 minutes at or near the boiling point to concentrate the solution down to 1 ml. After the solution was allowed to cool, it was diluted to 10 or 25 ml with 2 M KOH. Measurement of the absorbance at 415 nm for the sample

and using the known extinction coefficient of 1049 $M^{-1} cm^{-1}$,[20] it was possible to determine the ruthenium concentration and hence the molecular weight of the species. Reasonable results were obtained for $Ru(EDTA)(H_2O)^-$, $[Ru(NH_3)_5NCS](ClO_4)_2$ and trans-$Ru(NH_3)_4(NCS)(SO_4)$ (when it was vacuum dried because this species was very hydroscopic). In the case of $[Ru(NH_3)_5SCN](PF_6)_2$, the initial analysis of freshly prepared material was slightly lower than the predicted value (although no contamination could be detected by cyclic voltammetry or spectrally) and with time the complex (even in the solid state) seemed to decompose. However, all experiments with the S-bound ruthenium pentaammine thiocyanate were performed within 48 hours of its preparation and no further characterization of the decomposition was carried out.

In all the cases of trans-substituted ruthenium tetraammines reported in this study, the trans-configuration was proposed because no cis-trans rearrangements have been observed during the preparation of similar trans-Ru(II) complexes[3, 21] from the known trans-conformation of trans-$[Ru(NH_3)_4(SO_2)Cl]Cl$.[18] Formation of N-bound isothiocyanate ligands in trans-$Ru(NH_3)_4(NCS)(SO_4)$ and trans-$Ru(NH_3)_4(NCS)_2^+$ was postulated because of the similarity between the coordination reaction conditions for attachment of NCS^- to these complexes and the coordination reaction conditions used for the preparation of the known N-bonded $Ru(NH_3)_5NCS^{2+}$.[4] These syntheses for $Ru(NH_3)_5NCS^{2+}$ involve coordination of NCS^- to the ruthenium(II) centers which is very different from the reaction sequence used to obtain the S-bonded thiocyanate ruthenium(III) pentaammine.[10, 11]

Apparatus. Cyclic voltammograms were obtained with a Princeton Applied Research Model 173 potentiostat driven by a PAR Model 175 universal programmer and recorded on a Houston Model 2000 recorder. For scan rates greater than 1 V/sec. the transient current-potential curves were first recorded on a Textronik Model 5000 Digital Scope before being transferred to the Houston recorder. Controlled-potential electrolyses were conducted with the PAR Model 173 potentiostat equipped with a PAR Model 179 digital coulometer and using a cell modeled after the design of Moore and Peters.[22] Chronocoulometry experiments were accomplished by means of a computer-based data acquisition system[23] with the working electrode consisting of the modified (reference 40 in Part II of this thesis) PAR Model 303 static mercury drop electrode surrounded by a platinum gauze electrode as the auxiliary and a Ag/AgCl reference electrode.[24]

The amount of adsorption was determined by subtracting the intercept on the charge axis found in the substrate solution from the double layer charge obtained in a background experiment.[25] This was necessary because both oxidation states were adsorbed and it was not possible to use double-step chronocoulometry[26] to measure the double layer charge, thus the quantities of adsorbed material reported here were only approximate quantities. UV-visible spectra were obtained with a Hewlett-Packard Model 8450A Spectrometer.

RESULTS AND DISCUSSION

Spectral properties and formal potentials for several of the complexes examined in this study are listed in Table I. Formal potentials were evaluated from cyclic voltammetric curves, which in the case of trans-$Ru(NH_3)_4(NCS)(SO_4)$ required potential sweep rates high enough (10 V/sec or higher) to avoid the loss of $SO_4^=$ from the inner-coordination sphere of the electrogenerated Ru(II). The loss of $SO_4^=$ from Ru(II) species has been previously reported to occur with a half-life of 0.3 sec for trans-$(HO_2CC_5H_4N)Ru(NH_3)_4(SO)_4$.[27] In the present investigation, the rate of loss of $SO_4^=$ from trans-$Ru(NH_3)_4(NCS)(SO_4)^-$ was conveniently monitored by cyclic voltammetry (see Figure 1) both by the appearance of a new reversible couple at -0.24 V for trans-$Ru(NH_3)_4(NCS)(H_2O)^{2+/+}$ and by the loss of reoxidation current for trans-$Ru(NH_3)_4(NCS)(SO_4)^-$. Using the theory of Nicholson for a charge transfer process followed by an irreversible chemical reaction,[28] the rate constant for the loss of $SO_4^=$ from trans-$Ru(NH_3)_4(NCS)(SO_4)^-$ in 0.2 M CF_3COOH was found to be 4.6 sec^{-1} (see Table II). This value for the loss of $SO_4^=$ from the Ru(II) coordination sphere is slightly lower than that reported for trans-$(HO_2CC_5H_4N)Ru(NH_3)_4(SO_4)$ but in the same range for other aquation reaction rates of various substituted ruthenium(II) ammine complexes.[2-8]

N-Bound vs. S-Bound Thiocyanate

When the $[Ru(NH_3)_5NCS](ClO_4)_2$ prepared in this study is dissolved in 0.2 M CF_3COOH, a deep red-purple color results which is presumed to be the N-bound thiocyanate isomer. Its spectral and voltammetric responses are essentially identical to those of a complex prepared in a similar electrochemical fashion.[4] In this previous report,[4] infrared

TABLE I

Electronic Spectra and Formal Reduction Potentials of Several Ruthenium(III) Ammine Complexes

Ru(III) Complex	λ_{max}, nm (ϵ in $M^{-1} cm^{-1}$)[a]	E_f, in volts[b]
$Ru(NH_3)_5NCS^{2+}$	494(2175), 335(sm), 270(sm)	-0.21
$Ru(NH_3)_5NCS^{2+}$[c]	494(--), 335(sm)	-0.23
$Ru(NH_3)_5SCN^{2+}$	492(2150), 335(sm), 270(sm)	-0.20
$Ru(NH_3)_5SCN^{2+}$[c]	486(--), 335(sm)	-0.20
t-$Ru(NH_3)_4(NCS)(SO_4)$	468(3475), 308(1675)	-0.36
t-$Ru(NH_3)_4(NCS)_2^+$	746(sm), 525(--), 290(sh)	-0.24

a. sm = small peak; sh = shoulder.

b. Measured by cyclic voltammetry with a Ag/AgCl reference electrode.

c. Measured in 0.3 M NaCl solution.

TABLE II

Determination of the Aquation Rate Constant for trans-$Ru(NH_3)_4(NCS)(SO_4)^-$.

Scan Rate (V/sec)[a]	i_{p_a}/i_{p_c} [b]	τ(sec)[c]	$k_f(sec^{-1})$[d]
0.5	0.35	0.38	5.9
1.0	0.51	0.19	5.3
2.0	0.69	0.085	4.7
3.0	0.78	0.063	3.2
4.0	0.80	0.048	4.0
5.0	0.85	0.038	4.2
			av.-4.6

a. For a switching potential of -0.55 V. $E_{\frac{1}{2}}$ for the Ru(III/II) couple of trans-$Ru(NH_3)_4(NCS)(SO_4)$ is -0.36 V.

b. The ratio of anodic (i_{p_a}) to cathodic (i_{p_c}) peak currents calculated using Nicholson's method[28] to correct for baseline drift.

c. τ is the time between $E_{\frac{1}{2}}$ and the switching potential.

d. k_f found from Figure 12 in reference 28a.

Figure 1. Cyclic voltammogram for 1.5 mM trans-$Ru(NH_3)_4(NCS)(SO_4)$ on (BPG) carbon in 0.2 M CF_3COOH.

A. Scan rate = 50 mV/sec.

B. Scan rate = 1 V/sec.

C. Scan rate = 10 V/sec.

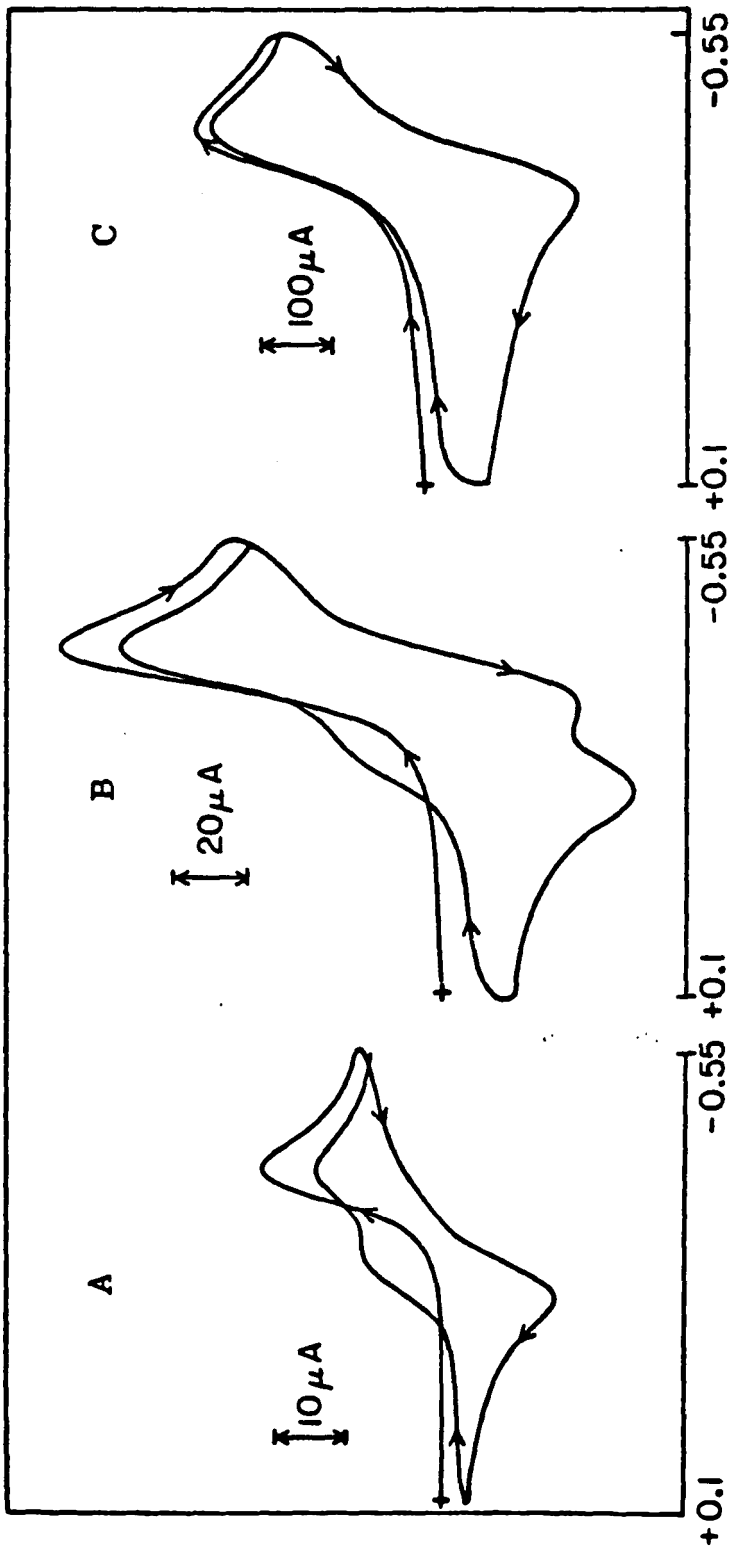
A
10μA
B
20μA
C
100μA
-0.55
+0.1
E vs Ag/AgCl, volts

absorption bands corresponding to the C-N stretching mode of the NCS ligand in $[Ru(NH_3)_5NCS](ClO_4)_2$ were measured in the solid state, compared to free thiocyanate and found to yield an integrated intensity five times larger than the uncoordinated thiocyanate. The relative ordering of intensities was used to support the assumption that the NCS ligand in $[Ru(NH_3)_5NCS](ClO_4)_2$ is N-bonded to the ruthenium.[4,12-14] Comparison of the proposed N-bound ruthenium pentaammine isothiocyanate to the species prepared in such a way as to form the S-bonded isomer[10,11] shows that these two complexes are not identical. Although the differences in the formal reduction potentials and visible spectral properties between the two ruthenium(III) linkage isomers are small (Table I), they are reproducible. In 0.3 M chloride ion media, there is an 8 nm shift toward higher energy for the ligand-to-metal charge transfer (LMCT) band and a 30 mV positive shift in the formal reduction potential for $Ru(NH_3)_5SCN^{2+}$ over that found for $Ru(NH_3)_5NCS^{2+}$. However, in 0.2 M CF_3COOH solutions, the spectral and potential differences between the two linkage isomers is only 2 nm and 10 mV, with the S-bound complex still at the higher energies and more positive potentials relative to the N-bonded ruthenium pentaammine isothiocyanate. The shift in the position of the visible absorption band to higher energies for $Ru(NH_3)_5SCN^{2+}$ in the presence of chloride ions may be due to an ion pairing effect, similar behavior has been observed for $Ru(NH_3)_5(pyridine)^{2+}$ in non-aqueous solvents with sodium chloride.[7]

Isomerization of the S-bonded ruthenium(II) pentaammine thiocyanate does not appear to occur on a cyclic voltammetric time scale (20 seconds or less) but if a solution of $Ru(NH_3)_5SCN^{2+}$ is allowed to sit

at room temperature, it converts into the N-bound isomer within several days. Similar results for the S-bound to N-bound conversion for solutions of $Ru(NH_3)_5SCN^{2+}$ were reported by Taube et al.[10] In addition, there was no indication of aquation of either $Ru(NH_3)_5NCS^{+}$ or $Ru(NH_3)_5SCN^{+}$ at the slowest scan rates employed (50 mV/sec), contrary to the implied aquation rate for the $Ru(NH_3)_5NCS^{+}$ complex.[4]

The reaction of $Ru(NH_3)_5NCS^{2+}$ with Hg^{2+} ions[4] has been cited as evidence in support of the proposed N-bound conformation, but in the present investigation, Hg^{2+} was found to react similarly with either ruthenium pentaammine thiocyanate isomer. Addition of $Hg(ClO_4)_2$ to red-purple solutions containing either S-bound or N-bound ruthenium(III) pentaammine thiocyanate immediately produces a yellow solution because of the following reactions:[4,29]

$$Ru(NH_3)_5NCS^{2+} + Hg^{2+} \rightleftharpoons Ru(NH_3)_5(NCS)Hg^{4+}$$

$$Ru(NH_3)_5SCN^{2+} + Hg^{2+} \rightleftharpoons Ru(NH_3)_5(SCN)Hg^{4+}.$$

The ruthenium(III) pentaammine thiocyanate mercury(II) adduct shows a small absorption band at 399 nm while the isothiocyanate derivative has an absorption maximum at 400 nm. Addition of chloride ions to either solution returns the respective spectrums to 92% of their original intensities with no apparent isomerization of the S-bonded ruthenium(III) pentaammine thiocyanate into the N-bound ruthenium(III) pentaammine isothiocyanate. Reaction of both ruthenium pentaammine thiocyanate linkage isomers with Hg^{2+} may be explained by proposing that the sulfur atom can coordinate both ruthenium and mercury simultaneously.

Thus, the reaction of Hg^{2+} with $Ru(NH_3)_5SCN^{2+}$ and $Ru(NH_3)_5NCS^{2+}$ can not be used to distinguish between the two isomers as previously proposed.[4]

As already discussed, the spectral and formal potential behavior for the two linkage isomers of the ruthenium pentaammine thiocyanate species are very similar although not identical, but in their adsorption properties on mercury electrodes there are large differences. Summarized in Figure 2 are the results of chronocoulometric adsorption measurements for the Ru(II) and Ru(III) pentaammine thiocyanate and isothiocyanate complexes as a function of potential and substrate concentration on mercury electrodes in 0.2 M trifluoroacetic acid. There appear to be only minor differences in the adsorption properties of the two Ru(II) species, with slightly larger quantities adsorbed and a greater potential dependence for the $Ru(NH_3)_5SCN^{+}$, but for the ruthenium(III) pentaammine thiocyanate and isothiocyanate complexes the adsorption profiles are quite distinctive. While $Ru(NH_3)_5NCS^{2+}$ is adsorbed almost as strongly as $Ru(NH_3)_5NCS^{2+}$, the S-bound isomer, $Ru(NH_3)_5SCN^{2+}$, is essentially not adsorbed at all. In addition, the potential for mercury oxidation in the presence of the N-bonded thiocyanate isomer was approximately 100 mV more negative than that for the S-bound ruthenium pentaammine thiocyanate. These two features, the difference in mercury oxidation potential in the presence of S-bound vs. N-bound thiocyanate ruthenium(III) pentaammine and only a little adsorption (less than 3 $\mu coul/cm^2$) of the $Ru(NH_3)_5SCN^{2+}$, more than any other were indicative of which linkage isomer of ruthenium pentaammine thiocyanate was present in solution.

Figure 2. Potential dependence of the adsorption of (A) Ruthenium pentaammine isothiocyanate and (B) Ruthenium pentaammine thiocyanate at mercury electrodes. The electrode was held for 30 sec. at the indicated potential in a solution of (A) $Ru(NH_3)_5NCS)^{2+}$ or (B) $Ru(NH_3)_5SCN^{2+}$ and then stepped to -0.6 V for Ru(III) reduction or +0.1 V for Ru(II) oxidation. Concentration of substrate, mM: ● - 0.2; ■ -0.5; ○ - 1.0; ▲ - 2.0. Supporting electrolyte: 0.2 M CF_3COOH; pH = 1.4.

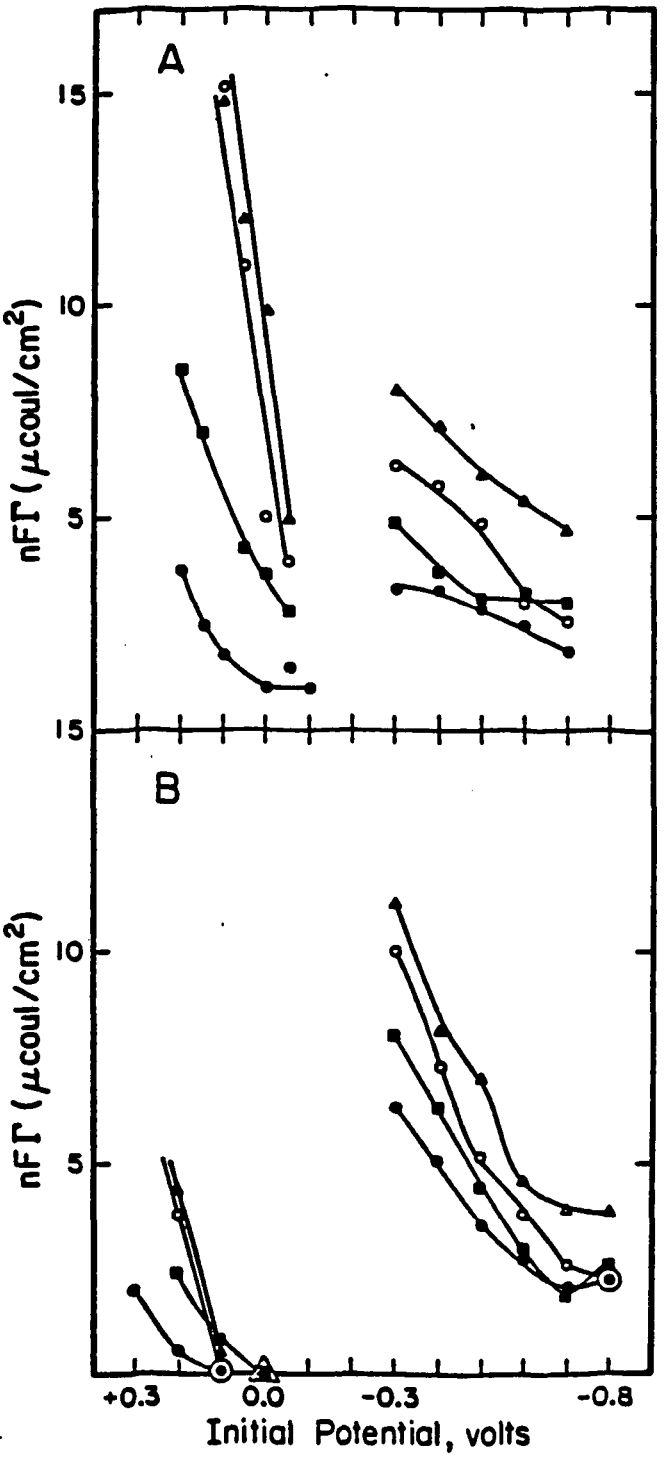
A
B
15
10
5
15
10
5
nFΓ (μcoul/cm²)
nFΓ (μcoul/cm²)
+0.3
0.0
-0.3
-0.8
Initial Potential, volts

The adsorption properties of the N-bound ruthenium(II) and ruthenium(III) pentaammine isothiocyanate complexes have also been studied in 0.2 M CF_3COONa (at pH = 6.5), in 1 M NH_4F[15] and in 0.32 M Na_2SO_4[15] solutions with analogous results to those reported in Figure 2. Based upon a molecular radius of 3.3 Å,[30] a concentration of 2 mM $Ru(NH_3)_5NCS^+$ shows about $\frac{1}{3}$ of a monolayer of adsorption, with repulsive rather than attractive interactions among the adsorbing molecules indicated[15] from a plot of the values of the quantities adsorbed in Figure 2 in Frumkin coordinates.[31] Also, the observed potential dependences follows the trend toward greater adsorption at the more positive potentials found for several other metal isothiocyanate complexes.[32] This probably reflects the increased interaction of the sulfur atom (in the NCS ligand) with the more positively charged mercury surface, similar to the affinity of several metal thiocyanate species (including $Ru(NH_3)_5NCS^{2+}$) with Hg^{2+}.[4, 32, 33] It has been suggested that the greater the value of the ligand field stabilization energy, the greater the extent of adsorption.[32, 33] The ruthenium pentaammine isothiocyanate species also appear to fit this correlation.

Formation of a Molecular Anchor - Redox Couple Complex

It has been proposed to exploit the moderate adsorption of ruthenium(II) ammine isothiocyanate complexes to prepare a molecule which could be used for attaching redox couples at a known distance from the mercury electrode.[17] The properties that such a molecule must have include strong adsorption on mercury in a known geometric conformation, electroinactive in the potential region where the redox couple is electroactive, possible coordination of a variety of redox

couples and convenient monitoring of the coordination of the redox couple to the molecular anchor either spectrally or voltammetrically. One possible candidate for such a complex that fulfills many of the above requirements is trans-$Ru(NH_3)_4(NCS)(4\text{-vinylpyridine})^+$.

Formation of trans-$Ru(NH_3)_4(NCS)(4\text{-vinylpyridine})^+$ was accomplished by electrochemical reduction of 2 mM solutions of either $Ru(NH_3)_5NCS^{2+}$ or trans-$Ru(NH_3)_4(NCS)(SO_4)$ at -0.6 V in 0.2 M CF_3COOH (pH = 1.4) containing approximately 40 mM 4-vinylpyridine (pKa 5.2-5.4[34]). The reducing potential of -0.6 V was maintained for 7 to 12 hours in the absence of oxygen and resulted in the complete coordination of the vinyl group to the ruthenium(II) atom. This coordination reaction is easily monitored by cyclic voltammetry (see Figure 3) because coordination of the olefin to the Ru(II) center shifts the formal potential of the Ru(II/III) couple over one volt more positive, similar to that observed for other ruthenium(II)-olefin species.[35] After the coordination reaction was complete, the pH of the solution was raised to 6.5 to deprotonate the pyridine nitrogen and the aqueous solution was extracted with three 20-ml portions of diethyl ether to remove excess 4-vinylpyridine. Then the resulting aqueous solution was exposed to reduced pressure to remove any remaining dissolved ether, the pH was readjusted to 6.0 and the chronocoulometric adsorption measurement made. At pH values above 5.0, the solution of trans-$Ru(NH_3)_4(NCS)$ (vinylpyridine)$^+$ was somewhat light sensitive, decomposing in only three to four hours, so this solution of trans-$Ru(NH_3)_4(NCS)$ (vinylpyridine)$^+$ was used immediately after preparation for adsorption measurements. After the chronocoulometric

Figure 3. A. Cyclic voltammogram of the solution produced by reducing 2 mM $[Ru(NH_3)_5Cl]Cl_2$ at -0.6 V in the presence of 40 mM 4-vinylpyridinium for three hours. B. Cyclic voltammogram of the solution generated by reducing 2 mM $Ru(NH_3)_5NCS^{2+}$ at -0.6 V in the presence of 40 mM 4-vinylpyridinium for eight hours. Carbon (BPG) electrode. Supporting electrolyte: 0.2 M CF_4COOH; pH = 1.4. Scan rate = 100 mV/sec.

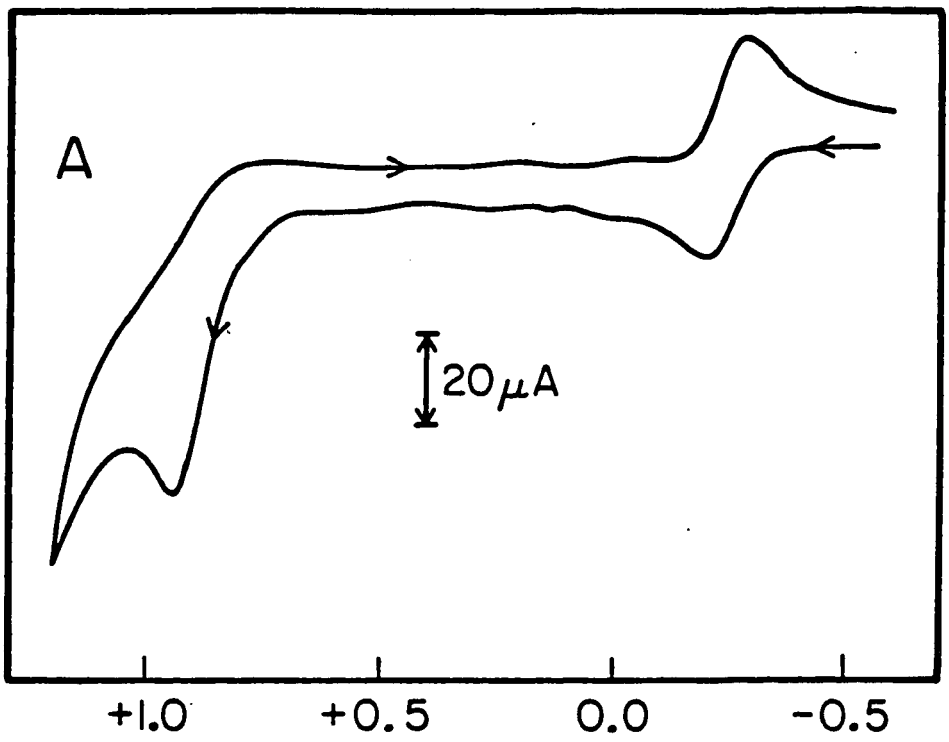
A
20μA
+1.0
+0.5
0.0
-0.5
E vs Ag/AgCl, volts

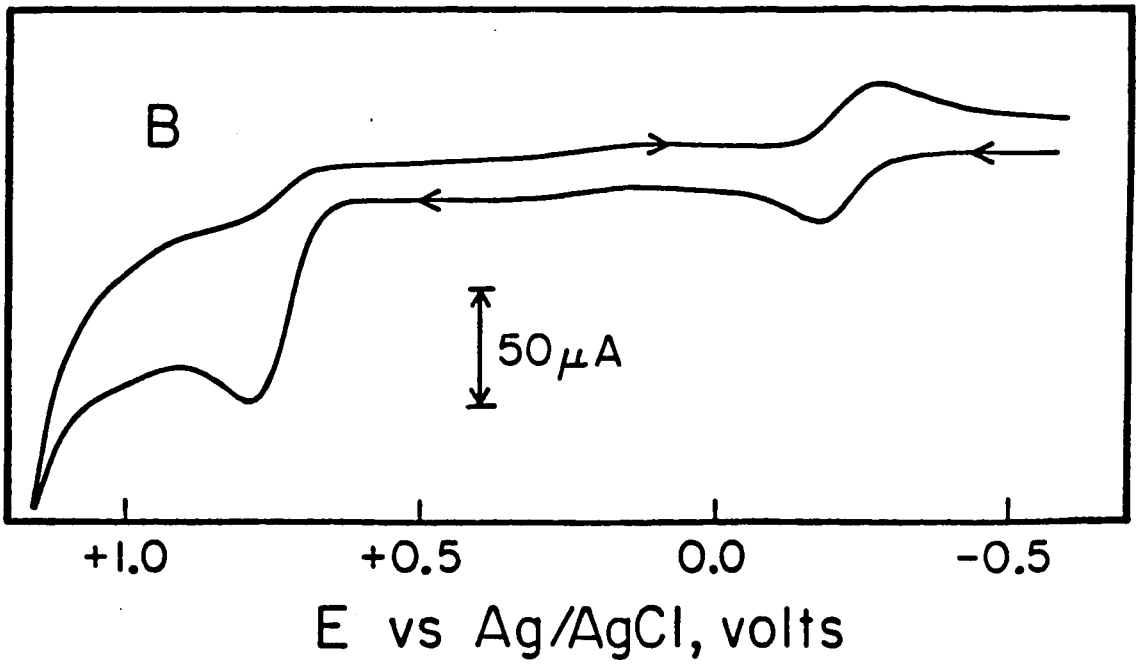
B
50μA
+1.0
+0.5
0.0
-0.5
E vs Ag/AgCl, volts

determination of the double layer charge on mercury for each potential step in the 2 mM trans-$Ru(NH_3)_4(NCS)(vinylpyridine)^+$ solution (trans-$Ru(NH_3)_4(NCS)(vinylpyridine)^+$ is electroinactive in the entire potential region accessible on mercury), a redox couple which coordinates the pyridine nitrogen was added and adsorption data were acquired as a function of applied potential and redox couple concentration.

$Ru(EDTA)(H_2O)^-$ was used as the redox couple because with its ruthenium atom in either oxidation state, Ru(II) or Ru(III), it binds strongly and quickly to the pyridine nitrogen[36, 37] and the formal potential for $Ru(EDTA)(pyridine)^-$ reduction is observable on mercury electrodes. In addition, coordination of the pyridine nitrogen to the inner-coordination sphere of Ru(EDTA) is easily monitored by cyclic voltammetry because of the +100 mV shift in the formal potential for $Ru(EDTA)(pyridine)^-$ *vs.* $Ru(EDTA)(H_2O)^-$ reduction (see Figure 4). Visible spectroscopy also could be used to follow the coordination of Ru(EDTA) to the pyridine nitrogen in trans-$Ru(NH_3)_4(NCS)(vinylpyridine)^+$, however this method was not as convenient as cyclic voltammetry because the spectral changes were relatively minor.[34] Under the experimental conditions used here, 2 mM trans-$Ru(NH_3)_4(NCS)(vinylpyridine)^+$ at pH = 6.0 with increasing concentrations of $Ru(EDTA)(H_2O)^-$ added (from 0.2 to 1.5 mM), complete coordination of the ruthenium(III) EDTA complex to the pyridine nitrogen of the molecular anchor, trans-$Ru(NH_3)_4(NCS)(vinylpyridine)^+$, was found. There was no indication in cyclic voltammograms of these solutions of $Ru(EDTA)^-$ in the presence of trans-$Ru(NH_3)_4(NCS)(vinylpyridine)^+$ that any $Ru(EDTA)(H_2O)^-$ remained uncomplexed.

Figure 4. A. Cyclic voltammogram of 1 mM $Ru(EDTA)(H_2O)^-$.
B. Cyclic voltammogram of 1 mM Ru(EDTA) in the presence of 2 mM 4-vinylpyridine.
Carbon (BPG) electrode. Supporting electrolyte: 0.2 M CF_3COONa; pH = 5.6. Scan rate = 100 mV/sec.

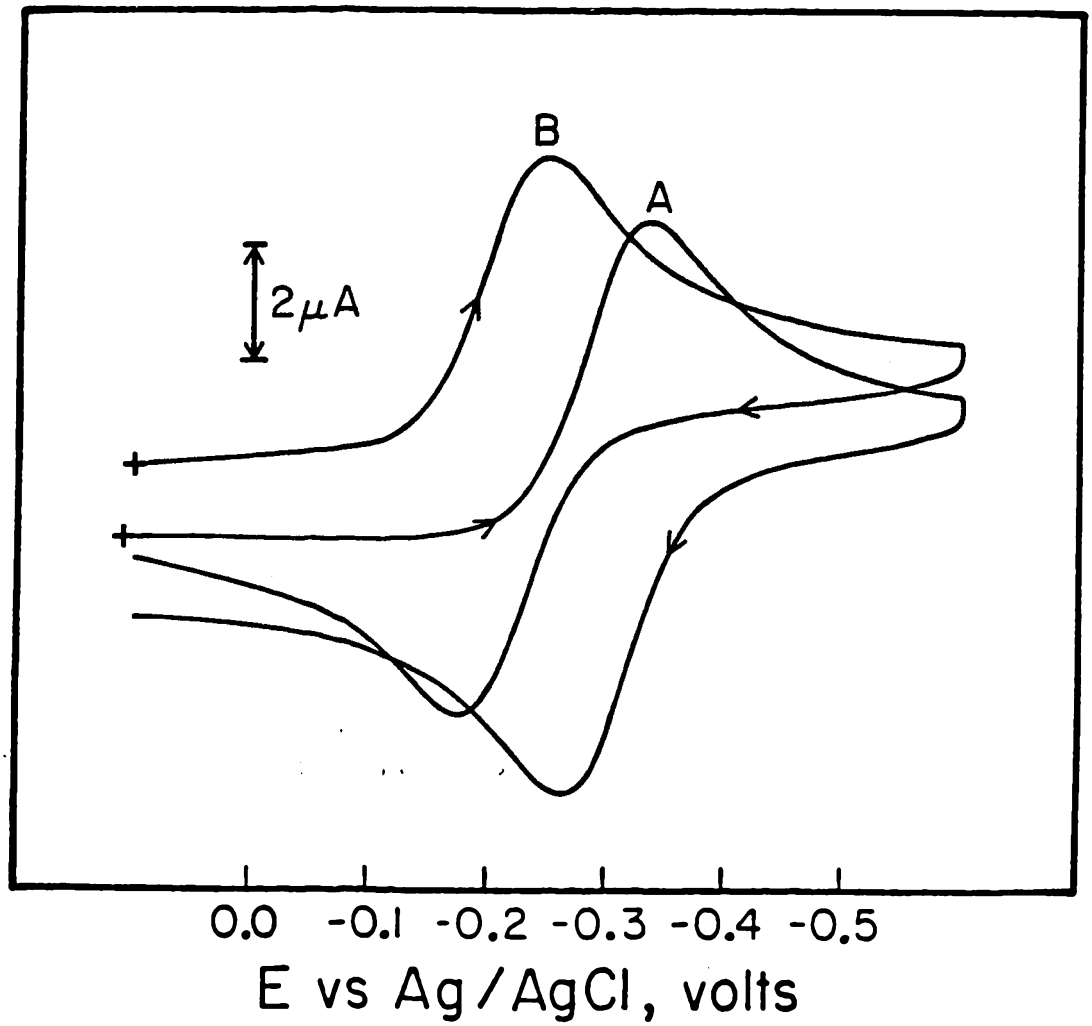
B
A
2μA
0.0 -0.1 -0.2 -0.3 -0.4 -0.5
E vs Ag/AgCl, volts

Adsorption measurements on mercury electrodes for solutions of trans-$Ru(NH_3)_4$(NCS)(vinylpyridine)Ru(EDTA) as a function of potential and concentration are shown in Figure 5. Although these solutions show some adsorption, the quantities involved (7-12 $\mu coul/cm^2$) are small, especially if the adsorbing molecules are perpendicular to the surface via adsorption through the thiocyanate ligand as anticipated. However, the potential dependence of the adsorption of trans-$Ru(NH_3)_4$-(NCS)(vinylpyridine)Ru(EDTA) species, more adsorption at more negative potentials, is in the opposite direction to that found for $Ru(NH_3)_5NCS^{2+}$ or $Ru(NH_3)_5NCS^{+}$ in the same media (Compare Figure 5 to Figure 2A). In fact, adsorption measurements performed on mM solutions of $Ru(NH_3)_5$(vinylpyridine)Ru(EDTA)$^{+}$, [38] which has no thiocyanate ligand to help induce adsorption, exhibits the same potential dependence and extent of adsorption as trans-$Ru(NH_3)_4$(NCS)(vinylpyridine)Ru(EDTA). This may imply that it is the size and solubility of the entire ruthenium ammine vinylpyridine ruthenium EDTA assembly which dictates its adsorption on mercury and that perhaps adsorption occurs with the molecule lying flat on the electrode surface. The possibility that the thiocyanate ligand is lost during the formation of trans-$Ru(NH_3)_4$(NCS)(vinylpyridinium)$^{2+}$ was ruled out from a comparison of the Ru(II) oxidation potential (E_{p_a}) for the product formed from electro-reductions of either $Ru(NH_3)_5NCS^{2+}$ or trans-$Ru(NH_3)_4$-(NCS)(SO_4) in the presence of 4-vinylpyridine ($E_{p_a} \sim +0.75$ V) to that for $Ru(NH_3)_5$(vinylpyridinium)$^{3+}$ ($E_{p_a} \sim +0.95$ V). Thus it appears that the ruthenium ammine isothiocynate complex is not suitable as a molecular anchor for attachment of redox couples to the mercury

Figure 5. Potential dependence of the adsorption at mercury electrodes of: □ - 2 mM $Ru(NH_3)_5$ (4-vinylpyridine) in the presence of 1 mM Ru(EDTA); ■ 2 mM trans-$Ru(NH_3)_4$(NCS)(4-vinylpyridine) in the presecce of 0.5 mM Ru(EDTA); ● - 2 mM trans-$Ru(NH_3)_4$(NCS)-(4-vinylpyridine) in the presence of 1 mM Ru(EDTA); ▲ 2 mM trans-$Ru(NH_3)_4$(NCS)(4-vinylpyridine) in the presence of 2 mM Ru(EDTA). Complete coordination of Ru(EDTA) to the pyridine nitrogen was observed. The electrode was held for 30 sec at the indicated potential and stepped to -0.6 V for Ru(III) reduction or + 0.1 V for Ru(II) oxidation. Supporting electrolyte: 0.2 M CF_3COONa; pH = 6.0.

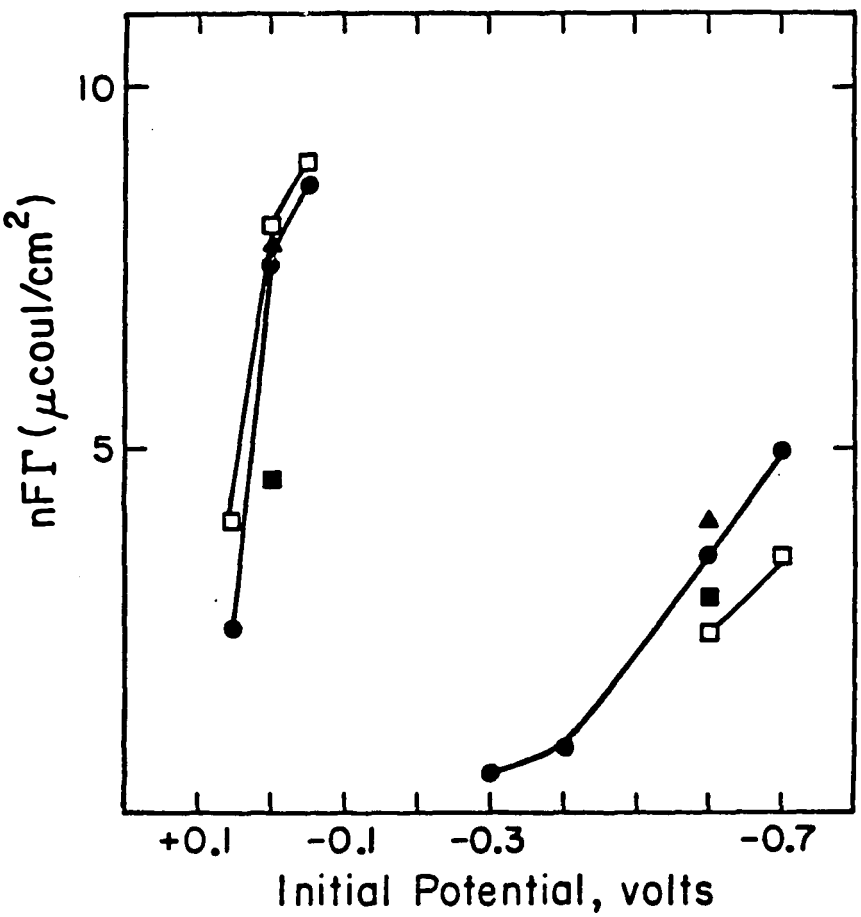
10
5
nFΓ (μcoul/cm²)
+0.1
-0.1
-0.3
-0.7
Initial Potential, volts

electrode only because its adsorption was not strong enough.

Attempts to modify the adsorption behavior of the ruthenium ammine vinylpyridine ruthenium EDTA species by using SeCN to help induce adsorption on mercury proved unsuccessful because of difficulties in preparing a complex with N-bound selenocyanate coordinated to the ruthenium ammine center. No further efforts were expended on this synthesis although it is still believed that the general approach of substituted ruthenium ammine complexes may yet prove fruitful in the preparation of a molecule which is adsorbed and can coordinate various redox couples so that their electrode kinetic parameters could be measured.

CONCLUSIONS

Comparison of the spectral and electrochemical properties of N-bound ruthenium pentaammine isothiocyanate versus S-bonded ruthenium pentaammine thiocyanate has shown that there are minor differences in their formal potentials and the position of their visible absorption bands. In particular, the adsorption behavior on mercury electrodes is very indicative of which linkage isomer is present. The lability of several substituted ruthenium(II) ammine complexes was exploited to prepare trans-$Ru(NH_3)_4(NCS)(4\text{-vinylpyridine})^+$. This molecule was used to both coordinate $Ru(EDTA)^-$ and to adsorb the resulting species on mercury. Unfortunately, the adsorption was not strong enough to allow measurement of the electrode kinetics to the adsorbed assembly.

ACKNOWLEDGMENTS

Initial exploratory experiments by Dr. Lorenz Walder aided and guided me in portions of the work described here.

REFERENCES

1. P. C. Ford, Coord. Chem. Rev., 5, 75 (1970).
2. R. E. Shepherd and H. Taube, Inorg. Chem., 12, 1392 (1973).
3. J. A. Marchant, T. Matsubara and P. C. Ford, Inorg. Chem., 16, 2160 (1977).
4. H. S. Lim, D. J. Barclay, and F. C. Anson, Inorg. Chem., 11,
5. S. Isied and H. Taube, Inorg. Chem., 15, 3070 (1976).
6. T. Matsubara and P. C. Ford, Inorg. Chem., 15, 1107 (1976).
7. P. C. Ford, De F. P. Rudd, R. Gaunder and H. Taube, J Am. Chem. Soc., 90, 1187 (1968).
8. S. S. Isied and H. Taube, Inorg. Chem., 13, 1545 (1974).
9. R. J. Allen and P. C. Ford, Inorg. Chem., 11, 679 (1972).
10. C. R. Brulet, S. S. Isied and H. Taube, J. Am. Chem. Soc., 95, 4758 (1973).
11. S. S. Isied, to be published, 1982.
12. R. Larsson and A. Miezis, Acta Chem. Scand., 23, 37 (1969).
13. C. Pecile, Inorg. Chem., 5, 210 (1966).
14. R. A. Bailey, S. L. Kozak, T. W. Michelsen and W. N. Mills, Coord. Chem. Rev., 6, 407 (1971).
15. S. Frank, unpublished results.
16. a) R. F. Lane and A. T. Hubbard, J. Phys. Chem., 77, 1401, 1411 (1973).

    b) A. P. Brown, C. Koval and F. C. Anson, J. Electroanal. Chem., 72, 379 (1976).

    c) R. J. Burt, G. J. Leigh and C. J. Pickett, Chem. Commun., 1940 (1976).

REFERENCES (continued)

d) J. R. Lenhard and R. W. Murray, J. Electroanal. Chem., 78, 195 (1977) and references cited therein.

e) J. F. Evans, T. Kuwara, M. T. Henne and G. P. Royer, J. Electroanal. Chem., 80, 409 (1977).

17. a) A. P. Brown and F. C. Anson, J. Electroanal. Chem., 92, 133 (1978).

b) M. Sharp, M. Petersson and K. Edstrom, J. Electroanal. Chem., 109, 271 (1980).

18. L. H. Vogt, J. L. Katz and S. E. Wiberley, Inorg. Chem., 4, 1157 (1965).

19. Roger Baar, unpublished results.

20. J. L. Woodhead and J. M. Fletcher, J. Chem. Soc., 5039 (1961).

21. a) P. C. Ford and C. Sutton, Inorg. Chem., 8, 1544 (1969).

b) J. Broomhead and L. Kane-Maguire, Proc. Int. Conf. Coord. Chem., 12th, 147 (1969).

c) F. Basolo, L. Kane-Maguire, P. S. Sheridan and R. G. Pearson, Proc. Int. Conf. Coord. Chem., 12th, 226 (1969).

22. W. M. Moore and D. G. Peters, J. Am. Chem. Soc., 97, 139 (1975).

23. a) G. Lauer, R. Abel and F. C. Anson, Anal. Chem., 39, 765 (1967).

b) J. A. Turner, Ph.D. Thesis, Colorado State University, 1977.

24. This reference electrode has a potential 45 mV negative of SCE.

25. F. C. Anson, Anal. Chem., 38, 54 (1966).

26. F. C. Anson, J. H. Christie and R. A. Osteryoung, J. Electroanal. Chem., 13, 343 (1967).

REFERENCES (continued)

27. S. S. Isied and H. Taube, J. Am. Chem. Soc., 95, 8198 (1973).

28. a) R. S. Nicholson and I. Shain, Anal. Chem., 36, 706, 1251 (1964).

b) R. S. Nicholson, Anal. Chem., 38, 1406 (1966).

29. J. Armor and A. Haim, J. Am. Chem. Soc., 93, 867 (1971).

30. G. M. Brown and N. Sutin, J. Am. Chem. Soc., 101, 883 (1979).

31. P. Delahay, "Doublr Layer and Electrode Kinetics", Ch 5, Wiley-Interscience, 1965.

32. a) D. J. Barclay, E. Passeron and F. C. Anson, Inorg. Chem., 9, 1024 (1970).

b) F. C. Anson and J. Caja, J. Electrochem. Soc., 117, 306 (1970).

33. S. Frank, Ph.D. Thesis, California Institute of Technology, 1974.

34. L. Walder, unpublished results.

35. H. Lehmann, K. J. Schenk, G. Chapuis and A. Ludi, J. Am. Chem. Soc., 101, 6197 (1979).

36. T. Matsubara and C. Creutz, Inorg. Chem., 18, 1956 (1979).

37. N. Oyama and F. C. Anson, J. Electroanal. Chem., 88, 289 (1978).

38. $Ru(NH_3)_5$(vinylpyridine)$Ru(EDTA)^+$ was generated from electroreduction of $[Ru(NH_3)_5Cl]Cl_2$ at -0.6 V in the presence of 40 mM 4-vinylpyridinium for 7 hours followed by precipitation of chloride ions with Ag^+. After filtering off the AgCl, the pH was raised to 6.5 and the aqueous solution washed with three 20-ml portions of diethyl ether. Then a slight vacuum was applied to remove

REFERENCES (continued)

dissolved ether and the pH readjusted to 6.0. $Ru(NH_3)_5$(vinylpyridine)Ru(EDTA)$^+$ was prepared by addition of Ru(EDTA)$(H_2O)^-$ to the $Ru(NH_3)_5$(vinylpyridine)$^{2+}$ solution.

APPENDIX I

Simple Electron Transfer Reactions: Comparison of Experimental Results to Theoretical Predictions

The following compilation of published rate constants for heterogeneous and homogeneous electron exchange reactions grew out of a search for complexes in which large intramolecular rearrangements accompany electron transfer (see Part II). It was intended to use such complexes in testing of several of the predictions of Marcus' theory.[1-7] With few exceptions, only experimentally measured rate constants as reported in the original publications are included in Table I. Electrode processes were restricted to those in which both reactant and product are soluble in the solute. (For a more extensive compilation of electrode reactions, including amalgam formation, see Tanaka.[8]) All values are uncorrected (i.e., the heterogeneous rate constants are not corrected for the effects of the electrical double layer and the homogeneous rate constants are not corrected for ionic strength effects) because suitable corrected values are rarely available. This table has proven useful to numerous members of the Anson group and is being included here in the hope that it may be helpful to future group members.

There are several well known theories of electron transfer, including those by Marcus,[1-7] Hush,[9-11] and Dogonadze,[12] but the theory proposed by Marcus for simple, outer-sphere electron transfer is particularly well-suited to providing theoretical equations with physical significance concerning the factors which influence the rate. Although there are several good references[2,7,13,14] which discuss Marcus theory and its application to electron transfer reactions, I will attempt to summarize some of the basic equations so that a discussion of several of the predictions of Marcus theory may be examined in light of this compilation.

TABLE I

Compilation of Heterogeneous Electron Transfer and Self-Exchange Rate Constants for Redox Reactions

METHOD ABBREVIATIONS

ACV = AC Voltammetry

ACI = AC Impendance

CV = Cyclic Voltammetry

CH = Chronocoulometry

CI = Current Impulse

ES = Exchange and Separation

ESR = Electron Spin Resonance

FR = Faradaic Rectification

G = Galvonastatic

GDP = Galvanostatic Double Pulse

HTE = Hydrodynamic Tubular Electrode

HV = Hydrodynamic Voltammetry

IR = Infrared Spectroscopy

IT = Isotopic Tracer

IV = Current-Voltage Curves

LOA = Loss of Optical Activity

NMR = Nuclear Magnetic Resonance

NPS = Normalized Potential Sweep

P = Potentiostatic

PG = Polarography

RD = Rotating Disk Voltammetry

RFPG = Radio Frequency Polarography

SV = Staircase Voltammetry

TD = Transfer Diffusion

CHEMICAL AND ELECTRODE MATERIAL ABBREVIATIONS

aq = Hydrated

bipy = 2,2′-bipyridine

C = Carbon (graphite) Electrode

Cp = cyclopentadienyl

CP = Carbon Paste Electrode

DMF = dimethylformamide

DMSO = dimethyl sulfoxide

DME = dimethoxyethane

en = ethylenediamine

EDTA = ethylenediaminetetraacetate

GC = Glassy Carbon Electrode

HMPA = hexamethyl phosphoramide

NB = nitrobenzene

Ox = oxalate

phen = 1,10-phenanthroline

TCNQ = 7,7′,8,8′-tetracyanoquinodimethane

TCNE = tetracyanoethylene

THF = tetrahydrofuran

TBAF = tetra-n-butylammonium hexafluorophosphate

TPAP = tetrapropylammonium perchlorate

TEAP = tetraethylammonium perchlorate

THAP = tetra-n-hexylammonium perchlorate

TEAB = tetraethylammonium bromide

TBAI = tetra-n-butylammonium iodide

TBAP = tetra-n-butylammonium perchlorate

REDOX COUPLE	SUPPORTING ELECTROLYTE (H_2O unless otherwise specified)	TEMP (°C)	ELECTRODE MATERIAL	k_s ($cm\ s^{-1}$)	k_{ex} ($M^{-1}s^{-1}$)	METHOD	REF.*
$Ce(aq)^{4+/3+}$	1.0 M H_2SO_4	25	GC	5.3×10^{-5}		CV,RD	7
"	1.0 M $HClO_4$	22	Pt	2.0×10^{-5}		RD	8*
"	1.0 M H_2SO_4	25	Pt	3.7×10^{-4}		RD	9
"	0.8 M H_2SO_4	0			0.42	IT	10*
$Co(aq)^{3+/2+}$	5.6 M $HClO_4$	2	Pt	1.8×10^{-7}		IV	11
"	3.0 M $NaClO_4$	25			3.3	IT	12*
"	H_2O only	0			0.75	IT	13
"	μ = 1.0 M	25			5	IT	14*
$Co(phen)_3^{3+/2+}$	H_2O only	13			6	IT	13*
"	1.0 M KCl	25	Pt	0.048		IV	15
$Co(NH_3)_6^{3+/2+}$	1.0 M NH_4Cl/7 M NH_3	25	Pt	5.25×10^{-4}		IV	16
"	1.0 M NH_4Cl/1 M NH_3	25	Pt	5×10^{-6}		HTE	17
"	μ = 1.0 M	65			$<10^{-10}$	IT	18
"	0.17 M NH_4Cl/5.7 M NH_3	45			$<6 \times 10^{-7}$	IT	19
"	1.0 M NH_4Cl/1 M NH_3	25	Pt	4.5×10^{-6}		HV	20
$Co(EDTA)^{-/2-}$	0.4 M $NaNO_3$/pH = 5	25	Hg	2.9×10^{-2}		P	21
"	H_2O only	100			1.4×10^{-4}	LOA	22*
"	0.1 M $HClO_4$	25	Hg	0.01		SV	6

* References with asterisks contain additional rate constants for the same redox couple under different conditions.

REDOX COUPLE	SUPPORTING ELECTROLYTE (H_2O unless otherwise specified)	TEMP (°C)	ELECTRODE MATERIAL	k_s ($cm\ s^{-1}$)	k_{ex} ($M^{-1}s^{-1}$)	METHOD	REF.*
$Co(EDTA)^{-/2-}$	pH = 2/$HClO_4$	85			2.1×10^{-4}	ES	23*
$Co(en)_3^{3+/2+}$	0.05 M $NaClO_4$	25	Hg	2.9×10^{-2}		SV	6
"	0.1 M $NaClO_4$	25	Hg	6.5×10^{-2}		SV	6
"	μ = 1.0 M	25			8.0×10^{-5}	IT	24
"	0.98 M KCl	25			7.5×10^{-5}	IT	13
"	μ = 0.9 M	25			5×10^{-5}	ES	19
$Cr(aq)^{3+/2+}$	1.0 M KCl	25	GC	10^{-4}		CV,RD	7*
"	1.0 M $NaClO_4$	25	Hg	5×10^{-6}		PG	25*
"	1.0 M $HClO_4$	25			$\leq 2 \times 10^{-5}$	IT	26*
"	1.0 M KCl	20	Hg	10^{-5}		NAC	27
"	1.0 M $NaClO_4$/pH = 2	24	Hg	7.5×10^{-6}		PG,CH	28*
"	1.0 M $LiClO_4$	25	Hg	3.6×10^{-6}		PG	29*
"	0.5 M $NaClO_4$	25	Hg	7.1×10^{-6}		PG	30*
$Cr(bipy)_3^{+/0}$	0.2 M TBAP/DMF	25	Hg	1.3		GDP	31
"	0.2 M TBAP/DMF	25	Pt	0.88		GDP	31
"	0.5 M $LiClO_4$/DMF	25	Hg	1.0		GDP	31
"	DMF only	25			1.5×10^9	ESR	32

* References with asterisks contain additional rate constants for the same redox couple under different conditions.

REDOX COUPLE	SUPPORTING ELECTROLYTE (H_2O unless otherwise specified)	TEMP (°C)	ELECTRODE MATERIAL	k_s ($cm\ s^{-1}$)	k_{ex} ($M^{-1}s^{-1}$)	METHOD	REF.*
$Eu(aq)^{3+/2+}$	1.0 M $NaClO_4$/pH = 3	25	Hg	2.5×10^{-4}		ACI	33
"	1.0 M KI	25	Hg	3.3×10^{-3}		ACI	34
"	1.0 M KCl	25	Hg	5×10^{-4}		ACI	34
"	1.0 M $NaClO_4$	25	Hg	9.5×10^{-5}		PG	35
"	1.0 M NaCl	25	Hg	1.2×10^{-4}		PG	35
"	1.0 M Na_2SO_4	25	Hg	1.8×10^{-5}		PG	35
"	1.0 M $NaClO_4$	25	Hg	2.9×10^{-4}		PG	33
"	0.1 M TPAP/DMF	20	Hg	1.6×10^{-4}		PG	36
"	μ = 2.0 M	25			$<10^{-4}$	IT	37*
"	1.0 M KCl	20	Hg	2.1×10^{-4}		ACI	27
"	1.0 M KI	20	Hg	1.6×10^{-3}		ACI	27
"	1.0 M KSCN	20	Hg	8×10^{-3}		ACI	27
"	1.0 M KSCN	25	Hg	3×10^{-4}		ACI	38*
"	0.5 M $NaClO_4$	25	Hg	1.3×10^{-4}		PG,ACV	39*
$Fe(aq)^{3+/2+}$	1.0 M $HClO_4$	20	Pt	5×10^{-3}		RD	40
"	0.1 M $HClO_4$	25	Pt	1.1×10^{-2}		HV	41
"	1.0 M $HClO_4$	20	Pt	5×10^{-3}		ACI	27

* References with asterisks contain additional rate constants for the same redox couple under different conditions.

REDOX COUPLE	SUPPORTING ELECTROLYTE (H_2O unless otherwise specified)	TEMP (°C)	ELECTRODE MATERIAL	k_s (cm s^{-1})	k_{ex} ($M^{-1}s^{-1}$)	METHOD	REF.*
$Fe(aq)^{3+/2+}$	1.0 M H_2SO_4	25	Pt	4.3×10^{-3}		RD	9
"	0.55 M $HClO_4$	22			10	ES	42*
"	1.0 M $HClO_4$	25	Pt	9×10^{-3}		RD	43*
"	0.5 M H_2SO_4	25	Pt	7×10^{-3}		RD	43*
"	1.0 M H_2SO_4	25	Pt	0.033		FR	44*
"	Na^+/pH = 2	0			0.87	ES	45*
"	1.0 M H_2SO_4	25	Hg	5.3×10^{-3}		G	46*
"	0.1 M $HClO_4$	25	Pt	7.6×10^{-3}		HV	20
"	0.15 M $NaClO_4$/0.05 M $HClO_4$	20			55	IT	47
"	μ = 0.5 M	25			4.0	IT	48*
"	0.9 M $HClO_4$	25	GC	1.3×10^{-3}		CV,RD	7*
"	0.45 M H_2SO_4	25	GC	8.6×10^{-4}		CV,RD	7*
"	0.45 M H_2SO_4	25	Pt	4.3×10^{-3}		CV,RD	7*
"	1.0 M H_2SO_4	25	GC	1.2×10^{-3}		CV	7
"	0.5 M H_2SO_4	25	Pt	3.6×10^{-3}		RD	49
$Fe(CN)_6^{3-/4-}$	1.0 M KCl	25	Pt(ox)	0.028		CI	50
"	1.0 M KCl	25	Pt	0.08		HV	41
"	1.0 M KCl	20	Pt	0.09		HV	51

* References with asterisks contain additional rate constants for the same redox couple under different conditions.

REDOX COUPLE	SUPPORTING ELECTROLYTE (H_2O unless otherwise specified)	TEMP (°C)	ELECTRODE MATERIAL	k_s ($cm\ s^{-1}$)	k_{ex} ($M^{-1}s^{-1}$)	METHOD	REF.*
$Fe(CN)_6^{3-/4-}$	1.0 M KNO_3	35	Pt	0.066		RFPG	52
"	1.0 M KCl	25	Pt	0.08		RD	9*
"	0.5 M K_2SO_4	25	Pt	0.13		RD	9*
"	1.0 M KCl	32			9.2×10^4	NMR	53*
"	0.5 M K_2SO_4	25	Pt	0.02		RD	43
"	0.25 mM EDTA/0.6 mM $(C_6H_5)_4As^+$	0.1			4.2	IT	54*
"	1.0 M KCl	20	Pt	0.09		ACI	27
"	0.5 M K_2SO_4	20	Pt	0.13		ACI	27
"	Na^+/pH = 2	50			10^3	ES	55
"	0.01 M KOH	25			3×10^2	ES	55
"	1.0 M KF	25	Au	8×10^{-2}		CI	56*
"	1.0 M LiCl	25	Au	2×10^{-2}		CI	56*
"	1.0 M NaCl	25	Au	3.8×10^{-2}		CI	56*
"	1.0 M LiCl	25	Au	1.3×10^{-2}		RD	57*
"	1.0 M NaCl	25	Au	2×10^{-2}		RD	57*
"	1.0 M KCl	25	Au	2×10^{-2}		RD	57*

* References with asterisks contain additional rate constants for the same redox couple under different conditions.

REDOX COUPLE	SUPPORTING ELECTROLYTE (H_2O unless otherwise specified)	TEMP (°C)	ELECTRODE MATERIAL	k_s ($cm\ s^{-1}$)	k_{ex} ($M^{-1}s^{-1}$)	METHOD	REF.*
$Fe(CN)_6^{3-/4-}$	0.5 M K_2SO_4	25	GC	0.025		CV,RD	7
"	1.0 M KCl	22	Pt	0.109		CV	58
$(Cp)_2Fe^{+/0}$	0.5 M LiCl/CH_3OH	25	Pt	0.7		GDP	5
"	0.035 M PF_6^-/CD_3CN	25			5.3×10^6	NMR	59*
"	0.1 M $DClO_4/CD_3OD$	25			4.8×10^6	NMR	59*
"	0.1 M TEAP/CH_3CN	25	Pt	0.044		CV	60*
"	0.1 M TEAP	25	Pt	0.166		CV	60*
"	0.6 M $NaClO_4/CD_3CN$	25			3.1×10^6	NMR	61*
"	0.02-0.2 M KPF_6/CD_3CN	25			5.3×10^6	NMR	61*
"	0.1 M $HClO_4$/aq CH_3OH	25			6.2×10^{10}	TD	62*
"	0.5 M LiCl	25	Hg	0.7		GDP	63
"	0.1 M TEAP/C_2H_5OH	25	Pt	0.016		CV	60*
"	0.05 M H^+/CH_3OH	25			2×10^{10}	TD	64*
"	0.05 M H^+/C_2H_5OH	25			10^{10}	TD	64*
"	H_2O - CH_3OH	0			$>7 \times 10^6$	IT	18*
"	H_2O - CH_3OH	-75			8.7×10^5	IT	18*
"	0.1 M TEAP/CH_3CN	25	Pt	0.22		CV	58

* References with asterisks contain additional rate constants for the same redox couple under different conditions.

REDOX COUPLE	SUPPORTING ELECTROLYTE (H_2O unless otherwise specified)	TEMP (°C)	ELECTRODE MATERIAL	k_s (cm s^{-1})	k_{ex} ($M^{-1}s^{-1}$)	METHOD	REF.*
$Fe(bipy)_3^{3+/2+}$	0.2 M KF	25	Pt	0.80		GDP	31
"	0.2 M TBAP/DMF	25	Pt	1.1		GDP	31
"	0.068 M PF_6^-/CD_3CN	25			3.7×10^6	NMR	65*
$Fe(phen)_3^{3+/2+}$	1.84 M Na_2SO_4	25			3.3×10^8	TD	66
"	0.5 M LiCl	25	Pt	0.7		GDP	5,63
"	0.05 M PF_6^-/CD_3CN	25			6×10^6	NMR	65
"	0.034 M ClO_4^-/CD_3CN	25			1.4×10^7	NMR	65
"	0.05 M Cl^-/D_2O	17			4.9×10^7	NMR	65
$IrCl_6^{2-/3-}$	1.0 M HCl	25	Pt	0.5		GDP	5
"	1.0 M HCl	25	Hg	0.5		GDP	63
"	0.1 M NH_4Cl	25			2.5×10^5	IT	67
$MnO_4^{-/2-}$	0.1 M NaOH	25	CP	2.4×10^{-2}		RD	68*
"	0.1 M NaOH/1.0 M $NaClO_4$	25	GC	3.7×10^{-3}		CV	68*
"	0.9 M NaOH	25	C	1.45×10^{-2}		RD	9
"	0.16 M NaOH	0			710	IT	69*
"	0.16 M NaOH	22			3000	IT	69*

* References with asterisks contain additional rate constants for the same redox couple under different conditions.

REDOX COUPLE	SUPPORTING ELECTROLYTE (H_2O unless otherwise specified)	TEMP (°C)	ELECTRODE MATERIAL	k_s (cm s^{-1})	k_{ex} ($M^{-1}s^{-1}$)	METHOD	REF.*
$Mo(CN)_8^{3-/4-}$	0.2 M KF	25	Pt	0.5		GDP	5
"	0.2 M KF	25	Hg	0.5		GDP	63
"	H_2O only	25			3×10^4	IT	70
$Os(bipy)_3^{3+/2+}$	0.034 M PF_6^-/CD_3CN	31			2.2×10^7	NMR	65
"	0.2 M TBAP/DMF	25	Hg	0.87		GDP	31
$Ru(bipy)_3^{3+/2+}$	0.2 M TBAP/DMF	25	Hg	0.01		GDP	31
"	0.2 M TBAP/DMF	25	Pt	0.24		GDP	31
"	0.045 M PF_6^-/CD_3CN	25			8.3×10^6	NMR	65
$Ru(NH_3)_6^{3+/2+}$	0.1 M $NaClO_4$	25	Hg	> 1		SV	6
"	0.013 M $DClO_4/D_2O$	25			8×10^2	IR	71*
"	0.16 M $NaOAc/D_2O$	25			4.3×10^3	IR	71*
$V(aq)^{3+/2+}$	1.0 M $HClO_4$	20	Hg	4×10^{-3}		ACI	27
"	0.1 M KPF_6/pH = 2.5	25	Hg	10^{-3}		PG,CV	3
"	1.0 M $NaClO_4$/pH = 2.5	25	Hg	10^{-3}		PG,CV	3
"	0.2 M $NaClO_4$/0.02 M $HClO_4$	25	Hg	6×10^{-3}		ACI	72
"	1.0 M $NaClO_4$/0.02 M $HClO_4$	25	Hg	5.3×10^{-3}		ACI	72
"	0.1 M $NaClO_4$	25	Hg	5.5×10^{-3}		ACI	72

* References with asterisks contain additional rate constants for the same redox couple under different conditions.

REDOX COUPLE	SUPPORTING ELECTROLYTE (H_2O unless otherwise specified)	TEMP (°C)	ELECTRODE MATERIAL	k_s ($cm\ s^{-1}$)	k_{ex} ($M^{-1}s^{-1}$)	METHOD	REF.*
$V(aq)^{3+/2+}$	1.0 M $HClO_4$	25			0.014	IT	73*
"	μ = 2.0 M	25			0.01	IT	73*
"	0.5 M K_2Ox	20	Hg	1.4×10^{-3}		NAC	27
"	1.0 M H_2SO_4	15	Hg	1.4×10^{-3}		PG	74
"	1.0 M $HClO_4$	25	Hg	3.6×10^{-3}		PG	74
"	1.0 M $HClO_4$	25	Hg	3.5×10^{-3}		PG,CH	75*
"	1.0 M $HClO_4$	25			0.007	IT	75*
"	1.0 M $HClO_4$	24	Hg	5.7×10^{-3}		IV	76
"	1.0 M $HClO_4$	25	Hg	3.6×10^{-3}		FR	77*
Anthracene$^{0/-}$	0.5 M TBAP/DMF	22	Hg	5		ACV	4
"	DMF only	25			1.8×10^{9}	NMR	4
"	DME only	25			1.8×10^{9}	NMR	78*
"	0.5 M TBAI/DMF	22	Hg	5		ACI	79
"	0.1 M TBAI/DMF	25	Hg	4		ACI	80
"	0.02 M TBAP/DMF	25			2.0×10^{8}	ESR	81
Benzonitrile$^{0/-}$	0.1 M TMAP/DMF	23	Hg	0.56		NPS	82
"	0.5 M TBAP/DMF	22	Hg	0.61		ACV	4
"	0.1 M TBAP/DMF	23			5.5×10^{8}	NMR	4

* References with asterisks contain additional rate constants for the same redox couple under different conditions.

REDOX COUPLE	SUPPORTING ELECTROLYTE (H_2O unless otherwise specified)	TEMP (°C)	ELECTRODE MATERIAL	k_s (cm s^{-1})	k_{ex} ($M^{-1}s^{-1}$)	METHOD	REF.*
m-Nitrobenzonitrile$^{0/\cdot-}$	0.5 M TBAP/DMF	22	Hg	1.8		ACV	4
"	0.01 M TEAP/DMF	23			1.6×10^8	NMR	4
Nitrobenzene$^{0/\cdot-}$	0.5 M TBAP/DMF	22	Hg	2.2		ACV	4
"	0.1 M TBAP/DMF	23			3.9×10^9	NMR	4
"	0.5 M TBAI/DMF	22	Hg	2.2		ACV	79
"	HMPA only	25			1.9×10^8	ESR	83*
p-Dinitrobenzene$^{0/\cdot-}$	0.5 M TBAP/DMF	22	Hg	0.93		ACV	4
"	0.01 M TEAP/DMF	25			6.0×10^8	NMR	4
m-Dinitrobenzene$^{0/\cdot-}$	0.1 M TBAI/DMF	30	Hg	5.0		ACI	84
"	0.5 M TBAP/DMF	22	Hg	2.7		ACV	4
"	0.1 M TEAP/DMF	25			5.2×10^8	NMR	4
"	0.5 M TBAI/DMF	22	Hg	2.7		ACV	79
Dibenzofuran$^{0/\cdot-}$	0.5 M TBAP/DMF	22	Hg	2.9		ACV	4
"	0.1 M TBAP/DMF	25			1.6×10^9	NMR	4
Naphthalene$^{0/\cdot-}$	0.1 M TBAI/DMF	30	Hg	1.0		ACI	85
"	Li^+/THF	-30			2.6×10^8	ESR	86*
"	Na^+/DME	-30			3.4×10^8	ESR	86*

* References with asterisks contain additional rate constants for the same redox couple under different conditions.

REDOX COUPLE	SUPPORTING ELECTROLYTE (H_2O unless otherwise specified)	TEMP (°C)	ELECTRODE MATERIAL	k_s (cm s^{-1})	k_{ex} ($M^{-1}s^{-1}$)	METHOD	REF.*
Naphthalene$^{0/:}$	Na^+/DME + THF	-55			1.7×10^8	ESR	86*
"	Na^+/DME + THF	24			1.2×10^9	ESR	86*
"	Na^+/THF	-70			1.5×10^8	ESR	86*
"	Na^+/DME	23			1.6×10^9	ESR	87
"	Na^+/THF	23			1.5×10^9	ESR	87
"	K^+/DME	23			2.2×10^9	ESR	87
"	K^+/THF	23			3.0×10^9	ESR	87
1,4-Naphthaquinone$^{0/:}$	0.5 M TBAP/DMF	22	Hg	2.1		ACV	4
"	0.01 M TBAP/DMF	25			4.2×10^8	NMR	4
"	0.3 M TEAP/DMF	22	Hg	0.35		CV	88
"	0.1 M TEAB/CH_3CN	23	Pt	0.83		CV	89*
Perylene$^{0/:}$	0.1 M TBAI/DMF	25	Hg	4		ACI	80
"	0.5 M TBAP/DMF	22	Hg	5		ACV	4
"	DME only	25			2.1×10^9	NMR	4
"	0.2 M TBAP/DMF	22	Hg	5		ACV	79
"	0.4 M TBAI/DMF	20	Pt	1.0		GDP	90
"	0.4 M TBAP/NB	25	Pt	0.7		GDP	91

* References with asterisks contain additional rate constants for the same redox couple under different conditions.

REDOX COUPLE	SUPPORTING ELECTROLYTE (H_2O unless otherwise specified)	TEMP (°C)	ELECTRODE MATERIAL	k_s (cm s^{-1})	k_{ex} ($M^{-1}s^{-1}$)	METHOD	REF.*
Phthalonitrile$^{0/:}$	1.5 M TBAP/DMF	22	Hg	1.4		ACV	4
"	0.1 M TBAP/DMF	23			1.2×10^9	NMR	4
"	0.5 M TBAI/DMF	22	Hg	1.42		ACV	79
Terephthalonitrile$^{0/:}$	0.5 M TBAP/DMF	22	Hg	0.68		ACV	4
"	0.1 M TBAP/DMF	23			1.4×10^9	NMR	4
"	0.5 M TBAI/DMF	22	Hg	0.68		ACV	79
4-Cyanopyridine$^{0/:}$	0.5 M TBAP/DMF	22	Hg	0.42		ACV	4
"	0.1 M TBAP/DMF	23			6.8×10^8	NMR	4
t-Stilbene$^{0/:}$	0.1 M TBAI/DMF	30	Hg	1.22		ACI	85*
"	0.1 M TBAI/DMF	30			6.8×10^8	ESR	85
"	0.5 M TBAI/DMF	22	Hg	1.6		ACV	79
"	0.1 M TBAI/DMF	25	Hg	2.5		ACI	80
α-Methyl-t-stilbene$^{0/:}$	0.1 M TBAI/DMF	30	Hg	0.43		ACI	85
"	DMF only	30			1.9×10^8	ESR	85
2,4,6,2',4',6'-hexa-methyl-t-stilbene$^{0/:}$	0.1 M TBAI/DMF	30	Hg	0.18		ACI	85
"	DMF only	30			8.0×10^7	ESR	85
Tetracene$^{0/:}$	DME only	25			1.9×10^9	ESR	92

* References with asterisks contain additional rate constants for the same redox couple under different conditions.

REDOX COUPLE	SUPPORTING ELECTROLYTE (H_2O unless otherwise specified)	TEMP (°C)	ELECTRODE MATERIAL	k_s (cm s^{-1})	k_{ex} ($M^{-1}s^{-1}$)	METHOD	REF.*
Tetracene$^{0/\cdot}$	0.1 M TBAI/DMF	30	Hg	1.64		ACI	85*
TCNE$^{0/\cdot}$	1.0 M KCl/CH_3CN	25	C	2×10^{-3}		CV	93
"	0.01-0.1 M Li^+/CH_3CN	25			1.7×10^9	ESR	94
TCNQ$^{0/\cdot}$	0.01-0.1 M K^+/CH_3CN	25			3.3×10^9	ESR	94
"	1.0 M KCl/CH_3CN	25	C	3.5×10^{-3}		CV	93
"	CH_3CN only	22			3.9×10^9	ESR	95*
Dibenzothiophene$^{0/\cdot}$	0.5 M TBAP/DMF	22	Hg	1.6		ACV	4
"	0.1 M TBAP/DMF	25			1.2×10^9	NMR	4
o-Toluenitrile$^{0/\cdot}$	0.5 M TBAP/DMF	22	Hg	0.63		ACV	4
"	0.1 M TBAP/DMF	23			8.6×10^8	NMR	4
p-Toluenitrile$^{0/\cdot}$	0.5 M TBAP/DMF	22	Hg	0.90		ACV	4
"	0.1 M TBAP/DMF	23			7.8×10^8	NMR	4
m-Toluenitrile$^{0/\cdot}$	0.5 M TBAP/DMF	22	Hg	0.63		ACV	4
"	0.1 M TBAP/DMF	23			5.6×10^8	NMR	4

* References with asterisks contain additional rate constants for the same redox couple under different conditions.

REFERENCES

1. R. A. Marcus, J. Phys. Chem., 67, 853 (1963).
2. N. S. Hush, Electrochim. Acta, 13, 1005 (1968).
3. M. J. Weaver, J. Phys. Chem., 84, 568 (1980).
4. H. Kojima and A. J. Bard, JACS, 97, 6317 (1975).
5. T. Saji, Y. Maruyama and S. Aoyagui, J. Electroanal. Chem., 86, 219 (1978).
6. J. F. Endicott, R. R. Schroeder, D. H. Chidester and D. R. Ferrier, J. Phys. Chem., 77, 2579 (1973).
7. R. J. Taylor and A. A. Humffray, J. Electroanal. Chem., 42, 347 (1973).
8. R. Greef, J. Electroanal. Chem., 18, 295 (1968).
9. Z. Galus and R. N. Adams, J. Phys. Chem., 67, 866 (1963).
10. P. B. Sigler and B. J. Masters, JACS, 79, 6353 (1957).
11. L. M. Boysova and A. L. Rotinyan, Soviet Electrochem., 3, 846, 1163 (1967).
12. H. S. Habib and J. P. Hunt, JACS, 88, 1668 (1968).
13. B. R. Baker, F. Basolo and H. M. Neumann, J. Phys. Chem., 63, 371 (1959).
14. N. A. Bonner and J. P. Hunt, JACS, 83, 3826 (1960).
15. H. Bartelt, Electrochim. Acta, 16, 629 (1971).
16. H. Bartelt and S. Landazury, J. Electroanal. Chem., 22, 105 (1969).
17. L. N. Klatt and W. J. Blaedel, Anal. Chem., 39, 1065 (1967).
18. D. R. Stranks, Disc. Faraday Soc., 29, 73 (1960).
19. W. B. Lewis, C. D. Corzell and J. W. Irvine, J. Chem. Soc., S386 (1949).

REFERENCES (continued)

20. J. Suzuki, Bull. Chem. Soc. Japan, 43, 755 (1970).

21. N. Tanaka and A. Yamada, Electrochim. Acta, 14, 491 (1969).

22. Y. Im and D. H. Busch, JACS, 83, 3357 (1961).

23. A. W. Adamson and K. S. Vorres, J. Inorg. and Nucl. Chem., 3, 206 (1956).

24. F. P. Dwyer and A. M. Sargeson, J. Phys. Chem., 65, 1892 (1961).

25. M. Zielinska-Iguaciuk and Z. Galus, J. Electroanal. Chem., 50, 41 (1974).

26. A. Anderson and N. A. Bonner, JACS, 76, 3826 (1954).

27. J. E. B. Randles and K. W. Somerton, Trans. Faraday Soc., 48, 937 (1952).

28. M. J. Weaver and F. C. Anson, Inorg. Chem., 15, 1871 (1976).

29. F. C. Anson, N. Rathjen and R. D. Frisbee, J. Electrochem. Soc., 117, 477 (1970).

30. R. Parsons and E. Passeron, J. Electroanal. Chem., 12, 524 (1966).

31. T. Saji and S. Aoyagui, J. Electroanal. Chem., 63, 31 (1975).

32. T. Saji and S. Aoyagui, Bull. Chem. Soc. Japan, 46, 2101 (1973).

33. B. Timmer, M. Sluyters-Rehback and J. Sluyters, J. Electroanal. Chem., 14, 181 (1967).

34. C. W. DeKreuk, M. Sluyters-Rehback and J. H. Sluyters, J. Electroanal. Chem., 28, 391 (1970).

35. Z. Borkowska and H. Elzanowska, J. Electroanal. Chem., 76, 287 (1977).

REFERENCES (continued)

36. N. S. Hush and J. M. Dyke, J. Electroanal. Chem., 53, 253 (1974).

37. D. J. Meier and C. S. Garner, J. Phys. Chem., 56, 853 (1952).

38. C. W. DeKreuk, M. Sluyters-Rehback and J. H. Sluyters, J. Electroanal. Chem., 33, 267 (1971).

39. B. Behr, Z. Borkowska and H. Elzanowska, J. Electroanal. Chem., 100, 853 (1979).

40. D. Jahn and W. Vielstich, J. Electrochem. Soc., 109, 849 (1962).

41. J. Jordan and R. A. Javick, Electrochim. Acta, 6, 23 (1962).

42. J. Silverman and R. W. Dodson, J. Phys. Chem., 56, 846 (1962).

43. D. H. Angell and T. Dickinson, J. Electroanal. Chem., 35, 55 (1972).

44. H. P. Agarwal, J. Electroanal. Chem., 5, 236 (1963).

45. J. Hudis and R. W. Dodson, JACS, 78, 911 (1956).

46. F. C. Anson, Anal. Chem., 33, 939 (1961).

47. J. Menashi, W. L. Reynolds and G. VanAuken, Inorg. Chem., 4, 299 (1965).

48. S. Fukushima and W. L. Reynolds, Talanta, 11, 283 (1964).

49. Z. Samec and J. Weber, J. Electroanal. Chem., 44, 229 (1973).

50. P. H. Daum and C. G. Enke, Anal. Chem., 41, 653 (1961).

51. J. Jordan, Anal. Chem., 27, 1708 (1955).

52. H. P. Agarwal, J. Electrochem. Soc., 110, 237 (1963).

53. M. Shporer, G. Ron, A. Lowenstein and G. Navon, Inorg. Chem., 4, 361 (1965).

REFERENCES (continued)

54. R. J. Campion, C. F. Deck, P. King and A. C. Wahl, Inorg. Chem., 6, 672 (1967).

55. C. F. Deck and A. C. Wahl, JACS, 76, 4054 (1954).

56. P. Bindra and H. Gerischer and L. M. Peter, J. Electroanal. Chem., 57, 435 (1974).

57. J. Kuta and E. Yeager, J. Electroanal. Chem., 59, 110 (1975).

58. M. Sharp, M. Petersson and K. Edstrom, J. Electroanal. Chem., 109, 271 (1980).

59. E. A. Yang, M. S. Chan and A. C. Wahl, J. Phys. Chem., 79, 2049 (1975).

60. J. W. Diggle and A. J. Parker, Electrochim. Acta, 18, 975 (1973).

61. E. S. Yang, M. S. Chan and A. C. Wahl, J. Phys. Chem., 84, 3094 (1980).

62. I. Ruff and I. Korosi-Odor, Inorg. Chem., 9, 186 (1970).

63. T. Saji, Y. Maruyama and S. Aoyagui, J. Electroanal. Chem., 86, 219 (1978).

64. I. Ruff, V. J. Friedrich, K. Demeter and K. Csillag, J. Phys. Chem., 75, 3303 (1971).

65. M. S. Chan and A. C. Wahl, J. Phys. Chem., 82, 2542 (1978).

66. I. Ruff and M. Zimonyi, Electrochim. Acta, 18, 515 (1973).

67. P. Hurwitz and K. Kustin, Trans. Faraday Soc., 62, 427 (1965).

68. K. Sekula-Brzezinska, P. Wrona and Z. Galus, Electrochim. Acta, 24, 555 (1979).

69. J. C. Sheppard and A. C. Wahl, JACS, 79, 1020 (1957).

REFERENCES (continued)

70. R. J. Campion, N. Purdie and N. Sutin, Inorg. Chem., 3, 1091 (1964).

71. T. J. Meyer and H. Taube, Inorg. Chem., 7, 2369 (1968).

72. D. Elliott, J. Electroanal. Chem., 22, 301 (1968).

73. K. V. Krishnamurity and A. C. Wahl, JACS, 80, 5921 (1961).

74. J. E. B. Randles, Can. J. Chem., 37, 238 (1959).

75. J. Lipkowski, A. Czerwinski, E. Cieszynska, Z. Galus, and J. Sobkowski, J. Electroanal. Chem., 119, 261 (1981).

76. V. S. Srinivasan, G. Torsi and P. Delahay, J. Electroanal. Chem., 10, 165 (1965).

77. D. Elliot and G. S. Buchanan, Anal. Chem., 39, 1245 (1967).

78. K. Suga and S. Aoyagui, Bull. Chem. Soc. Japan, 46, 755 (1973).

79. H. Kojima and A. J. Bard, J. Electroanal. Chem., 63, 117 (1975).

80. A. C. Aten and G. J. Hoytink, "Advances in Polarography," 1961.

81. K. Suga, H. Mizota, Y. Kanzaki and S. Aoyagui, J. Electroanal. Chem., 41, 313 (1973).

82. B. Aalstad, E. Ahlsabet and V. D. Parker, J. Electroanal. Chem., 122, 195 (1981).

83. G. R. Stevenson and R. Concepcion, JACS, 96, 4696 (1974).

84. M. E. Peover and J. S. Powell, J. Electroanal. Chem., 20, 427 (1969).

85. R. Dietz and M. E. Peover, Disc. Faraday Soc., 45, 154 (1968).

86. N. Hirota, R. Carraway and W. Schook, JACS, 90, 3611 (1968).

87. R. Chang and C. S. Johnson, JACS, 88, 2338 (1966).

REFERENCES (continued)

88. T. Rosanske and D. E. Evans, J. Electroanal. Chem., 72, 277 (1976).

89. R. Samuelsson and M. Sharp, Electrochim. Acta, 23, 315 (1978).

90. H. Mizota, K. Suga, Y. Kanzaki and S. Aoyagui, J. Electroanal. Chem., 44, 471 (1973).

91. N. Korzumi and S. Aoyagui, J. Electroanal. Chem., 55, 452 (1974).

92. K. Suga, S. Ishikawa and S. Aoyagui, Bull. Chem. Soc. Japan, 46, 808 (1973).

93. M. Sharp, Electrochim. Acta, 21, 973 (1976).

94. M. A. Komarynskz and A. C. Wahl, J. Phys. Chem., 79, 695 (1975).

95. N. Haran, Z. Luz and M. Shporer, JACS, 96, 4788 (1974).

Marcus applies transition state theory to describe the intersection of the two energy curves for electron transfer (reactants and products) and from this analysis he finds that the rate constant, k, measured for the electron transfer process is related to the free energy of activation, ΔG^*, for this reaction via

$$k = \kappa \rho Z \exp(-\Delta G^*/RT), \tag{1}$$

where κ is the transmission coefficient (usually assumed to be one for adiabatic reactions), i.e., the probability that the activated complex for the system will transfer from the energy surface of the reactants to that of the products; ρ is a ratio[5, 6] usually assumed to be unity; Z is a factor that measures the collision frequency of the redox molecules in solution with other redox molecules in solution or with the electrode, Z_{ex} and Z_{el}, respectively:

$$Z_{el} = \left(\frac{kT}{2\pi m}\right)^{\frac{1}{2}} \qquad Z_{ex} = R^2 \left(\frac{8\pi KT}{0.5m}\right)^{\frac{1}{2}} \tag{2}$$

where m = the molecular weight and R = collision diameter (usually taken as two times the molecular radius); and ΔG^* is the free energy of activation, assuming that the Franck-Condon principle holds (which states that internuclear distances and nuclear velocities do not change during an electronic transition).

The factors which influence the free energy of activation (ΔG^*) can be expressed by the following equation:

$$\Delta G^* = \frac{w_r + w_p}{2} + \frac{\lambda}{4} + \frac{\Delta G^\circ}{2} + \frac{(\Delta G^\circ + w_p - w_r)^2}{4\lambda} \tag{3}$$

where w_r, w_p represent the work needed to bring the reactant and the product to the reaction site from the bulk, ΔG° is the standard free energy of reaction at the reaction site ($\Delta G^\circ = -RT \ln K$, K being the equilibrium constant for the electron transfer reaction) and λ is the reorganization energy which can be subdivided into λ_i, the inner-sphere reorganization energy, and λ_o, the outer-sphere reorganization energy. The inner-sphere reorganization energy (treating the molecular changes as harmonic oscillators) is given by:

$$\lambda_i = \tfrac{1}{2}[\sum_{j,k} (k_{jk} \Delta q_j \Delta q_k)] \tag{4}$$

(where k_{jk} are the reduced force constants and $\Delta q_j, \Delta q_k$ are differences in equilibrium bond lengths and angles between the oxidized and reduced forms.) The outer-sphere reorganization energy (based upon a dielectric continuum for the solvent) for homogeneous (self-exchange) reactions is given by

$$(\lambda_o)_{ex} = (ne)^2(\frac{1}{2a_1} + \frac{1}{2a_2} - \frac{1}{R})(\frac{1}{D_{op}} - \frac{1}{D_s}) \tag{5a}$$

and for heterogeneous electron transfers (including the image potential) by

$$(\lambda_o)_{el} = \frac{(ne)^2}{2} (\frac{1}{2a_1} - \frac{1}{R'})(\frac{1}{D_{op}} - \frac{1}{D_s}) \tag{5b}$$

(where a_1, a_2 are radii of the ions, R' is twice the distance from the center of ion 1 to the electrode surface (usually taken as $2a_1$), D_{op} is the optical dielectric constant of the medium and D_s is the static dielectric

constant of the medium).

In calculating the work terms, w_r and w_p, an approximation normally applied[13,14] is given in equation 6

$$w = \frac{q_1 q_2}{D_s(d)(1+\beta d\sqrt{\mu})} \tag{6}$$

where q_1, q_2 are the charges on the ions, d is the distance from the center of ion 1 to ion 2, μ is the ionic strength of the medium and β is defined as

$$\beta = \left(\frac{8N^2e^2}{1000\,D_s RT}\right)^{\frac{1}{2}}, \tag{7}$$

where N is Avogadro's number and R, in this instance, is the molar gas constant. In circumstances where the work terms and ΔG° are small, then ΔG^* reduces to $\frac{\lambda_i + \lambda_0}{4}$.

Probably the most frequently cited and experimentally tested relationship that can be derived from Marcus' treatment is

$$k_{12} = (k_{11}k_{22}K_{12}f_{12})^{\frac{1}{2}}, \tag{8}$$

where k_{11} and k_{22} are the rate constants for the two homonuclear self-exchange reactions, k_{12} and K_{12} are the rate and equilibrium constant, respectively, for the cross reaction and f_{12}, defined as:

$$\log f_{12} = \frac{(\log K_{12})^2}{4\log\left(\frac{k_{11}k_{22}}{Z^2_{ex}}\right)} \tag{9}$$

is close to one except for reactions with large values of K_{12}. This

equation has been used to predict both cross reaction rates and self-exchange rates for a wide variety of reactions.[15-19]

A second result derivable from the Marcus treatment is:

$$\frac{k_s}{Z_{el}} = \left(\frac{k_{ex}}{Z_{ex}}\right)^{\frac{1}{2}} \quad \text{or} \quad \Delta G^*_{el} = \Delta G^*_{ex}/2 \; . \tag{10}$$

The rate data in Table I and the corresponding free energies in Table II are useful for testing these predicted relationships.

An alternate relationship between the activation energies for heterogeneous and homogeneous electron transfer has been proposed (although not derived) by Hush;[9]

$$\Delta G^*_{el} = \Delta G^*_{ex} \; . \tag{11}$$

Equation 11 is based upon the assertion that the image potential can be ignored for heterogeneous electron transfers. In Table III and in Figure 1 some results derived from the first two tables are shown. Nine systems seem to follow the Marcus prediction (when R = 2a), and thirteen the Hush prediction. About fifteen to twenty complexes do not appear to fit either expression and about three fall in between the two. Closer inspection reveals that the Marcus equation adequately predicts the relationship between heterogeneous and homogeneous electron transfer rates for complexes with k_{ex} between 10^{-4} and $10^{4}\ M^{-1}s^{-1}$, while the Hush equation works better for systems with k_{ex} in the 10^{7} to $10^{9}\ M^{-1}s^{-1}$ range. However, for many of the redox couples with k_{ex} greater than $10^{9}\ M^{-1}s^{-1}$ (i.e., near the diffusion-limited rate) neither

TABLE II

Free Energies of Activation for Heterogeneous and Homogeneous Electron Transfer Reactions

Case Number	Redox Couple	r(Å)[a]	Z_{el} (cm/sec)[b]	Z_{ex} ($M^{-1}s^{-1}$)[b]	ΔG^*_{el}(eV)[c]	ΔG^*_{ex}(eV)[c]
1	$Ce^{3+/4+}$	3.74	$3.9*10^3$	$2.4*10^{11}$	0.42-0.49	0.63
2	$Co(aq)^{2+/3+}$	3.48	$5.0*10^3$	$2.5*10^{11}$	0.57	0.58-0.69
3	$Co(NH_3)_6^{2+/3+}$	3.35	$4.95*10^3$	$2.4*10^{11}$	0.41-0.52	>1.21
4	$Co(EDTA)^{-/2-}$	--	$3.8*10^3$	$2.0*10^{11}$	0.34	<1.02
5	$Co(en)^{2+/3+}$	--	$4.06*10^3$	$2.0*10^{11}$	0.29-0.30	0.91
6	$Cr(aq)^{2+/3+}$	3.49	$5.0*10^3$	$2.6*10^{11}$	0.50-0.55	0.95
7	$Cr(bipy)^{0/+}$	6.1	$2.8*10^3$	$4.4*10^{11}$	0.20	0.15
8	$Eu(aq)^{2+/3+}$	--	$5.0*10^3$	$2.0*10^{11}$	0.36-0.50	>0.89
9	$Fe(aq)^{2+/3+}$	3.51	$5.0*10^3$	$2.6*10^{11}$	0.31-0.36	0.58-0.64
10	$Fe(CN)_6^{3-/4-}$	4.65	$4.3*10^3$	$4.0*10^{11}$	0.25-0.40	0.39-0.60
11	$Cp_2Fe^{0/+}$	3.5	$4.6*10^3$	$2.9*10^{11}$	0.30	0.29
12	$Fe(bipy)_3^{2+/3+}$	--	$2.7*10^3$	$2.0*10^{11}$	0.20	0.28
13	$Fe(phen)_3^{2+/3+}$	--	$2.6*10^3$	$2.0*10^{11}$	0.21	0.17-0.26
14	$IrCl_6^{2-/2-}$	--	$3.1*10^3$	$2.0*10^{11}$	0.22	0.35

TABLE II (continued)

Case Number	Redox Couple	r(Å)[a]	Z_{el} (cm/sec)[b]	Z_{ex} ($M^{-1}s^{-1}$)[b]	ΔG^*_{el}(eV)[c]	ΔG^*_{ex}(eV)[c]
15	$MnO_4^{-/2-}$	3.09	$5.8*10^3$	$2.4*10^{11}$	0.34	>0.46
16	$Mo(CN)_8^{3-/4-}$	--	$3.6*10^3$	$2.0*10^{11}$	0.22	0.40
17	$Os(bipy)_3^{2+/3+}$	--	$2.4*10^3$	$2.0*10^{11}$	(0.24)	0.23
18	$Ru(bipy)_3^{2+/3+}$	6.1	$2.6*10^3$	$4.3*10^{11}$	~0.24	0.27
19	$Ru(NH_3)_6^{2+/3+}$	3.3	$4.4*10^3$	$2.1*10^{11}$	<0.21	0.45-0.49
20	$V(aq)^{2+/3+}$	3.48	$5.1*10^3$	$2.6*10^{11}$	0.33-0.40	0.78-0.82
21	Anthracene$^{0/\cdot-}$	3.84	$4.7*10^3$	$3.0*10^{11}$	0.18	0.13-0.19
22	Benzonitrile$^{0/\cdot-}$	3.4	$6.2*10^3$	$3.2*10^{11}$	0.24	0.16
23	m-Nitrobenzonitrile$^{0/\cdot-}$	--	$5.2*10^3$	$2.7*10^{11}$	0.20	0.19
24	p-Dinitrobenzene$^{0/\cdot-}$	3.5	$4.9*10^3$	$2.5*10^{11}$	0.18-0.19	0.16
25	m-Dinitrobenzene$^{0/\cdot-}$	3.5	$4.8*10^3$	$2.5*10^{11}$	0.22	0.15
26	Dibenzofuran$^{0/\cdot-}$	3.8	$4.6*10^3$	$2.9*10^{11}$	0.19	0.13
27	Naphthalene$^{0/\cdot-}$	3.54	$5.5*10^3$	$3.0*10^{11}$	0.22	0.12-0.19
28	1,4-Naphthaquinone$^{0/\cdot-}$	3.5	$5.0*10^3$	$2.7*10^{11}$	0.20-0.24	0.17
29	Perylene$^{0/\cdot-}$	4.3	$3.9*10^3$	$3.0*10^{11}$	0.17-0.21	0.13

TABLE II (continued)

Case Number	Redox Couple	r(Å)[a]	Z_{el} (cm/sec)[b]	Z_{ex} ($M^{-1}s^{-1}$)[b]	ΔG^*_{el} (eV)[c]	ΔG^*_{ex} (eV)[c]
30	Phthalonitrile$^{0/\cdot-}$	3.6	$5.6*10^3$	$3.0*10^{11}$	0.21	0.14
31	Terephthalonitrile$^{0/\cdot-}$	--	$5.6*10^3$	$3.0*10^{11}$	0.23	0.14
32	4-Cyanopyridine$^{0/\cdot-}$	3.2	$6.2*10^3$	$2.7*10^{11}$	0.25	0.15
33	t-Stilbene$^{0/\cdot-}$	4.2	$4.3*10^3$	$3.6*10^{11}$	0.19-0.21	0.16
34	α-Methyl-t-stilbene$^{0/\cdot-}$	--	$4.5*10^3$	$2.0*10^{11}$	0.24	0.18
35	Tetracene$^{0/\cdot-}$	4.12	$4.2*10^3$	$3.0*10^{11}$	0.18-0.20	0.13
36	Dibenzothiophene$^{0/\cdot-}$	3.7	$4.8*10^3$	$2.8*10^{11}$	0.21	0.10
37	o-Toluenitrile$^{0/\cdot-}$	3.6	$5.8*10^3$	$3.3*10^{11}$	0.23	0.15
38	p-Toluenitrile$^{0/\cdot-}$	3.6	$5.8*10^3$	$3.3*10^{11}$	0.23	0.15
39	m-Toluenitrile$^{0/\cdot-}$	3.6	$5.8*10^3$	$3.3*10^{11}$	0.23	0.16

a. Measured experimentally.

b. Calculated using equation 2.

c. Calculated using equation 1.

TABLE III

Heterogeneous and Homogeneous Electron Transfer Rates and Comparison to Marcus and Hush Predictions.

	cm/sec		$M^{-1} s^{-1}$	
	k_s	Z_{el}	k_{ex}	Z_{ex}
A. FIT MARCUS PREDICTION (R = 2a)				
$Co(phen)_3^{2+/3+}$	0.048	2.6×10^{3}	12	2×10^{11}
$Cr(aq)^{2+/3+}$	8×10^{-6}	5×10^{3}	$<2\times10^{5}$	2.6×10^{11}
$Eu(aq)^{2+/3+}$	10^{-4}	5×10^{3}	$<10^{-4}$	2×10^{11}
$Fe(aq)^{2+/3+}$	0.01-0.001	5×10^{3}	10-40	2.6×10^{11}
$Fe(CN)_6^{3-/4-}$ [a]	0.01-0.1	4.3×10^{3}	10^{2-4}	2.6×10^{11}
$IrCl_6^{2-/3-}$ [a]	0.5	3.1×10^{3}	2.5×10^{5}	2×10^{11}
$Mo(CN)_8^{3-/4-}$	0.5	3.6×10^{3}	3×10^{5}	2×10^{11}
$Ru(NH_3)_6^{2+/3+}$ [b]	>1	4.4×10^{3}	$1\text{-}4\times10^{3}$	2.1×10^{11}
$V(aq)^{2+/3+}$	3×10^{-3}	5.1×10^{3}	0.01	2.6×10^{11}
B. FIT HUSH PREDICTION				
$Co(aq)^{2+/3+}$	1.8×10^{-7}	5×10^{3}	4.4	2.4×10^{11}
$Cr(bipy)_3^{0/-}$ [a]	1.0	2.8×10^{3}	1.5×10^{9}	4.4×10^{11}

TABLE III (continued)

	cm/sec		$M^{-1}s^{-1}$	
	k_s	Z_{el}	k_{ex}	Z_{ex}
$Cp_2Fe^{0/+}$ [b]	0.05-0.2	4.6×10^{3}	10^{7-9}	2.9×10^{11}
$Fe(phen)_3^{2+/3+}$	0.7	2.6×10^{3}	5×10^{7}	2×10^{11}
$Os(bipy)_3^{2+/3+}$	0.87	2.4×10^{3}	2.3×10^{7}	2×10^{11}
$Ru(bipy)_3^{2+/3+}$	0.15	2.6×10^{3}	9×10^{6}	4.3×10^{11}
Anthracene$^{0/\cdot-}$	5	4.7×10^{3}	2×10^{8}	3×10^{11}
m-Nitrobenzenitrile$^{0/\cdot-}$	1.8	5.2×10^{3}	1.6×10^{8}	2.7×10^{11}
m-Dinitrobenzene$^{0/\cdot-}$	0.93	4.8×10^{3}	6×10^{8}	2.5×10^{11}
Naphthalene$^{0/\cdot-}$	1.0	5.5×10^{3}	10^{8-9}	3×10^{11}
1,4-Naphthaquinone$^{0/\cdot-}$	1.5	5×10^{3}	4.2×10^{8}	2.7×10^{11}
Perylene$^{0/\cdot-}$	4	3.9×10^{3}	2.1×10^{9}	3×10^{11}
t-Stilbene$^{0/\cdot-}$	1.5	4.3×10^{3}	6.8×10^{8}	3.6×10^{11}
C. IN BETWEEN THE PREDICTIONS				
$Ce(aq)^{3+/4+}$	$3\times10^{-4(-5)}$	3.9×10^{3}	4.4	2.4×10^{11}
$Fe(bipy)_3^{2+/3+}$	1.0	2.7×10^{3}	3.7×10^{6}	2×10^{11}
$MnO_4^{-/2-}$	10^{-2}	5.8×10^{3}	3000	2.4×10^{11}

TABLE III (continued)

	cm/sec		$M^{-1} s^{-1}$	
	k_s	Z_{el}	k_{ex}	Z_{ex}
D. k_s VALUES TOO LARGE BASED UPON k_{ex}				
$Co(NH_3)_6^{2+/3+}$	$5\times10^{-5(-6)}$	5×10^{3}	10^{-11}	2.4×10^{11}
$Co(EDTA)^{-/2-}$	0.02	3.8×10^{3}	10^{-4}	2×10^{11}
$Co(en)_3^{2+/3+}$	0.06	4×10^{3}	6.5×10^{-5}	2×10^{11}
E. k_s VALUES TOO SMALL BASED UPON k_{ex}				
Benzonitrile$^{0/\cdot-}$	0.6	6.2×10^{3}	5.5×10^{8}	3.2×10^{11}
Nitrobenzene$^{0/\cdot-}$	2.2	5.7×10^{3}	3.9×10^{9}	2.9×10^{11}
p-Dinitrobenzene$^{0/\cdot-}$ [c]	0.93	4.8×10^{3}	6×10^{8}	2.5×10^{11}
Dibenzofuran$^{0/\cdot-}$ [c]	2.0	4.6×10^{3}	1.6×10^{9}	2.9×10^{11}
Phthalonitrile$^{0/\cdot-}$	1.41	5.6×10^{3}	1.2×10^{9}	3×10^{11}
Terephthalonitrile$^{0/\cdot-}$	0.68	5.6×10^{3}	1.4×10^{9}	3×10^{11}
4-Cyanopyridine$^{0/\cdot-}$	0.42	6.2×10^{3}	6.8×10^{8}	2.7×10^{11}
α-Methyl-t-stilbene$^{0/\cdot-}$ [c]	0.43	4.5×10^{3}	1.9×10^{8}	2×10^{11}
2,4,6,2′,4′,6′-hexyl-methyl-t-stilbene$^{0/\cdot-}$ [c]	0.18	5×10^{3}	8×10^{7}	2×10^{11}

TABLE III (continued)

	cm/sec		$M^{-1} s^{-1}$	
	k_s	Z_{el}	k_{ex}	Z_{ex}
Tetracene$^{0/\dot{-}}$ [c]	2.5	4.2×10^{3}	1.9×10^{9}	3×10^{11}
TCNE$^{\dot{-}/=}$	2×10^{-3}	5×10^{3}	1.7×10^{9}	2×10^{11}
TCNQ$^{0/\dot{-}}$	3.5×10^{-3}	5×10^{3}	2×10^{9}	2×10^{11}
Dibenzothiophene$^{0/\dot{-}}$ [c]	1.6	4.8×10^{3}	1.2×10^{9}	2.8×10^{11}
o-Toluenitrile$^{0/\dot{-}}$	0.63	5.8×10^{3}	8.6×10^{8}	3.2×10^{11}
p-Toluenitrile$^{0/\dot{-}}$	0.90	5.8×10^{3}	7.8×10^{8}	3.2×10^{11}
m-Toluenitrile$^{0/\dot{-}}$ [c]	0.63	5.8×10^{3}	5.6×10^{8}	3.2×10^{11}

a. Barely within one order of magnitude of prediction.

b. Probably within prediction if believe experimental values.

c. Almost within one order of magnitude of Hush prediction.

Figure 1. Comparison of the Energies of Activation for Heterogeneous Electron Transfer (ΔG^*_{el}) versus Homogeneous (Self-Exchange) Electron Transfer (ΔG^*_{ex}) Reactions. Values plotted are from those listed in Table II.
Marcus Prediction (for R = 2a): $\Delta G^*_{el} = \Delta G^*_{ex}/2$.
Hush Prediction: $\Delta G^*_{el} = \Delta G^*_{ex}$.

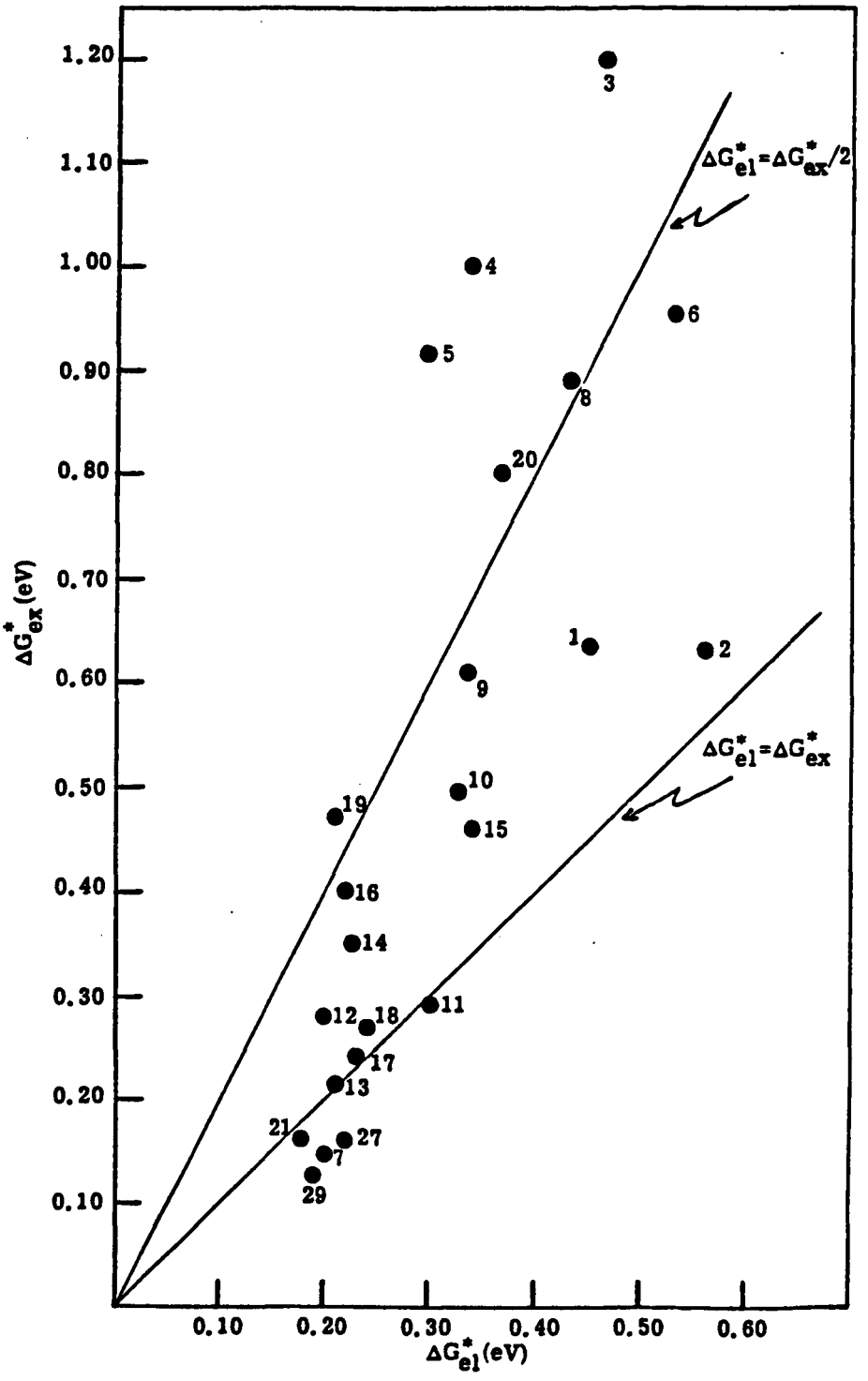
1.20
1.10
1.00
0.90
0.80
0.70
0.60
0.50
0.40
0.30
0.20
0.10
ΔG^*_{ex} (eV)
0.10
0.20
0.30
0.40
0.50
0.60
ΔG^*_{el} (eV)
$\Delta G^*_{el}=\Delta G^*_{ex}/2$
$\Delta G^*_{el}=\Delta G^*_{ex}$
3
4
6
5
8
20
1
2
9
10
19
15
16
14
12
18
11
17
13
21
27
7
29

equation works well. (Both equations predict k_s values much larger than the experimentally measured values.) Both equations also fail for numerous cobalt (III/II) complexes.

Failure of the Marcus theory (when R = 2a) adequately to predict the relationship between the heterogeneous and homogeneous rates may be due to the fact that most heterogeneous electron transfer reactions occur with the complex at the Outer Helmholtz Plane of the electrode[20] (which is usually 3-5 Å from the electrode) so that $R > 2a$. When R is allowed to be larger than or equal to 2a, the Marcus prediction becomes closer to the Hush prediction (especially when the outer-sphere reorganization energy dominates the ΔG^* for electron transfer) and almost half of the systems measured to date can be predicted by the Marcus equation. Finally, some of the lack of agreement between theory and experiment can be explained by the fact that only uncorrected rate constants were compared because of the paucity of corrected rate constants, and uncertainties about the theory applied to obtain the corrected rate constants.[21]

With the data compiled in Table I and values of λ_i and λ_o taken from references,[13,22-24] it was possible to test two empirical equations that have been proposed in the literature[25,26] relating k_{ex} and k_s. These equations are:

$$\log k_{ex} = \left(\frac{2r+2}{2r+1}\right) \log k_s + \frac{14r+3}{2r+1} \qquad (12)$$

where $r = (\lambda_o/\lambda_i)_{ex}$[25] and from reference 26:

$$\log k_{ex} = (2 \pm 0.5) \log k_s + (4 \pm 1). \qquad (13)$$

Neither of these equations adequately describes the correlation between homogeneous and heterogeneous electron transfer rates, although equation 13 does seem to hold for those systems for which the Marcus prediction (when R = 2a) also is valid.

REFERENCES

1. R. A. Marcus, J. Chem. Phys., 24, 979 (1956).
2. R. A. Marcus, Electrochim. Acta, 13, 995 (1968).
3. R. A. Marcus, Ann. Rev. Phys. Chem., 15, 155 (1964).
4. R. A. Marcus, J. Chem. Phys., 24, 966 (1956).
5. R. A. Marcus, J. Chem. Phys., 43, 679 (1965).
6. R. A. Marcus, Can. J. Chem., 37, 155 (1959).
7. R. A. Marcus, J. Phys. Chem., 67, 853 (1963).
8. N. Tanaka and R. Tamamushi, Electrochim. Acta, 9, 963 (1964).
9. N. S. Hush, Electrochim. Acta, 13, 1005 (1968).
10. N. S. Hush, J. Chem. Phys., 28, 962 (1958).
11. N. S. Hush, Trans. Faraday Soc., 557 (1960).
12. R. R. Dogonadze, A. M. Kuznetsov and T. A. Marsagishvila, Electrochim. Acta, 25, 1 (1980).
13. G. M. Brown and N. Sutin, JACS, 101, 883 (1979).
14. M. Chou, C. Creutz and N. Sutin, JACS, 99, 5615 (1977).
15. R. G. Linck in "Homogeneous Catalysis", G. N. Schrauzer, Ed., Marcel Dekker, New York, Ch 7 (1971).
16. L. E. Bennett, Progr. Inorg. Chem. 18. 1 (1973).
17. N. Sutin, Inorg. Biochem., Ch 19 (1973).
18. R. G. Linck, MTP Int. Rev. Sci., Inorg. Chem. Ser. Two, Ch 7 (1974).
19. R. G. Linck, Surv. Prog. Chem., 7, 89 (1976).
20. M. J. Weaver, J. Phys. Chem., 84, 568 (1980).
21. H. Mizota, K. Suga, Y. Kanzaki and S. Aoyagui, J. Electroanal. Chem., 44, 471 (1973).

REFERENCES (continued)

22. P. Siders and R. A. Marcus, JACS, 103, 741 (1981).

23. N. Hale in "Reactions of Molecules at Electrodes", Ed., N. S. Hush, Ch 4 (1971).

24. N. Sutin in "Tunnelling in Biological Systems", 1979.

25. T. Saji, Y. Maruyama and S. Aoyagui, J. Electroanal. Chem., 86, 219 (1978).

26. J. F. Endicott, R. R. Schroeder, D. H. Chidester and D. R. Ferrier, J. Phys. Chem., 77, 2579 (1973).

APPENDIX II

Several Techniques Used for the Measurement of Electrode Kinetic Parameters

In Part II of this thesis, the techniques of cyclic voltammetry, chronocoulometry and AC impedance were applied to the measurement of the heterogeneous electron transfer rate constants for several species. Although a brief discussion of each technique was presented, the major emphasis of the research was on the values of the rate constants, not so much on how they were acquired and calculated. In this appendix, I will expand on the experimental and theoretical considerations used for the measurement of the electrode kinetics by these techniques.

Cyclic Voltammetry

Experimentally, cyclic voltammetry is one of the easiest methods to apply to measurement of electrode rate constants (k_s), because of the simplicity of the instrumentation used and the ease of calculation from the measured parameters of interest. Essentially all one needs is a triangular waveform generator (for example the PAR Model 175 universal programmer) which is used to drive a potentiostat that is connected to the electrochemical cell. The electrochemical cell consists of the substrate solution, the working electrode, auxiliary electrode and a reference electrode. To obtain the electrode kinetics, the scan rate is varied and the resulting current-voltage curves are monitored with an x-y recorder or a storage oscilloscope. From the potential difference between the anodic and cathodic peak currents, it is possible to calculate the value of the rate constant. The major experimental difficulty is in eliminating the effect of ohmic potential (iR) drop, which occurs because current is flowing in a solution with finite resistance. Ohmic resistance affects the parameters used to measure

the electrode kinetics in cyclic voltammetry in a very similar way to that of the kinetics themselves and in many cases it is hard to distinguish between the two. Even in situations where positive-feedback circuitry[1] has been employed to reduce iR, care must be taken in setting the value of feedback.[2] Usually must researchers increase the amount of feedback until a point just before oscillation of the entire system, however, this value depends on many variables and will vary from one set-up to another.

There are several other methods that experimentally can be used to reduce the effects of ohmic potential loss. These include using low concentrations of substrate and small electrode areas to minimize the current, decreasing the resistance of the solution by increasing the supporting electrolyte concentration and eliminating physical barriers such as glass frits between the electrodes, and by arranging the electrodes as close together as possible. It has also been proposed[3] to use a model substrate which has a measured rate constant greater than 1.0 cm/sec to calibrate the iR feedback setting. Many of the aforementioned precautions to measure the rate constants were used for the values reported in Part II.

To reiterate, the experimenter varies the scan rate for a potential scan from where no faradaic reaction occurs to potentials 113/n mV past the half-wave potential ($E_{\frac{1}{2}}$) for the substrate where the scan is reversed back to the initial potential and monitors the resulting current-voltage curves. The potential difference between the anodic and cathodic peak currents (ΔE_p) is then used to calculate the rate constant.[4] The theoretical work of Nicholson[4] has shown that ΔE_p is a function of the

TABLE I

Variation of the Peak Potential Separation (ΔE_p) With the Kinetic Parameter ψ.[4]

ψ[a]	ΔE_p[b]
20	61
7	63
6	64
5	65
4	66
3	68
2	72
1	84
0.75	92
0.50	105
0.35	121
0.25	141
0.10	212

a. For a scan reversal potential 113/n mV past the $E_{\frac{1}{2}}$ and ψ defined in equation 1.

b. The potential separation between the anodic and cathodic peak currents for n = 1.

scan rate (ν), the rate constant for electron transfer (k_s), the transfer coefficient (α) and the potential at which the scan is reversed. However, for a reversal potential of 113 mV (for n = 1) past the $E_{\frac{1}{2}}$ for the substrate and for α between 0.3 and 0.7, the ΔE_p is nearly independent of these parameters and is related to a dimensionless parameter, ψ, via Table I.[4]

Once ΔE_p is known as a function of scan rate, ψ as a function of scan rate can be determined and the rate constant is calculated by equation 1:[4]

$$\psi = \frac{(\frac{D_{ox}}{D_{red}})^{\frac{\alpha}{2}} k_s}{[D_{ox}\pi\nu(\frac{nF}{RT})]^{\frac{1}{2}}} \qquad (1)$$

where D_{ox}, D_{red} are the respective diffusion coefficients of the oxidized and reduced forms of the redox couple (usually assumed to be equal), α is assumed to be 0.5 (as a first approximation) and $\frac{nF}{RT}$ is 38.92 V^{-1} (at 25° C and n = 1). In general, only values of ψ between 0.1 and 7.0 are useful for determining the apparent k_s values at each scan rate, from which the heterogeneous electron transfer rate constant is calculated by averaging the apparent k_s values over the entire scan rate range.

AC Impedance[5]

The basic operational procedure involves applying an AC voltage of known frequency and amplitude (usually 5.0 - 10.0 mV) to an electrochemical cell and measuring the in-phase and out-of-phase components of the resulting current.[6] This is easily accomplished with a lock-in

amplifier. The amplifier is used to generate the AC signal and to measure the in- and out-of-phase components of the current with respect to the AC voltage. The amplifier also converts the AC voltages to DC levels which are read off a voltmeter. These values are then used to calculate impedances from which the electrode kinetics can be extracted after corrections for solution resistance and double layer capacity.[5]

The equipment needed to perform an AC impedance experiment are a lock-in amplifier, a fast potentiostat (i.e., a potentiostat with no capacitors on the current output), a frequency counter and several voltmeters. Everything should be turned on and allowed to warm up for at least 15 minutes. Each instrument should be plugged into the same power outlet (separate plugs though). For measurements on mercury the PAR Model 303 Automatic Electrode (very high precision area reproducibility) can be used as the working electrode, a Pt gauze electrode around the mercury drop for the auxiliary electrode and either a silver wire or SCE as reference electrodes (although no glass frits should be used to separate the reference electrode as this causes phase shifts and the SCE or Ag/AgCl reference electrodes do leak a little). The potentiostat can be used in a 3-electrode configuration (normal) or in a 2-electrode set-up where the reference and auxiliary electrodes are tied together and the DC potential is measured by a voltmeter.[7] If the potentiostat has iR compensation capabilities, it should be applied before the AC voltage is set and should <u>totally</u> compensate the solution resistance (otherwise an unknown amount of uncompensated solution resistance remains and makes the calculations of the kinetics

unreliable by that amount). However, in many cases it is better not to apply iR feedback and to use substrate concentrations of 1 mM or less so that the AC currents are small ($\leq 10^{-5}$ Ampere) which minimizes any potential drop due to resistance. This technique works well unless the solution resistance is much greater than about 300 Ω or if the double layer capacity is larger than 0.2 μF.

Calculation of the kinetic parameters assume that the cell can be represented by an equivalent circuit as shown in Figure 1A. This can be further reduced to an equivalent RC series circuit as shown in Figure 1B, from which the electrode kinetics may be extracted after corrections for the solution resistance (R_Ω) and the double layer capacitance (C_{dl}).

Operationally then one first measures the in- and out-of-phase AC currents (as voltages from the lock-in amplifier, appropriately scaled) for a solution containing the compound of interest at several different DC potentials at and near the $E_{\frac{1}{2}}$ for the complex and at several different frequencies (freq.). Then the in- and out-of-phase AC currents are calculated by

$$i_{in} = \frac{V_{in}}{R_m} \qquad i_{out} = \frac{V_{out}}{R_m} \tag{2}$$

where V_{in} and V_{out} are the in- and out-of-phase voltages from the lock-in amplifier and R_m is the measuring resistor on the potentiostat. The admittances are then calculated via:

$$Y_{in} = \frac{i_{in}}{V_{RMS}} \quad \text{and} \quad Y_{out} = \frac{i_{out}}{V_{RMS}} \tag{3}$$

Figure 1. A. Equivalent circuit for an electrochemical cell with electrode kinetics.

B. An RC series circuit.

A

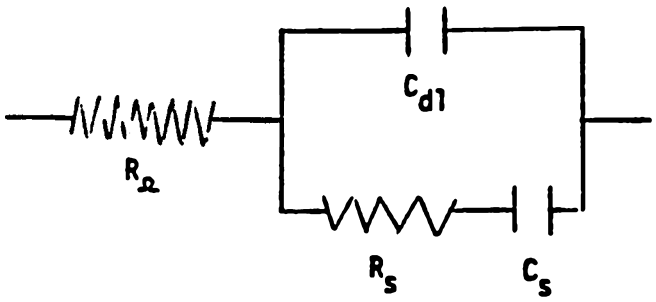

B

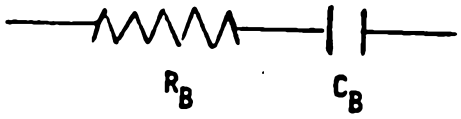

where V_{RMS} is the applied AC voltage. The admittances are converted to impedances by:

$$Z_{in} = \frac{Y_{in}}{(Y_{in})^2 + (Y_{out})^2} \qquad Z_{out} = \frac{Y_{out}}{(Y_{in})^2 + (Y_{out})^2} \tag{4}$$

from which the in-phase component gives R_B directly (in ohms) and the out-of-phase component gives C_B (in farads) by:

$$C_B = \frac{1}{2\pi\,(\text{freq.})Z_{out}} \,. \tag{5}$$

Next a background solution is run, which in this case gives R_Ω and C_{dl} directly from the R_B and C_B calculated for this solution. Once R_Ω and C_{dl} are known, the parameters R_B and C_B measured at each potential and frequency in the complex solution can be converted into impedances R_s and C_s (the kinetically useful parameters) via the following equations:[5]

$$R'_B = R_B - R_\Omega \tag{6}$$

$$R_p = R'_B \left[\frac{1 + [2\pi(\text{freq.})R'_B C_B]^2}{[2\pi(\text{freq.})R'_B C_B]^2} \right] \tag{7}$$

$$C_p = \frac{C_B}{1 + [2\pi(\text{freq.})R'_B C_B]^2} \tag{8}$$

$$C'_B = C_p - C_{dl} \tag{9}$$

$$R_s = \frac{R_p}{1 + [2\pi(\text{freq.})R_pC'_B]^2} \tag{10}$$

$$C_s = C'_B\left[\frac{1 + [2\pi(\text{freq.})R_pC'_B]^2}{[2\pi(\text{freq.})R_pC'_B]^2}\right]. \tag{11}$$

And once C_s and R_s have been calculated at each frequency and at each DC potential, a plot of $\cot\theta$ vs. DC potential is made (as in Figure 2A) and the potential(s) of maximum $\cot\theta$ at each frequency are found.

$$\cot\theta = \frac{R_s}{2\pi(\text{freq.})C_s}\ . \tag{12}$$

If one is lucky enough to have $\alpha = 0.5$ and $D_{ox} = D_{red}$, then the $\cot\theta$ maximum at each frequency should occur at the $E_{\frac{1}{2}}$ for the complex and the kinetics are simply calculated from the slope of a plot of $(\cot\theta)_{max}$ vs. $[2\pi(\text{freq.})]^{\frac{1}{2}}$ as shown in Figure 2B. However, in the cases where α does not equal 0.5, more complicated expressions for the slope have to be applied[5] or as a first approximation the simpler expression can be used. In this method one does not need to know the concentration of the complex or the area of the electrode, although D_{ox} or D_{red} must have been independently determined.

An alternate (and perhaps a more diagnostically useful) route to acquire the kinetics are to plot the impedances R_s and $\frac{1}{2\pi(\text{freq.})C_s}$ at $E_{\frac{1}{2}}$ (assuming $\alpha = 0.5$) at each frequency versus $\frac{1}{[2\pi(\text{freq.})]^{\frac{1}{2}}}$ as in Figure 2C. One should obtained straight lines with

Figure 2. A. $\text{Cot}\,\theta$ versus DC potential at each frequency.

B. $(\text{Cot}\,\theta)_{max}$ versus $(2\pi \text{ frequency})^{\frac{1}{2}}$.

C. In-phase (R_s) and out-of-phase $\left(\frac{1}{2\pi \text{ frequency } C_s}\right)$ impedances versus $(2\pi \text{ frequency})^{-\frac{1}{2}}$.

A

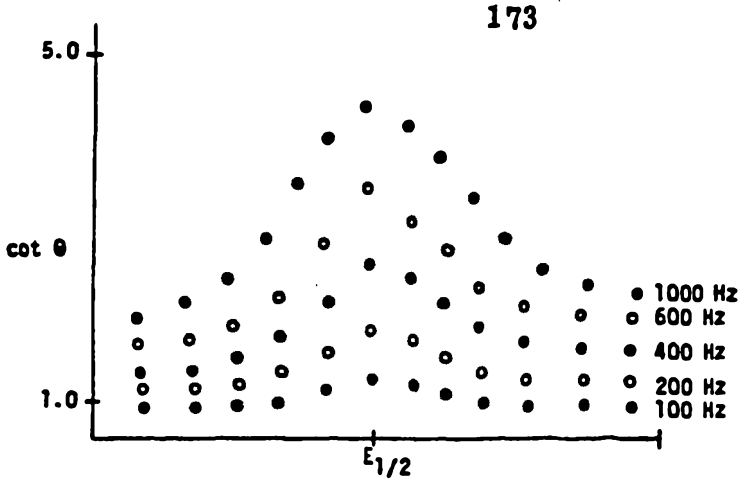

B

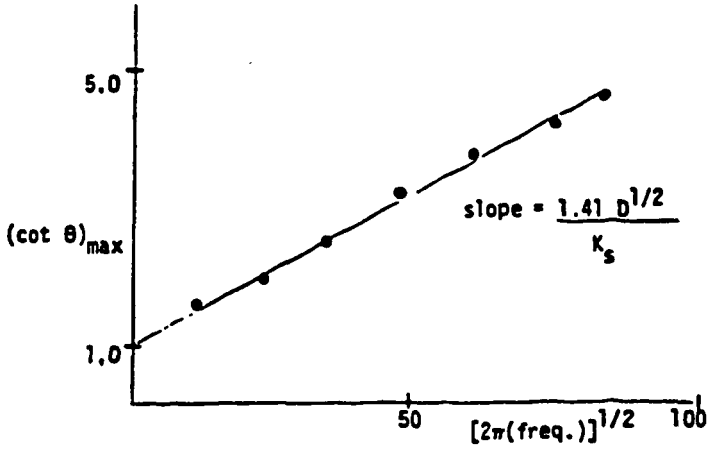

note - line should intercept the $(\cot \theta)_{max}$ axis at 1.00.

C

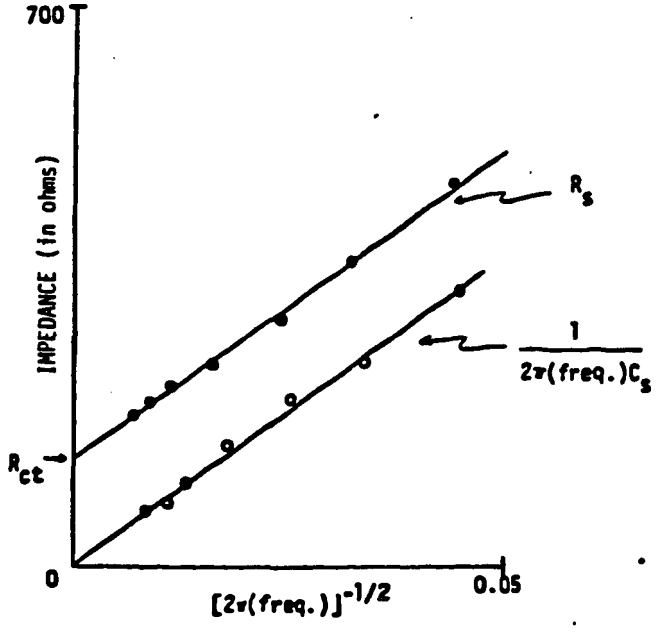

equal slopes, σ:

$$\sigma = \frac{4}{n^2F}\ \frac{RT}{F}\ \frac{1}{\sqrt{2}\,D^{\frac{1}{2}}C^bA} \tag{13}$$

where the units are: $\frac{RT}{F} = 0.02569$ V, $F = 96500\ \frac{\text{Amp-sec}}{\text{mole-e}^-}$, $A = \text{cm}^2$, $C^b = \frac{\text{mole}}{\text{cm}^3}$, $D^{\frac{1}{2}} = \frac{\text{cm}}{\text{sec}^{\frac{1}{2}}}$. If you do not obtain equal slopes or a positive intercept for R_s vs. $\frac{1}{[2\pi(\text{freq.})]^{\frac{1}{2}}}$ plots on the impedance axis and a zero intercept for $\frac{1}{2\pi(\text{freq.})C_s}$ vs. $\frac{1}{[2\pi(\text{freq.})]^{\frac{1}{2}}}$ plots, there are problems either with the electronics, such as the iR compensation circuit, or with the chemical system (such as chemical kinetics or adsorption). Electronic problems can be tested by running a dummy cell composed of resistors and capacitors arranged as the equivalent circuit cell in Figure 1A. For systems with equal slopes and a positive intercept, the electrode kinetics are extracted from the intercept (R_{ct}) of (the in-phase component) R_s. This is because R_{ct} is related to the exchange current (i_o) by $R_{ct} = \frac{RT}{nFi_o}$ where $i_o = \frac{nFAk_sC^b}{2}$ (if at $E_{\frac{1}{2}}$).[5] All values of the rate constants measured in Part II by this technique were calculated using plots of R_s and $(2\pi \text{ frequency } C_s)^{-1}$ versus $(2\pi \text{ frequency})^{-\frac{1}{2}}$ although essentially identical values were obtained from the $(\cot\theta)_{max}$ versus $(2\pi \text{ frequency})^{\frac{1}{2}}$ plots.

Chronocoulometry

Chronocoulometric experiments to determined the kinetic parameters involve stepping from a potential where no faradaic reaction occurs to potentials up the rising portion of the wave for the substrate

of interest, and measuring the charge as a function of time. In the present investigation a computer-based,data-acquisition system[8] with iR compensation was used to acquire, calculate and display the charge versus $(\text{time})^{\frac{1}{2}}$ behavior. Under conditions when the potential step is not onto the diffusion-limited plateau, the charge for the initial time after the potential step is controlled by a mixture of kinetic and diffusive elements. Eventually though, the charge becomes linear with $(\text{time})^{\frac{1}{2}}$ (this occurs at times where $y \geq 5$, y defined as in reference 9). Extrapolation of the linear portion of the charge versus $(\text{time})^{\frac{1}{2}}$ curve back to time = 0 (after subtraction of the double layer charge[10]) will intercept the charge axis at zero if there

However, if the electrode kinetics control a significant portion of the initial current after the potential step, then the extrapolated line will intercept the charge axis at negative values (see Figure 3). From the slope of the charge versus $(\text{time})^{\frac{1}{2}}$ plot and the negative intercept on the charge axis, the positive intercept on the $(\text{time})^{\frac{1}{2}}$ axis (defined as $t_i^{\frac{1}{2}}$) for the charge = 0, can be calculated.

Operationally, the experimenter varies the potential steps and determines the $t_i^{\frac{1}{2}}$ values for these potential steps. Then using the relationship given in equation 14, λ is found:

$$\lambda = \frac{\pi^{\frac{1}{2}}}{2t_i^{\frac{1}{2}}} \cdot \tag{14}$$

The minimum value of λ occurs when $t_i^{\frac{1}{2}}$ is at a maximum, which occurs at the potential defined by:

Figure 3. A plot of charge versus (time)$^{\frac{1}{2}}$ for a potential step onto the rising portion of the faradaic wave for the redox couple (after subtraction of the double layer charge).

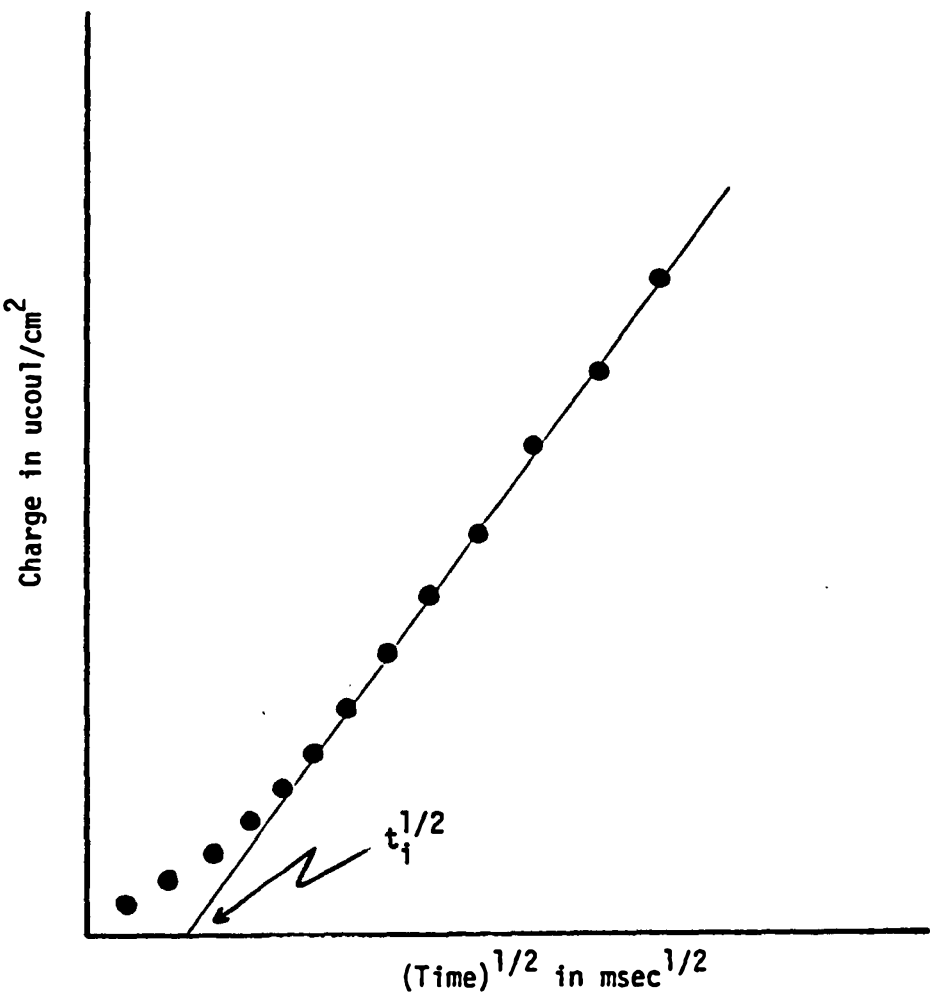
Charge in ucoul/cm^2
$t_i^{1/2}$
(Time)$^{1/2}$ in msec$^{1/2}$

$$E_{\lambda_{min}} = E^{\frac{1}{2}} + \frac{RT}{nF} \ell n\left(\frac{\alpha}{1-\alpha}\right) \qquad (15)$$

For $\alpha = 0.5$ and equal diffusion coefficients for the oxidized and reduced species, the λ_{min} is found at $E_{\frac{1}{2}}$ and the heterogeneous electron transfer rate constant is calculated from:[9]

$$\lambda_{min} = \frac{2k_s}{D^{\frac{1}{2}}} \qquad (16)$$

where the diffusion coefficient (D) is calculated from the chronocoulometric slope for a step to a potential on the diffusion-limited plateau via equation 17:[9,11]

$$\text{chronocoulometric slope} = \frac{2nFAD^{\frac{1}{2}}C^b}{\pi^{\frac{1}{2}}} \; . \qquad (17)$$

When the minimum value of λ does not occur at $E_{\frac{1}{2}}$, more complicated expressions have to be used to extract the electrode kinetic information[9,12] however a discussion of these equations is beyond the scope of this appendix and the reader is referred to the original references.[9,12]

REFERENCES

1. a) D. T. Sawyer and J. L. Robert, "Experimental Electrochemistry for Chemists", Ch. 5, Wiley, New York, 1974.
   b) R. R. Schroeder in "Computers in Chemistry and Instrumentation", Ch 10, V 2, "Electrochemistry", J. S. Mattson, H. B. Mark, Jr. and H. C. MacDonald, Jr., Eds., Marcel Dekker, New York, 1972.
2. a) D. E. Smith, Crit. Rev. Anal. Chem., 2, 247 (1971).
   b) D. Britz, J. Electroanal. Chem., 88, 309 (1978).
3. M. Sharp, M. Petersson and K. Edstrom, J. Electroanal. Chem., 109, 271 (1980).
4. R. S. Nicholson, Anal. Chem., 37, 1351 (1965).
5. A. J. Bard and L. R. Faulkner, "Electrochemical Methods", Ch 9, Wiley, New York, 1980.
6. a) M. Sluyters-Rehbach and J. H. Sluyters, J. Electroanal. Chem., 4, 1 (1970).
   b) J. E. B. Randles, Disc. Faraday Soc., 1, 11 (1947).
   c) D. D. MacDonald, "Transients Techniques in Electrochemistry", Ch 5, Plenum, New York, 1977.
7. H. Kojima and A. J. Bard, J. Electroanal. Chem., 63, 117 (1975).
8. G. Lauer, R. Abel and F. C. Anson, Anal. Chem., 39, 765 (1967).
9. J. H. Christie, G. Lauer and R. A. Osteryoung, J. Electroanal. Chem., 7, 60 (1964).
10. F. C. Anson, Anal. Chem., 38, 54 (1966).

REFERENCES (continued)

11. F. C. Anson, J. H. Christie and R. A. Osteryoung, J. Electroanal. Chem., 13, 343 (1967).

12. P. J. Lingaine and J. H. Christie, J. Electroanal. Chem., 10, 284 (1965).

PROPOSITIONS

PROPOSITION 1

Abstract

[2.2.1] and [2.2.2] propellanes may be trapped in situ via a Diels-Alder reagent which has a specific stereochemistry such that the formation of other intermediates, instead of the highly strained, small-ring propellane, is excluded.

Most of the research on the preparation, identification and reactions of propellanes ([a.b.c.0] tricyclic hydrocarbons) has occurred in the last 20 years.[1-4] Of special interest is the formation of small-ring propellanes, which have been proposed as intermediates in a number of studies,[5-40] although the [2.2.1] propellane and [2.2.2] propellane, 2 and 3 respectively, have never been isolated. Production of these highly-strained compounds was attempted via chemical[6-8] and electrochemical reduction[5,9] of the corresponding bridgehead-bridgehead dihalo bicyclic hydrocarbons. Due to the apparently transient existence of these species, various trapping agents like Br_2[7,8] and Cl_2[6,9] were used in an attempt to isolate products which could be ascribed to the propellanes. (These halogenation products were found in low yields of 10-25%.) In addition, the intermediacy of propellanes were based upon the final products when no trapping agents were added.[5,7] However, none of these reports necessarily excludes the possibility of the formation of the products from non-propellane intermediates such as free radicals, anions or organolithium compounds.

Recently there has appeared a report on the matrix isolation of [2.2.1] propellane at 29°K[10] formed by gas-phase dehalogenation of the dihalide precursor with metal atoms. Formation of the propellane was postulated based upon the IR absorption spectrum obtained and via trapping with Br_2, although attempts to isolate the propellane product were unsuccessful.

Therefore, to try to unequivocally show the presence of the small-ring propellanes under the conditions employed for chemical or electrochemical reduction of the dihalo species, it is proposed to attempt to

trap the propellanes with a Diels-Alder reagent that has a specific stereochemistry. The Diels-Alder reaction has been previously used before to trap other propellanes,[11-13] although no direct stereochemical evidence was obtained. Since the Diels-Alder reaction (1,4-addition) is a concerted process, if one allowed (E,E)-dideutero-1,2-dimethylene cyclopentane (1) to react with either the [2.2.1] propellane (2) or [2.2.2] propellane (3), the expected Diels-Alder products [(4) and (5) respectively] would be isomers with both deuterium atoms on the same side of the molecular plane (cis-like).

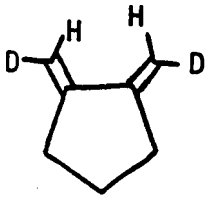

1

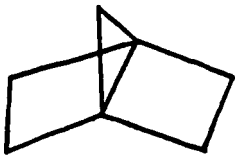

2

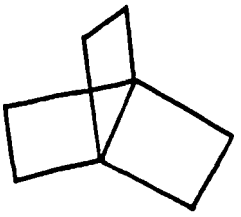

3

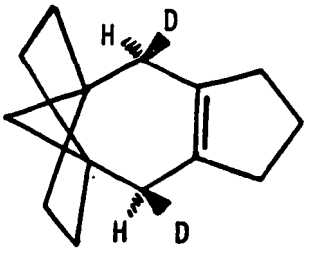

4

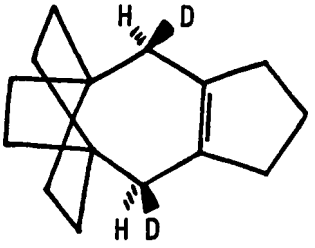

5

However, if adducts with (1) are formed from radical[14] or anionic species, it may be possible to see products where the two deuterium atoms are on opposite sides of the molecular plane (trans-like), (6) and (7), or derived from 1,2-attack,[15] (8) and (9), on the Diels-Alder reagent.

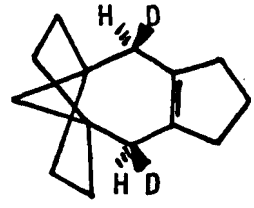

6

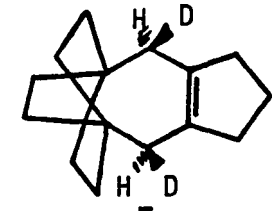

7

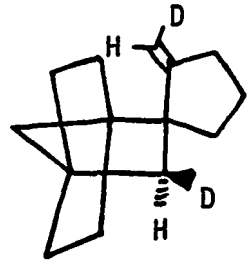

8

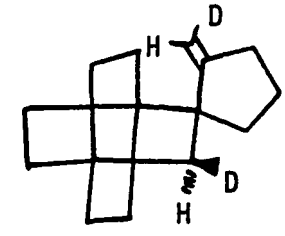

9

Isolation of reasaonable yields of product derived from 1,2-attack or with the trans-like configuration of the deuterium atoms would preclude the [2.2.1] propellane (or the [2.2.2] propellane) as a major intermediate. If, however, only the product with the cis-like configuration of the deuterium atoms is found, this only strongly suggests that the propellane was formed, it is not proof-positive. An advantage of the Diels-Alder reagent over previous traps is that it is electroinactive[16] and should be stable towards organolithium compounds; thus it can be added in a 10-fold excess (versus starting dihalo bicyclic material) to the solutions used previously[5,7,8] to generate the propellane intermediates, thereby increasing the possibility of reaction to form adducts.

Synthesis of (E,E)-dideutero-1,2-dimethylene cyclopentane (1) may be accomplished by first preparing (E,E)-6,7-dichloro-1,2-dimethylene cyclopentane via the following procedure:[17,18]

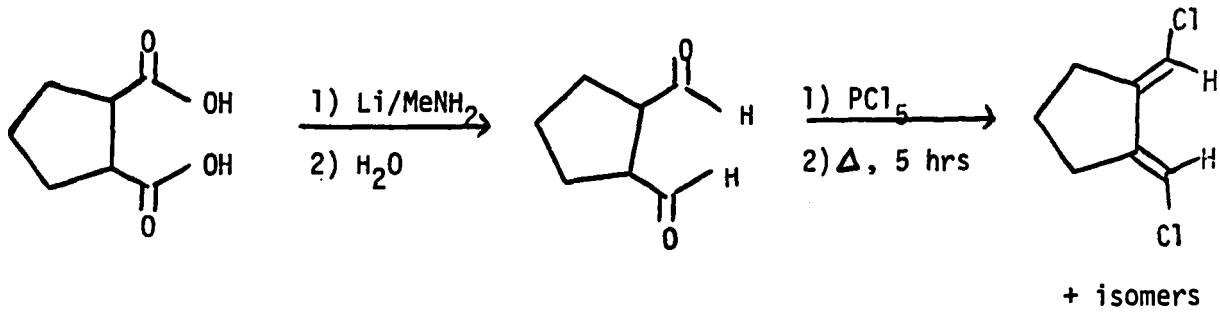

+ isomers

The (E,E)-dichloro isomer is easily separated from the other dichloro isomers by preparative-scale vapor phase chromatography[19-23] and low-temperature crystallization.[24] Then using a Zn-Cu catalyst, the chloride atoms on the vinyl groups can stereospecifically be converted to deuterium atoms by addition of D_2O.[25] Identification of 1 and the relevant adduct products would be possible using mass spectrometry and nuclear magnetic resonance techniques.[21,23,26] In particular, NMR using Lanthanide shift reagents[13] or double resonance NMR[27-39] (taking advantage of the Nuclear Overhauser effect[30]) should distinguish between the deuterium atoms on the same side or opposite sides of the molecular plane. However, it may also be necessary to perform NMR on model compounds such as (cis and trans)-3,6-dideutero-1,4-cyclohexadiene (10) or (cis and trans)-5,8-dideutero-1,3,6-cyclooctatriene (11)

to help identify the conformations of the products.

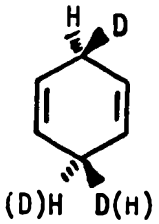

10

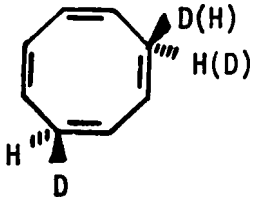

11

REFERENCES AND NOTES

1. D. Ginsburg, Tetrahedron, 30, 1487 (1976).
2. D. Ginsburg, Accounts of Chem. Research, 2, 121 (1969).
3. D. Ginsburg, Accounts of Chem. Research, 5, 249 (1972).
4. D. Ginsburg, Accounts of Chem. Research, 7, 286 (1974).
5. W. F. Carroll, Jr. and D. G. Peters, J. Org. Chem., submitted for publication.
6. K. B. Wiberg, W. F. Bailey and M. E. Jason, J. Org. Chem., 41, 2711 (1976).
7. K. B. Wiberg, W. E. Pratt and W. F. Bailey, J. Am. Chem. Soc. 99, 2297 (1977).
8. J. J. Dannenburg, T. M. Prociv and C. Hutt, J. Am. Chem. Soc. 96, 913 (1974).
9. K. B. Wiberg, G. A. Epling and M. Jason, J. Am. Chem. Soc. 96, 912 (1974).
10. F. H. Walker, K. B. Wiberg, and J. Michl, J. Am. Chem. Soc. 104, 2056 (1982).
11. J. Kalo, J. M. Photis, L. A. Paquette, E. Vogel and D. Ginsburg, Tetrahedron, 32, 1013 (1976).
12. O. Szeimies-Seebach and G. Szeimies, J. Am. Chem. Soc. 100, 3966 (1978).
13. L. A. Paquette and G. L. Thompson, J. Am. Chem. Soc. 94, 7118 (1972).
14. If radicals attack the Diels-Alder reagent, the resulting radical should be free to rotate, thus losing the stereochemistry of the deuterium atoms with respect to each other.

15. Products derived from 1,2-attack cannot be from a concerted process, such as the Diels-Alder reaction, since a 2 + 2 reaction is thermally forbidden.

16. Non-phenyl conjugated double bonds are not reducible electrolytically.

17. R. C. Fuson and W. Cole, J. Am. Chem. Soc. 60, 1238 (1938).

18. M. S. Newman, G. Fraenkel and W. N. Kim, J. Org. Chem. 28, 1851 (1963).

19. D. E. Applequist and J. A. Landgrebe, J. Am. Chem. Soc. 86, 1543 (1964).

20. A. Cocks and H. M. Frey, J. Chem. Soc. B, 952 (1970).

21. P. Kelso, A. Yeshurun, C. N. Shih and J. J. Gajewski, J. Am. Chem. Soc. 97, 1513 (1975).

22. J. A. Berson, E. W. Petrillo and P. Bickart, J. Am. Chem. Soc. 96, 636 (1974).

23. T. C. Shields, D. W. Peck and A. N. Kurtz, Chem. and Ind. 269 (1969).

24. P. D. Bartlett and G. E. H. Wallbillich, J. Am. Chem. Soc. 91, 409 (1969).

25. L. M. Stephenson, R. V. Gemmer and S. P. Current, J. Org. Chem. 42, 212 (1977).

26. J. J. Gajewski and C. N. Shih, J. Am. Chem. Soc. 91, 5900 (1969).

27. J. Nouls, Tet. Letters, 4605 (1967).

28. O. Sciacovelli, W. von Philipsborn, C. Smith and D. Ginsburg, Tetrahedron, 26, 4589 (1970).

29. D. Y. Curtin, H. Gruen and B. A. Shoulder, Chem and Ind. 1205 (1958).

30. J. Noggle, The Nuclear Overhauser Effect, Academic Press, New York, 1971.

PROPOSITION 2

Abstract

Synthesis of a 4-substituted-2,2'-bipyridine ligand in which a fluorescent side group has been attached at the 4-position is proposed for the preparation of cobalt and ruthenium bis(2,2'-bipyridine) (4-substituted-2,2'-bipyridine) complexes. When the emission of the fluorescent unit depends upon the polarity of the environment around it, it can be used to monitor the interior of polymer films which incorporate the modified bipyridine metal complexes. The combination of the electroactive redox group which contains a ligand with a fluorescent tag would enable the correlation between electrochemistry and polarity inside polymer-modified electrodes, in particular for Nafion (a sulfonic acid polymer).

Polymer-modified electrodes have become an area of increasing activity in the past five years,[1] especially in the field of electrocatalysis.[2] Many different redox couples have been incorporated into a variety of polymer films via covalent[3] and electrostatic[2,4] binding and then used to mediate electron transfer[5] and/or catalyze chemical reactions of solution-phase complexes.[2] One of the primary concerns in these polymer modified electrodes which contain inorganic redox couples is how charge transport occurs through the film from the electrode surface to the solution-phase and which process is rate (current) limiting. Several rate limiting steps can be envisaged[5,6] including: (1) electron transfer from the electrode to the redox couple inside the film; (2) diffusion of the redox couple through the polymer layer to the electrode; (3) diffusion of counterions in or out of the polymer region to keep electroneutrality within the film; (4) electron hopping (via self-exchange) from one redox couple to another within the polymer layer, or (5) any combination of the above.

In many of the cases studied to date,[5] diffusion of the redox couple through the polymer region[7] or the electron hopping pathway[7] was found to be the rate determining step limiting the maximum current flow possible. Recently, electrochemical investigations into the mechanism of charge transport through nafion polymer films (adsorbed on carbon electrodes) containing electrostatically bound Ru(2,2'-bipyridine)$_3^{2+}$, Co(2,2'-bipyridine)$_3^{2+}$ or Ru(NH$_3$)$_6^{3+}$ were completed.[7] Measurement of the apparent diffusion coefficients as a function of the concentration of incorporated reactant was used to comment on the rate limiting processes in these systems.[5,7] It was postulated that

inside the polymer there exist two different areas where the redox couple resides,[7] one a polar (similar to a bulk solution phase) region and the other a non-polar phase (the fluorocarbon backbone of the polymer), each having different electron transfer properties. However, no further characterization of these two regions was attempted.

The microenvironments of several polymer films have been investigated by NMR techniques,[8] electrochemically-generated chemiluminescence[9] and non-electroactive fluorescent complexes.[10] For the method of fluorescence, there are many compounds which have been used to probe the local environments of biomolecules,[11] several of which have absorption and emission spectra that depend very strongly on the polarity of the environment they are in. For these types of complexes, examples of which are dansyl chloride,[12] substituted naphthalenes[13] and 7-(p-methoxybenzylamino)-4-nitrobenzoxadiazole,[14] their emission spectra are shifted to lower energies (with very low quantum yields) in polar solvents like water, while in less polar solvents such as benzene or 1-octanol the emission maxima are at higher energies (a shift of 30-100 nm from the polar maximum) and the quantum efficiencies are near 0.5. Excited state lifetimes and polarization data also yield information on the local environment "sensed" by the fluorescent molecule.

It is proposed that the coupling of an electroactive redox couple which contains a fluorescent tag would be used to provide insights into the microenvironments inside polymer-modified electrodes through a comparison of the electrochemical and fluorescent properties observed.

The specific examples recommended are the ruthenium and cobalt bis(2,2'-bipyridine)(4-fluorescent side chain 2,2'-bipyridine) complexes incorporated into nafion films adsorbed on graphite. The 4-fluorescent side chain 2,2'-bipyridine ligand would be prepared from 4-amino-2,2'bipyridine(I)[15] and 7-chloro-4-nitrobenzoxodiazole(II)[14] as shown in reaction 1:[14,16]

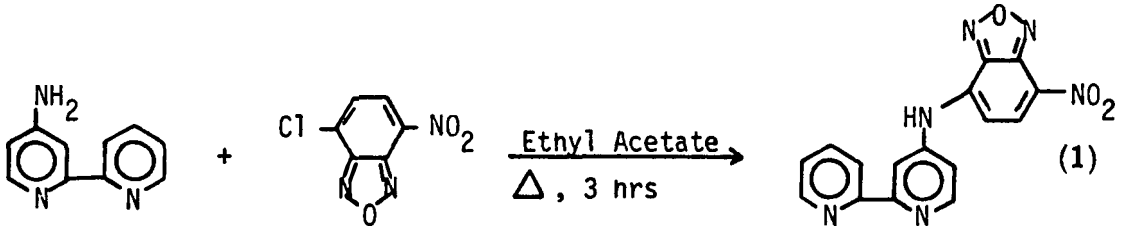

Synthesis of the mono- or tris-(4-fluorescent side chain 2,2'-bipyridine) metal species would be accomplished following standard procedures.[17] After incorporation of the redox couple-fluorescent tag molecule into the nafion film, measurements of the electrochemical and fluorescent properties would be carried out. To determine the polarity inside the polymer film, fluorescent experiments with the redox couple-fluorescent tag complex in solvents of varying polarity and compositions (similar structures to the fluorocarbon backbone and bulk aqueous phase) would be necessary. It is hoped that this technique would provide information not only on the kinds of environments inside the polymer but also perhaps how the incorporated ions are partitioned among the various regions.

However, several caveats must be kept in mind when interpreting the fluorescent results. These include: (1) rigidity of the solvent around the fluorescent probe, such that solvent reorientation during the the excited state liftime is inhibited, can make a polar region appear non-polar;[18] (2) pH effects on the fluorescence;[19] (3) metal ions and supporting electrolyte ions may alter the fluorescent properties;[20] (4) because of the size of the fluorescent probe-redox couple; the microenvironment "sensed" by one may not be identical to that "sensed" by the other;[21] (5) quenching of the excited state by the redox couple (this could be minimized by elongating the side chain that attaches the fluorescent tag to the bipyridine ligand although this would increase the possibility of (4), and (6) because of the size of the redox couple-fluorescent probe (it is larger than just the redox couple), this molecule may reside in different regions than it would have if the fluorescent side chain was not present. Despite the above restrictions, it is believed that this coupling of electrochemistry and fluorescence will yield new and useful data on polymer-modified electrodes.

REFERENCES

1. See, for example: a) W. R. Heinman and P. T. Kissinger, Anal. Chem. 50, 166R (1978).
b) K. D. Snell and A. G. Keenan, Chem. Soc. Rev. 8, 259 (1979).
2. See, for example: a) K. C. Shigehara and F. C. Anson, J. Electroanal. Chem. 132, 107 (1982), and references therein.
b) N. Oyama and F. C. Anson, Anal. Chem. 52, 1192 (1980), and references therein.
3. See, for example: N. Oyama and F. C. Anson, J. Am. Chem. Soc. 101, 739, 3450 (1979) and references therein.
4. See, for example: N. Oyama and F. C. Anson, J. Electrochem. Soc. 127, 247 (1980).
5. See, for example: D. Buttry and F. C. Anson, J. Electroanal. Chem. 130, 333 (1981).
6. F. C. Anson, J. M. Saveant and K. Shigehara, submitted for publication.
7. D. Buttry and F. C. Anson, J. Am. Chem. Soc., in press.
8. See, for example: a) A. Pines, M. G. Gibby and J. S. Waugh, J. Chem. Phys. 56, 1775 (1972).
b) I. Ya Slonim and A. N. Lyubimov, "The NMR of Polymers", Plenum Press, New York (1970), and references therein.
9. See, for example: a) I. Rubinstein and A. J. Bard, J. Am. Chem. Soc. 103, 5007 (1981).
b) D. Buttry and F. C. Anson, submitted for publication.
10. See, for example: a) H. Morawertz, Science, 203, 405 (1979).
b) Y. Nishijima in "Progress in Polymer Science, Japan",

S. Onogi and K. Uno, Eds., pp. 199-251, Wiley, New York, 1973.

11. A. Azzi, Quart. Rev. Biophys. 8, 237 (1975), and references therein.
12. G. Weber, Biochem. J. 51, 155 (1952).
13. See, for example: a) L. Stryer, J. Mol. Biol. 13, 482 (1965).
    b) G. Weber and D. J. Laurence, Proc. Biochem. Soc. xxxi (1954).
14. R. A. Kenner and A. A. Aboderin, Biochem. 10, 4433 (1971).
15. a) M. J. Cook, A. R. Katrizky and S. Nadji, J. Chem. Soc., Perkin Trans. 2, 1215 (1978).
    b) R. A. Jones, B. D. Roney, W. H. Sasse and K. O. Wade, J. Chem. Soc. B, 106 (1967).
    c) J. March, "Advanced Organic Chemistry", 2nd ed. pp. 1125, 1129 (1977), and references therein.
16. a) A. J. Boulton, P. B. Ghosh and A. R. Katritzky, J. Chem. Soc. B, 1004 (1966).
    b) A. J. Boulton, P. B. Ghosh and A. R. Katritzky, Tetrahedron Lett. 2887 (1966).
17. See, for example: W. R. McWhinnie and J. D. Miller, Adv. Inorg. Chem. Radiochem. 12, 135 (1969).
18. See reference 11, p. 250, and references therein.
19. See reference 11, pp. 298-300, and references therein.
20. See reference 11, pp. 278-280, and references therein.
21. See reference 11, pp. 249-253, and references therein.

PROPOSITION 3

Abstract

Adsorption of aromatic molecules on carbon electrodes in aqueous media may be utilized to prepare an adsorbed aromatic-susbstituted ferricinium layer on rotating graphite disk electrodes. Under conditions when: (1) more than or equal to a monolayer of adsorbed complex is present which completely blocks the electrode surface from solution-phase material; (2) the formal potential for the adsorbed species is essentially the same as for the same solution complex; (3) the cross reaction between adsorbed substituted-ferricinium and solution-phase substituted-ferrocene is the rate determining step in electron transfer from the electrode to solution material, then the cross reaction rate constant measured from the limiting currents in rotating disk experiments is bascially identical to the homogeneous (self-exchange) electron transfer rate constant for the aromatic-substituted ferrocene/ferricinium redox couple.

There are several examples of aromatic molecules which have been found to adsorb quite strongly (a full monolayer) on graphite electrodes in aqueous media.[1,2] Usually those complexes which are less soluble in water and with the greater number of aromatic ring systems tend to adsorb stronger and with greater stability on the surface.[2] Adsorption can occur spontaneously just be dipping the graphite electrode in an aqueous solution containing the aromatic compound[2] or by coating the species on the surface by first dissolving the complex in a non-aqueous solvent, syringing several μL of solution onto the electrode and then allowing the nonaqueous solvent to evaporate.[3] In some cases, the adsorbed material is stable on the electrode for many hours, even sitting in only pure supporting electrolyte. Alternatively, an adsorbed layer may be formed by electrochemically generating the species in situ which spontaneously adsorbs on the graphite surface.[4]

The amount adsorbed in a given system can be determined from cyclic voltammetry,[1,2] differential pulse voltammetry[1,2] or chronocoulometry.[5] Usually these techniques are applied after the electrode has been coated with the adsorbed material and then transferred to a pure supporting electrolyte solution, however, it is sometimes possible to perform these experiments with solution-phase complex present as long as the solution-phase concentration is low.

Recently, there has appeared a study in which the apparent homogeneous electron transfer rate constant $(k_{ex})_{app}$ for $IrCl_6^{3-/2-}$ was measured by rotating disk voltammetry.[6] This was accomplished by electrostatically binding $IrCl_6^{3-}$ into a polyelectrolyte polymer film

(protonated polyvinylpyridine) which irreversibly adsorbs on the rotating disk, graphite electrode and then varying the rotation rate of the electrode (which is coated with the polymer-$IrCl_6^{3-}$ matrix) in solutions of different concentrations of $IrCl_6^{2-}$. Measurements of the limiting current as a function of rotation rate and then analyzing the resulting data by means of Koutecky-Levich reciprocal plots[7] (as shown below) was used to calculate the apparent self-exchange rate constant $(k_{ex})_{app}$ from the finite intercepts on the (current)$^{-1}$ axis.

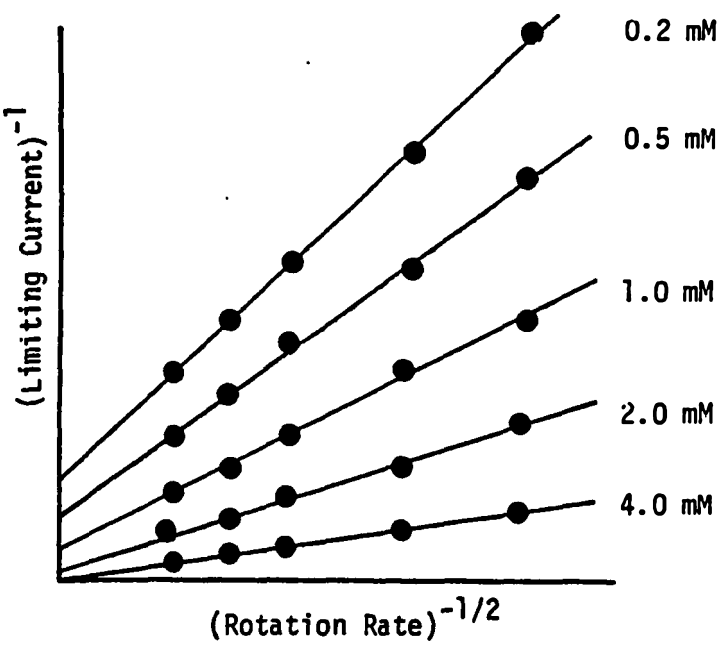

The slopes of the straight lines were inversely proportional to the bulk concentration of $IrCl_6^{2-}$ in solution and the intercepts were inversely proportional to k_{ex} by equation 1:[6]

$$(\text{intercept})^{-1} = F(k_{ex})_{app}\Gamma_{ads}C^b \qquad (1)$$

where F is the faraday constant; $(k_{ex})_{app}$ is the apparent electron transfer rate constant (in M^{-1} cm^3 s^{-1}) between the adsorbed, polymer-bound species and the solution-phase complex (which is the other half of the redox couple); Γ_{ads} is the total amount of adsorbed material ($IrCl_6^{3-}$ in this case) or in some cases it is just the calculated monolayer coverage of the adsorbed redox couple (in mol cm^{-2}); C^b is the solution-phase concentration for the redox partner ($IrCl_6^{2-}$) of the complex in the film (in mol cm^{-3}).

All of the above discussion depends upon the following conditions being met: (1) the adsorbed layer prevents solution material from reaching the electrode; (2) the formal potential for the adsorbed couple is essentially the same as for the solution couple; (3) the rate limiting step in electron transfer from the electrode to solution-phase complex is the cross reaction between the adsorbed and solution materials, which implies (4) that electron transfer from the electrode to the adsorbed layer and also electron transfer through the adsorbed layer are not rate limiting. This was the case for thin polymer-$IrCl_6^{3-}$ films and mM concentrations of $IrCl_6^{2-}$ in solution[6] and also in the investigation of the self-exchange rate constant for Cu(1,10-phenanthroline)$_2^{2+/+}$ in aqueous media measured by the rotating disk method.[4]

The ferrocene/ferricinium redox couple has been extensively studied in non-aqueous and aqueous media.[8-11] Both homogeneous

(self-exchange)[8-11] and heterogeneous[12-14] electron transfer rate constants have been measured. Ferrocene undergoes only very little intramolecular changes upon oxidation[15] so that the rate of electron transfer is basically governed by the outer-sphere reorganizational energy. In non-aqueous media, the self-exchange rate for $(C_5H_5)_2Fe^{0/+}$ is approximately 10^7 M^{-1} s^{-1} [8,9] while it may be as high as 10^9 M^{-1} s^{-1} in aqueous media.[10] In order to probe further the application of rotating disk voltammetry to the measurement of self-exchange rate constants and to study in greater detail the ferrocene/ferricinium redox couple it is proposed to: (1) prepare several aromatic-substituted ferrocenes which should adsorb on either basal or edge plane graphite electrodes in either the Fe(II) or Fe(III) oxidation state; (2) measure the amount of adsorbed material via chronocoulometry[5] or cyclic voltammetry[2] and determine if it blocks the electrode from solution material; (3) measure the formal potential for the solution couple and also for the adsorbed couple; (4) perform rotating disk experiments with the coated electrodes at different rotation rates and in solutions of differing concentrations of the redox partner; (5) make Koutecky-Levich plots[7] of the resulting limiting currents as a function of rotation rate and bulk solution concentration of the redox partner; (6) calculate the apparent self-exchange rate constant from the intercepts (if there are any; will not have any intercepts if the cross reaction rate is too high) on the $(current)^{-1}$ axis using equation 1 if the plots are linear; (7) make sure that electron transfer from the electrode to the adsorbed layer and also electron transfer through the adsorbed layer are not rate limiting by examining

the adsorbed layer in the absence of any solution redox complex by rotating disk and coulostatic[16] experiments.

Candidates for aromatic-substituted ferrocenes include helical ferrocene(I), a synthesis of which has just appeared,[17] the substituted ferrocene(II) which could be prepared from commercially available 2,3-dibenzofluorene and $FeCl_2$ according to standard procedures[18] or possibly even bis(1,2,3,4-tetraphenylcyclopentadienyl)iron, (III), synthesized in a similar manner from the commercial ligand (Aldrich). The latter complex, although not having all its phenyl rings planar, may be better suited to intercalation of the rings into edge plane graphite. It is believed that for all of the above complexes, a full monolayer or more of adsorbed material would be found.

Values of the self-exchange rate constant for the substituted ferrocene redox couples measured by the rotating disk technique can be compared to those previously measured for the unsubstituted ferrocene or NMR experiments[8,11] on the freshly prepared aromatic-substituted ferrocenes would also be performed.

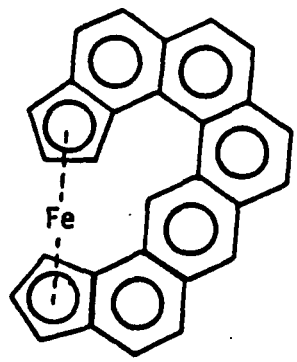

I

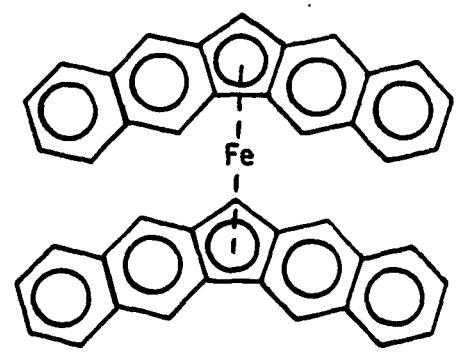

II

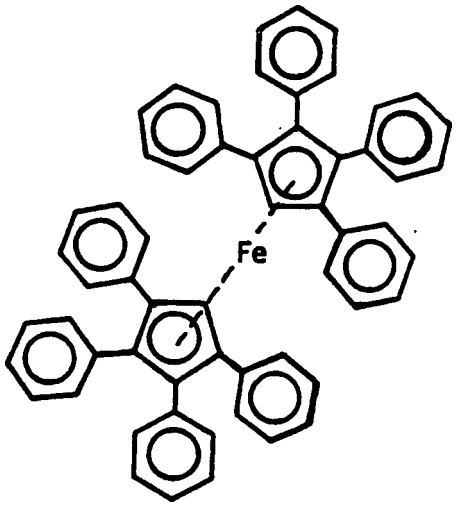

III

REFERENCES

1. a) A. P. Brown and F. C. Anson, Anal. Chem. 49, 1589 (1977). b) A. P. Brown, C. Koval and F. C. Anson, J. Electroanal. Chem. 72, 379 (1976), and references therein.
2. C. Koval, Ph.D. Thesis, California Institute of Technology, 1979.
3. Ths technique is commonly used for the polymer-modified research. See, for example: (a) N. Oyama and F. C. Anson, Anal. Chem. 52, 1192 (1980).
4. C. Lee and F. C. Anson, to be published.
5. F. C. Anson, Anal. Chem. 38, 54 (1966).
6. K. Shigehara, N. Oyama and F. C. Anson, Inorg. Chem. 20, 518 (1981).
7. a) J. Koutecky and V. G. Levich, Zh. Fiz. Khim. 32, 1565 (1956). b) V. G. Levich, "Physicochemical Hydrodynamics", Prentice Hall, Englewood, NJ, 1962.
8. E. S. Yang, M. S. Chan and A. C. Wahl, J. Phys. Chem. 84, 3094 (1980).
9. I. Ruff, V. J. Friedrich, K. Demeter and K. Csillag, J. Phys. Chem. 75, 3303 (1971).
10. D. R. Stranks, Disc. Faraday Soc. 29, 73 (1960).
11. E. A. Yang, M. S. Chan and A. C. Wahl, J. Phys. Chem. 79, 2049 (1975).
12. J. H. Higgle and A. J. Parker, Electrochim. Acta 18, 975 (1973).
13. T. Saji, Y. Maruyama and S. Aoyagni, J. Electroanal. Chem. 86, 219 (1978).

14. M. Sharp, M. Peterson and K. Edstrom, J. Electroanal. Chem. 109, 271 (1980).

15. a) T. Bernstein and P. H. Herbstein, Acta Cryst. B24, 1640 (1968).

b) J. W. Bats, J. J. de Boer and D. Bright, Inorg. Chim. Acta, 5, 605 (1971).

16. a) H. P. van Leeuwen, Electrochim. Acta, 23, 207 (1978).

b) J. M. Kudirka, P. H. Daum, and C. C. Enke, Anal. Chem. 44, 309 (1972).

17. T. J.Katz and J. Pesti, J. Am. Chem. Soc. 104, 346 (1982).

18. F. A. Cotton and G. Wilkinson, "Advanced Inorganic Chemistry. A Comprehensive Text", 4th ed., p. 1163, Interscience, New York, 1980.

PROPOSITION 4

Abstract

Preparation of the ruthenium(II) and (III) analogs of the caged metal ion [(1,3,6,8,10,13,16,19-octaazabicyclo[6.6.6]eicosane)cobalt(III)]$^{3+}$, which has been given the trivial name of Co(sepulchrate)$^{3+}$, via condensation of the tris(ethylenediamine)ruthenium(III) ion with formaldehyde and ammonia is proposed. Formation of the chiral Δ-Ru(sepulchrate)$^{3+}$ and Λ-Ru(sepulchrate)$^{2+}$ complexes could then be used to determine the homogeneous (self-exchange) electron transfer rate constant for the Ru(sepulchrate)$^{3+/2+}$ redox couple, which would be compared to the previously measured value for Ru(ethylenediamine)$_3^{3+/2+}$.

Ligands which encapsulate metal ions, such as cryptates[1] and crown ethers,[2] have been an area of much current research due to their unusual chemical specificity and stability. Very recently there has appeared a synthesis of an encapsulating ligand-metal ion complex [(1,3,6,8,10,13,16,19-octaazabicyclo[6.6.6]eicosane)cobalt(III)]$^{3+}$. Co(sepulchrate)$^{3+}$ for short, which was formed when Co(ethylenediamine)$_3^{3+}$ was condensed with NH_3 and CH_2O in basic media in greater than 95% yield.[3] The sepulchrate ligand endows the cobalt-sepulchrate species with unusual stability, in both the Co(II) and Co(III) oxidation states,[3,4] and reactivity (for example with oxygen[3,4]). Several other metal-sepulchrate complexes have been prepared,[5] including those with Pt(IV), Rh(III) and Cr(III), although their chemical properties and the synthetic procedures involved in their preparation have not yet been published.

One of the unique features of the sepulchrate-metal ion complex is that if the synthesis is performed with chiral Co(ethylenediamine)$_3^{3+}$, Δ or Λ, only the one chiral isomer (Δ or Λ respectively) is formed[3,4] because of the inflexibility of the imine backbone produced upon intramolecular condensation. This property has been exploited to prepare chiral Δ-Co (sepulchrate)$^{3+}$ and Λ-Co(sepulchrate)$^{2+}$. When equal concentrations of the two chiral species are mixed together, it was possible to determine the homogeneous electron transfer rate constant from the rate of racemization, defined by the change in optical rotation at 500 nm.[3] At 25°C and μ = 0.2 (NaCl, HCl), a homogeneous electron transfer rate constant (k_{ex}) of 5.1 M^{-1} s^{-1} was found.[3] This value for the self-exchange rate constant of Co(sepulchrate)$^{3+/2+}$ is approximately

10^5 times larger than that measured for Co(ethylenediamine)$_3^{3+/2+}$ (k_{ex} of 5×10^{-5} M^{-1} s^{-1}) by the same method[6] or isotopic exchange[7] under similar conditions.

It is very difficult to explain this dramatic difference in the self-exchange rate constants for these very similar cobalt-imine complexes especially considering that the electronic states (determined from the ligand field spectra and the paramagnetism found for the high spin cobalt(II) species[3,4]) and intramolecular bond distance changes are essentially identical for the Co(ethylenediamine)$_3^{3+/2+}$ and Co(sepulchrate)$^{3+/2+}$ couples. At present, there is no explanation for the dissimilarity in the homogeneous electron transfer rate constants of Co(sepulchrate)$^{3+/2+}$ and Co(ethylenediamine)$_3^{3+/2+}$, therefore it is proposed to see if a rate difference is also observed for the ruthenium analogs, Ru(sepulchrate)$^{3+/2+}$ and Ru(ethylenediamine)$_3^{3+/2+}$.

Preparation of the two chiral forms of Ru(sepulchrate)$^{3+}$ would be attempted in a similar manner to that performed for the chiral Co(sepulchrate)$^{3+}$ isomers[3,4] via condensation of the appropriate chiral Ru(ethylenediamine)$_3^{3+}$ with ammonia and formaldehyde in basic solutions. Once both Δ- and Λ-Ru(sepulchrate)$^{3+}$ isomers have been synthesized and characterized, spectrally and physically (crystal structure), in both the Ru(II) and Ru(III) oxidation states then mixing of equal concentrations of Δ-Ru(sepulchrate)$^{3+}$ and Λ-Ru(sepulchrate)$^{2+}$ should allow the determination of the homogeneous electron transfer rate constant for this redox couple.[3] This value, once measured, can then be compared to the previously measured self-exchange rate constants for Ru(ethylenediamine)$_3^{3+/2+}$ (k_{ex} is approximately 200 M^{-1} s^{-1})[8] and Ru$(NH_3)_6^{3+/2+}$

(k_{ex} is 1000 M^{-1} s^{-1}).[8]

Under identical experimental conditions (i.e., same temperature and ionic strength) the homogeneous electron transfer rate constants for Ru(sepulchrate)$^{3+/2+}$ and Ru(ethylenediamine)$_3^{3+/2+}$ might (a priori) be expected to be comparable since both complexes should have similar inner- and outer-sphere rearrangements and ligand environments. If indeed this is the case, then this suggests that there is something peculiar about the Co(sepulchrate)$^{3+/2+}$ and Co(ethylenediamine)$_3^{3+/2+}$ comparison, perhaps due to non-adiabatic effects or ligand dissocation[4] in the Co(ethylenediamine)$^{3+/2+}$ couple. However, on the other hand, if there is a large increase in the homogeneous electron transfer rate constant for Ru(sepulchrate)$^{3+/2+}$ over that found for Ru(ethylenediamine)$_3^{3+/2+}$, then one would be tempted to say that there is something very special about the sepulchrate ligand. The possibilities that there may be electronic interactions through the lone pairs on the capping nitrogens or intercalation of one molecule into another have been ruled out in the cobalt derivatives.[4] Finally, if the Ru(sepulchrate)$^{3+/2+}$ self-exchange rate is really 10^5 times larger than that observed for Ru(ethylenediamine)$_3^{3+/2+}$, it would be in the same range (approximately 10^7 to 10^9 M^{-1} s^{-1}) as that found for Ru(2,2'-bipyridine)$_3^{3+/2+}$.[9] This value is not outside the realm of possibility although it would not be predicted by Marcus theory.[10]

In addition to the comparison of self-exchange rate constants, it may also be possible to compare heterogeneous electron transfer rate constants measured for the ruthenium imine complexes and to use the Ru(sepulchrate)$^{2+}$ as a simple, outer-sphere, one-electron transfer agent.

REFERENCES AND NOTES

1. J. M. Lehn, Pure Appl. Chem. 49, 857 (1977) and references therein.
2. a) C. J. Pedersen, J. Am. Chem. Soc. 89, 7017 (1867).
   b) D. J. Cram and J. M. Cram, Acc. Chem. Res. 11, 8 (1978) and references therein.
3. I. I. Creaser, J. M. Harrowfield, A. J. Herlt, A. M. Sargeson, J. Springborg, R. J. Geue and M. R. Snow, J. Am. Chem. Soc. 99, 3181 (1977).
4. A. M. Sargeson, Chem. in Brit. 23 (1979)
5. H. Boucher et al., unpublished work.
6. F. P. Dwyer and A. M. Sargeson, J. Phys. Chem. 65, 1892 (1961).
7. a) W. B. Lewis, C. D. Coryell and J. W. Irvine, J. Chem. Soc. Suppl., No. 2, 386 (1949).
   b) B. R. Baker, F. Basolo and H. M. Neumann, J. Phys. Chem. 63, 371 (1959).
8. T. J. Meyer and H. Taube, Inorg. Chem. 7, 2369 (1968).
9. a) M. S. Chan and A. C. Wahl, J. Phys. Chem. 82, 2542 (1978).
   b) R. C. Young, F. R. Keene and T. S. Meyer, J. Am. Chem. Soc. 99, 2468 (1977).
10. a) R. A. Marcus, J. Chem. Phys. 24, 979 (1956).
    b) R. A. Marcus, Electrochim. Acta, 13, 995 (1968).

PROPOSITION 5

Abstract

A synthetic route to 5- and 6-membered dimetallocycles containing metals other than cobalt is proposed via reaction of the stable radical anions of several dinuclear metal species with various dibromoalkyls. Decomposition of these dimetal-carbon ring systems, where the dimetal fragment is either Fe-Fe or Ni-Ni, may occur through other pathways than those observed for the dicobalt ring complexes. In addition, reaction of the radical anion of $[(C_5H_5)Co(CO)_2]_2$ with 1,1'-methyl bromide ferrocene would allow formation of a previously unknown trinuclear metallocycle containing two different metals.

Metallocycles have been identified as intermediates in a variety of organic transformations catalyzed by metal complexes,[1] and many different ring sizes and different metals have been prepared.[2] Dimetallocycles, in which there are two metals in the ring, are also proving to have quite interesting chemistry and many kinetically stable 3-membered dimetallocycles have been synthesized.[3] However, there have not been many examples of larger ring dimetallocycles, especially when four[4] or six[5,6] atoms are in the ring. The larger dimetallocycles are of interest because they may be models for alkene and diene oligomerization, as well as possibilities for CO insertion reactions into the ring.

Recently, a study has appeared dealing with the preparation and chemistry of a dimetallocyclohexene species containing a cobalt-cobalt metal bond.[6] Synthesis of the dimetallocycle was accomplished via reaction of the radical anion, derived from $[(C_5H_5)Co(CO)_2]_2$ and Na, of the dicobalt compound with α,α'-dibromo-o-xylene. Attempts to prepare the saturated version proved unsuccessful due to facile β-hydrogen elimination reactions,[7] although this was not a problem in the 5-membered dicobalt analogue.[8] The dicobalt metallocyclohexene was stable below room temperature but in solution above 22°C, it was found to undergo decomposition into a previously unknown mononuclear o-xylylene species, which, when heated to 70°C in the presence of CO, inserted to carbon monoxide to form 2-indanone.[6] Decomposition of the dicobalt metallocyclohexene also occurred upon addition of various phosphines.[6]

To investigate the general utility of the synthetic procedure used

to prepare the larger ring dimetallocycles (i.e., by reaction of dimetal radical anions with dibromoalkyls) and to see how the identity of the metals in the ring effect any decomposition, it is proposed to react the stable radical anions of $[Ni(CO)_2P(C_6H_5)_2]_2$[9] and $[Fe(NO)_2P(C_6H_5)_2$[9] with α,α'-dibromo-o-xylene. If formation of the unsaturated dimetallocyclohexenes is successful, then further experiments to try and prepare the fully saturated version, by reaction of the dimetal radical anion with 1,4-dibromobutane, would be attempted since the β-hydrogen elimination may be sensitive to the identity of the metals present in the ring.

Any thermal or ligand-induced decomposition reactions would also be characterized (by NMR and IR techniques[5,6]) to determine any similarities of the Fe-Fe and Ni-Ni dimetallocyclohexenes with the dicobalt analogue. Preparation and characterization of products would all be performed in an inert atmosphere box using techniques similar to that already described.[5,6]

Finally it is proposed to further exploit the reaction of dimetal radical anions with dibromo complexes in the synthesis of a unique trimetallocycle containing a ferrocene subunit. This could be accomplished (see reaction 1) by reaction of the radical anion of $[(C_5H_5)Co(CO)_2]_2$ with 1,1'-methylbromide ferrocene (prepared from commercially available 1,1'-formaldehyde ferrocene[10]).

Reaction 1.

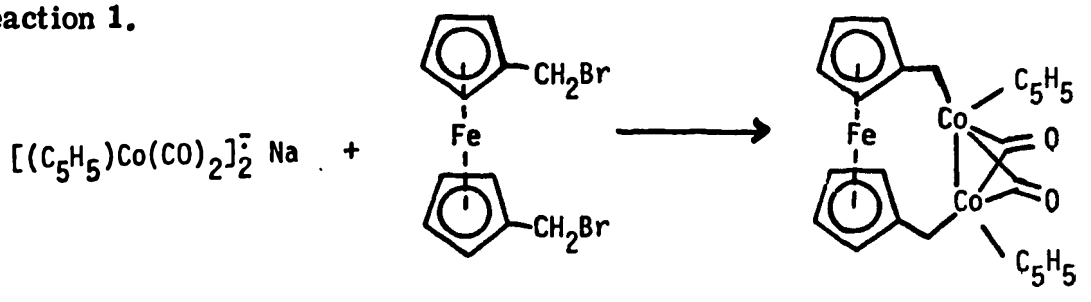

This trinuclear metallocycle does not have the same decomposition pathways available to it that the benzannulated derivative has and therefore may be more thermally stable. However, any decomposition that may occur will probably generate new and reactive intermediates not previously observed. It is also hoped that the presence of the third metal might allow insertion of small molecules into the trinuclear complex and provide interesting redox behavior.

REFERENCES

1. See, for example: a) J. X. McDermott, J. F. White and G. M. Whitesides, J. Am. Chem. Soc. 95, 4451 (1973), and references therein.

b) R. H. Grubbs, A. Miyashita, M. Liu, and P. Burk, J. Am. Chem. Soc. 100, 2418 (1978), and references therein.

c) K. C. Bishop, Chem. Rev. 76, 461 (1976).

2. F. A. Cotton and G. Wilkinson, "Advanced Inorganic Chemistry. A Comprehensive Text", pp. 1238-42, Wiley, New York, 1980.

3. See, for example: a) R. A. Jones, G. Wilkinson, A. M. Galas, M. B. Hursthouse, and M. K. Abdul Malik, J. Chem. Soc., Dalton Trans. 1771 (1980).

b) W. A. Herrmann, J. Plank, D. Riedel, K. Ziegler, K. Weidenhammer, E. Guggolz and B. Balbach, J. Am. Chem. Soc. 103, 63 (1981).

c) K. H. Theopold and R. G. Bergman, J. Am. Chem. Soc. 103, 2489 (1981).

4. See, for example: a) N. Boag, M. Green and F. G. Stone, J. Chem. Soc. Chem. Commun. 1281 (1980).

b) R. S. Dickson, C. Mok and G. J. Pain, J. Organometal Chem. 166, 385 (1979).

c) M. D. Rausch, R. G. Gastinger, S. A. Gardner, R. K. Brown, and J. S. Wood, J. Am. Chem. Soc. 99, 7870 (1977).

5. See, for example: a) L. E. Swart, J. Browning, M. Green, A. Zaguna, J. L. Spencer and F. G. Stone, J. Chem. Soc. Dalton Trans. 1777 (1977).

b) S. A. Knox, R. F. Stansfield and F. Stone, J. Chem. Soc. Chem. Commun. 221 (1978).

c) J. Slater and E. L. Muetterties, Inorg. Chem. 20, 946 (1981).

6. W. H. Hersh and R. G. Bergman, J. Am. Chem. Soc. 103, 6992 (1981).

7. K. H. Theopold, W. H. Hersh and R. G. Bergman, Israel J. Chem. in press.

8. K. H. Theopold and R. G. Bergman, J. Am. Chem. Soc. 102, 5694 (1980).

9. R. E. Dessy, R. Kornmann, C. Smith and R. Hayton, J. Am. Chem. Soc. 90, 2001 (1968).

10. Mild reduction of 1,1'-formadelhyde ferrocene to the 1,1'-methyl alcohol ferrocene followed by reaction with HBr or $SoBr_2$ should yield the desired product.